

University of Bath



PHD

Ultrasonic compatibilisation of polymers

Crook, Simon Thomas

Award date:
1999

Awarding institution:
University of Bath

[Link to publication](#)

General rights

Copyright and moral rights for the publications made accessible in the public portal are retained by the authors and/or other copyright owners and it is a condition of accessing publications that users recognise and abide by the legal requirements associated with these rights.

- Users may download and print one copy of any publication from the public portal for the purpose of private study or research.
- You may not further distribute the material or use it for any profit-making activity or commercial gain
- You may freely distribute the URL identifying the publication in the public portal ?

Take down policy

If you believe that this document breaches copyright please contact us providing details, and we will remove access to the work immediately and investigate your claim.

Download date: 13. May. 2019

ULTRASONIC COMPATIBILISATION OF POLYMERS

submitted by Simon Thomas Crook

for the degree of PhD

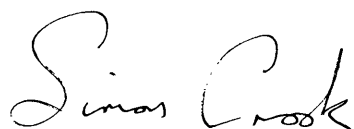
of the University of Bath

1999

COPYRIGHT

Attention is drawn to the fact that copyright of this thesis has been supplied on condition that anyone who consults it is understood to recognise that its copyright rests with its author and that no quotation from the thesis and no information derived from it may be published without the prior consent of the author.

Signed:

A handwritten signature in black ink that reads "Simon Crook". The signature is written in a cursive style with a large initial 'S' and a long, sweeping underline.

UMI Number: U601453

All rights reserved

INFORMATION TO ALL USERS

The quality of this reproduction is dependent upon the quality of the copy submitted.

In the unlikely event that the author did not send a complete manuscript and there are missing pages, these will be noted. Also, if material had to be removed, a note will indicate the deletion.



UMI U601453

Published by ProQuest LLC 2013. Copyright in the Dissertation held by the Author.
Microform Edition © ProQuest LLC.

All rights reserved. This work is protected against
unauthorized copying under Title 17, United States Code.



ProQuest LLC
789 East Eisenhower Parkway
P.O. Box 1346
Ann Arbor, MI 48106-1346

UNIVERSITY OF BATH LIBRARY		
30	20 JUN 2000	
PHD		

Acknowledgements

Many thanks must go to the following people who have made life more enjoyable and work easier whilst researching and writing this thesis:

My colleagues in the laboratory, Phil Drake, David Brown, Simon Hickling, Dave Snell and not forgetting the honorary member, Roger Jardine. Also to Liz for always being happy, helpful and cleaning the glassware!

To Dr Gareth Price for having the patience to read this thesis through and for his many useful comments and suggestions. Also thanks to TWI for the funding and especially to Roger Wise who is always an enthusiastic helpful fellow.

Finally special thanks go to my parents for helping me through university and especially to Jenny for her support and love.

Abstract

Presented in this thesis is an introduction to sonochemistry and general polymer compatibilisation research. The use of ultrasound on various polymer systems has been examined, both in solution and in the molten state. Examination of these systems was achieved using scanning electron microscopy (SEM), gel permeation chromatography (GPC), differential scanning calorimetry (DSC) and dynamic mechanical thermal analysis (DMTA).

Results are displayed for the ultrasonic degradation of homopolymer solutions via GPC degradation plots and for ultrasonic compatibilisation of polymer pairs in solution via SEM photographs. A study of ultrasonic effects in molten systems was also undertaken, with results for homopolymer melt degradation in the form of GPC degradation plots and for melt compatibilisation via SEM photographs, DSC thermograms and DMTA plots. Similar research was also carried out for pressurised, sonicated melts.

From the results it is shown that ultrasonic techniques degrade homopolymers in solution and compatibilise most polymer pairs in solution. Evidence of chain branching of polybutadiene via ultrasonic degradation was also shown by NMR spectroscopy. It was also found that ultrasound has little effect, other than mixing, on polymer melts unless pressure is also applied. This improves the coupling between the sonic horn and polymer melt, so allowing cavitation to take place.

Aims

The overall aim of this project was to investigate the possibility of ultrasonic compatibilisation of immiscible polymer pairs in the molten state. It was also envisaged that experiments involving polymer solution systems would be studied, in order to gain a background of knowledge and to further understand the effect of ultrasound on polymer solutions. This was carried out for both single polymer solutions (degradation) and in pairs (compatibilisation).

CONTENTS

	<u>Page</u>
Abstract	3
Aims	4
<u>INTRODUCTION</u>	
1. Sonochemistry	10
1.1. Ultrasonic Waves	10
1.2. Cavitation	13
1.3. Factors Affecting Cavitation	15
1.4. History Of Ultrasound	17
1.5. Generation Of Ultrasound	20
<i>1.5.1. The Piezoelectric Effect</i>	20
<i>1.5.2. Equipment For Power Ultrasound</i>	20
1.6. Industrial Applications Of Ultrasound	23
<i>1.6.1. Ultrasonic Welding</i>	23
<i>1.6.2. Ultrasonic Cleaning</i>	25
<i>1.6.3. Engineering Applications</i>	25
<i>1.6.4. Chemical Engineering Applications</i>	26
<i>1.6.5. Medicinal Uses</i>	27
1.7. Research In Ultrasound	28
<i>1.7.1. Basic Understanding</i>	28
<i>1.7.2. Sonoluminescence</i>	29
<i>1.7.3. Ultrasound in Heterogeneous Chemistry</i>	30
<i>1.7.4. Decomposition Of Metal Carbonyls</i>	33
<i>1.7.5. Sonication Of Metals</i>	34
<i>1.7.6. Ultrasonic Degradation Of Water Contaminants</i>	34
2. Ultrasound and Polymers	36
2.1. Polymer Degradation	36
<i>2.1.1. Mechanism of degradation</i>	37
<i>2.1.2 Factors affecting ultrasonic degradation</i>	40
<i>2.1.3. Kinetics of ultrasonic polymer degradation</i>	41

	<u>Page</u>
2.1.4. <i>Products of polymer chain degradation</i>	43
2.2. Polymer Synthesis	44
3. Compatibilisation Of Polymers	47
3.1. Polymer-Polymer Thermodynamics	47
3.1.1. <i>The Ideal Solution</i>	47
3.1.2. <i>The Regular Solution</i>	48
3.1.3. <i>Polymer-Solvent Systems</i>	48
3.1.4. <i>Polymer-Polymer Systems</i>	50
3.1.5. <i>Polymer Incompatibility</i>	51
3.2. Compatibilisation Of Polymer Mixtures	52
3.2.1. <i>Ultrasonic Compatibilisation</i>	52
3.3. Some Current Research In Polymer Compatibilisation	53
4. Polymer Recycling	57
4.0.1. <i>Polymer Recycling In The Automotive Industry</i>	57
4.0.2. <i>Polymer Recycling In Europe</i>	58
4.1. Methods Of Recycling Plastics	59
4.1.1. <i>Mixed Waste</i>	59
4.1.2. <i>Pyrolysis</i>	59
4.1.3. <i>Hydrolysis</i>	60
4.1.4. <i>Hydrogenation</i>	60
4.1.5. <i>Other Depolymerisation Methods</i>	61
4.1.6. <i>Incineration</i>	61
4.1.7. <i>Composite Materials</i>	62
4.1.8. <i>Biodegradation</i>	62
4.1.9. <i>Landfill</i>	63
4.1.11. <i>Rubber Reclamation</i>	63
4.1.12. <i>Other</i>	64
4.2. Economic Considerations For Polymer Recycling	64
4.3. Overview	65
5.0. Experimental Introduction	67
5.1. Gel Permeation Chromatography	67

	<u>Page</u>
5.2. Differential Scanning Calorimetry & Dynamic Mechanical	
Thermal Analysis	70
5.3. Scanning Electron Microscopy	74
5.4. Experimental Methods	75
5.5. Sonication of Model Solutions	76
5.6. Electron Microscope Study of the Effects of Ultrasound on	
Polymer Mixtures in Solution	77
5.7. Sonication of Polymer Melts	78
5.8. Polymer Melt Degradation	80
5.9. Polymer Melt Compatibilisation	81
5.10. Scanning Electron Microscopy of Polymer Melts	81
5.11. Sonication of Polymer Melts Under Pressure	81
5.12. Sonication of PMMA/Silica Layers	84
5.13. Materials used in study	84
6.0 RESULTS	85
6.1. Ultrasonic Degradation of Polymers in Solution	85
<i>6.1.1 Polystyrene/Toluene</i>	85
<i>6.1.2. Cis Polybutadiene/Toluene</i>	89
<i>6.1.3. Poly(isoprene)/toluene</i>	95
<i>6.1.4. PVC/Tetrahydrofuran</i>	98
6.3. Section Discussion	99
7.0. Electron Microscope Study Of The Effects Of Ultrasound On	102
Solutions Containing Two Polymer Species	
<i>7.0.1 Polystyrene/Polyisoprene 1:1</i>	102
<i>7.0.2. Polystyrene/Polymethylmethacrylate in tetrahydrofuran</i>	105
<i>7.0.3 Polystyrene/Polymethylmethacrylate in Toluene</i>	111
<i>7.0.4 Polyisoprene/Polymethylmethacrylate</i>	112
<i>7.0.5. Polyethylene / Polypropylene in Decalin</i>	116
7.1. Section Discussion	119
8.0. Polymer Degradation in the Melt	123
8.1. Observation of Melt Flow due to Ultrasonic Mixing	123

	<u>Page</u>
8.1.1 <i>PDMS Melt Flow Simulation</i>	123
8.1.2 <i>Sonication of PMMA / Silica layers</i>	124
8.2. Ultrasonic Degradation of Molten Polymers	125
8.2.1 <i>Polystyrene</i>	126
8.2.2 <i>Polystyrene (under N₂)</i>	127
8.0.3 <i>Polymethylmethacrylate</i>	130
8.0.4 <i>Polyethylene</i>	131
8.3 Section Discussion	133
9.0. Melt Compatibilisation	134
9.0.1. <i>Polyethylene/ Polystyrene electron micrograph studies</i>	134
9.0.2. <i>Polyethylene/Polypropylene electron micrograph studies</i>	137
9.0.3 <i>DSC Results for Melt Sonicated PE/PP</i>	144
9.0.4 <i>DMTA of PE/PP</i>	146
9.0.5. <i>Polyvinylidifluoride/Polyethylene electron micrograph studies</i>	149
9.0.6. <i>DSC results for PE/PVDF Melt Sonication</i>	151
9.0.7. <i>PVDF/PE DMTA Results</i>	153
9.0.8 <i>Polyvinylidifluoride/Polypropylene</i>	156
9.1. Section Discussion	156
10.0 Sonication of Pressurised Polymer Melt Systems	158
10.1.1. <i>SEM of Polypropylene/Polyethylene</i>	158
10.1.2. <i>DSC of pressurised melt samples</i>	161
10.1.3. <i>DMTA of pressurised PE/PP Melt</i>	166
10.1.4. <i>Sonication of pressurised PE/PVDF in the melt</i>	169
10.1.5. <i>DSC of pressurised PE/PVDF</i>	169
10.1.6 <i>DMTA Results for pressurised sonication of PE/PVDF Melts</i>	171
10.2 Section Discussion	172
11.0. Discussion & Conclusions	175
11.1 Discussion	175
11.1.1 <i>Sonochemical Polymer Solution Degradation</i>	175

	<u>Page</u>
<i>11.1.2. Compatibilisation</i>	176
<i>11.1.3. Melt Sonochemistry-Atmospheric Pressure</i>	177
<i>11.1.4. Pressurised Melt Sonocation</i>	179
<i>11.1.5. Possible Uses & Industrial Scale Up</i>	180
11.2 Conclusions	182
11.3. Further Work Arising From This Research	183
REFERENCES	184

1. SONOCHEMISTRY

Sonochemistry is the study of the effect of sound on chemical reactions, of which most work has been done using ultrasound¹⁻⁶. Sound is a waveform consisting of density variations in an elastic medium, moving away from a source. Sound is generally categorised into different regimes depending on the frequency (measured in Hz). Human hearing is effective in the range 20-16000 Hz, although we lose sensitivity to the higher frequencies as we age. From the human hearing range, the terms infrasonic, sonic and ultrasonic are defined. Infrasonic refers to sounds with frequencies below 20 Hz, sonic to sounds within the range of human hearing, and ultrasonic to sounds of frequencies above 16 kHz.

Whilst the lower limit of ultrasound is set at 16 kHz, the upper limit of ultrasound is less exact and is around 500 MHz for liquids. There are two main categories of ultrasound, these are low power (high frequency) and high power (low frequency) ultrasound. High frequency ultrasound has frequencies greater than 1 MHz and is used in sonar, many chemical applications and in medicine for non-destructive testing and diagnostics as it gives high resolution. This range of ultrasound does not generally cause chemical change to a system. Low frequency ultrasound has frequencies between 20 and 100 kHz and is of use in chemistry due to its effects on a wide range of reactions. The frequency of power ultrasound is much lower than frequencies associated with molecular vibrations, so any effect is usually due to the action of sound on the solvent in the system.

Ultrasound is also found at work in nature, in the use of echo-location⁷ by bats (30-90 kHz) and dolphins (upto 120 kHz).

1.1 Ultrasonic Waves

Ultrasonic waves^{8,9} must pass through an elastic medium in order to propagate. This causes the particles in the medium to be displaced. In liquids and gases, the waves are longitudinal. In solids the waves can be both transverse and longitudinal. For transverse waves the displacement of the particles in the medium

through which the wave travels is perpendicular to the direction of the wave. For longitudinal waves the particles are displaced parallel to the motion of the wave. In both cases the particles are only displaced locally i.e. it is the wave that travels, not the particles.

The speed of propagation, c , of an acoustic wave is given by $c = \lambda f$, where λ is the wavelength of the wave and f is the frequency. The velocity of the sound wave in a fluid, c , depends upon the density and compressibility of the medium according to:

$$c = \{ 1/(B_{ad} \rho) \}^{1/2} \quad (1)$$

where B_{ad} is the adiabatic compressibility of the medium and ρ is the density of the fluid.

As already described, acoustic waves cause the particles in a medium to vibrate, so for an individual particle the displacement, x , from rest (equilibrium) at time, t , is given by:

$$x = x_0 \sin 2\pi ft \quad (2)$$

where x_0 is the maximum displacement of a particle.

The vibrational velocity of the particle is given by the equation:

$$v = dx/dt = x_0 (2\pi f) \cos 2\pi ft = v_0 \cos 2\pi ft \quad (3)$$

where v_0 is the maximum velocity of the particle.

This displacement causes variations in the pressure of the medium as the particles are compressed and decompressed. This creates an acoustic pressure in the medium, P_A , which will vary with time, t , and is positive for compressions and negative for rarefactions. This acoustic pressure is given for any point by:

$$P_A = P_{max} \sin 2\pi ft \quad (4)$$

where P_{max} is the maximum pressure amplitude.

From this equation, the acoustic intensity, I , defined as the energy transmitted through unit area of a fluid per unit time, can be given by:

$$I = (P_{\max})^2 / 2\rho c \quad (5)$$

where ρ is density. As the sound wave propagates, the intensity is attenuated due to the transfer of energy to the surroundings. The molecules of the liquid vibrate causing viscous interactions and energy loss as heat. This attenuation is shown as:

$$I = I_0 \exp(-2\alpha d) \quad (6)$$

where α is the absorption coefficient. The value of α depends on factors such as the thermal conductivity, specific heat capacity, the density and pressure. At a constant temperature the ratio α / v^2 must also be constant so that the attenuation is larger at higher frequencies.

In a fluid, the dissipation of mechanical energy to heat results from viscosity, thermal conduction and thermal relaxation. The friction from viscous interactions as the molecule vibrates causes heating and attenuation. Ultrasonic energy is also absorbed when thermal relaxation in a polyatomic molecule occurs between the translational and the internal degrees of freedom (rotational and vibrational).

In liquids various structural relaxations can occur depending upon the molecular arrangement. Ultrasonic energy is absorbed as the molecules rearrange themselves. A good example, shown in Figure 1, is cyclohexene which exists as a conformational isomer in either of two equivalent half chair forms or a half boat form, with the half chair forms being approximately 11 kJ/mol more stable than the half boat form. For this molecule the energy from the ultrasonic wave can be absorbed to enable the conversion from the half chair form to the half boat form, attenuating the ultrasound.

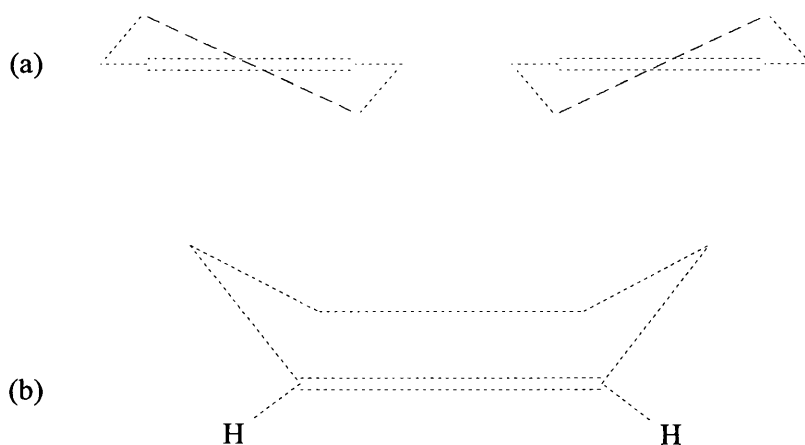


Figure 1: (a) Half chair forms and (b) half boat form of cyclohexene. Four carbons, two on either side of the double bond, are co-planar.

1.2 Cavitation

As already stated, the passage of an acoustic wave through a liquid medium causes molecular vibration. During compression the average distance between molecules is decreased, but during rarefaction the distances are increased. If a sufficiently large negative pressure occurs during the rarefaction stage, then the distance between molecules required to hold the liquid together may be exceeded, causing the formation of voids or cavities in the liquids, i.e. cavitation (figure 2).

In practice, this occurs at pressures much lower than those required to overcome the tensile strength of a liquid ¹⁰. The pressure required to overcome the tensile strength of liquids are of the order of hundreds of bar, whereas the pressure change caused by ultrasonic waves is only a few bar. The reason for the reduced pressure being able to produce cavitation is explained by the presence of small dust particles and dissolved gases which act as “weak spots” or nucleating sites for cavitation, even the fluids container walls can have an effect. These cavitation bubbles can oscillate in size as the sound waves propagate. There are also several different forms of cavities which may occur, these are empty cavities, vapour and gas filled cavities.

Cavitation bubbles may also be classified as one of two types, stable and transient cavitation.

Stable cavitation bubbles can exist for many acoustic cycles. They are thought to contain mainly gas and vapour. These bubbles may grow significantly via diffusion of gas and solvent vapour, and may also transform into a transient cavity. The collapse of these cavities is less violent than that of transient cavities due to the cushioning effect of the gas in the bubble. It was initially thought that this form of cavity played little part in chemical reactivity, although the large shear gradients around these bubbles give rise to many of the mechanical effects found during sonication.

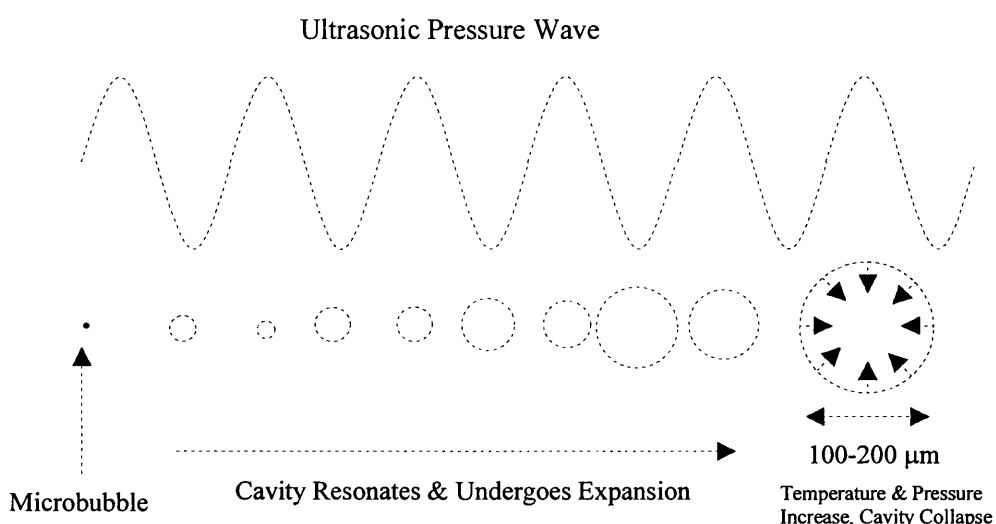


Figure 2: Ultrasonic waves form microbubbles that grow & collapse, producing high temperatures and pressures.

Transient cavitation bubbles have short lifetimes, usually existing for one acoustic cycle during which the bubble grows to a relatively large size (100-200 μm) before collapsing violently and rapidly (1-10 μs). These can break up into smaller bubbles which may nucleate further cavities. As the lifetime of these cavities is so short, it is assumed that diffusion of gases into the bubble does not occur. This means that the cavities are either empty or vapour filled. The collapse

of these bubbles is much more violent than that for stable cavitation bubbles as there is no gas cushioning them.

The pressures¹¹ and temperatures^{2,12,13,14,15} found at the site of cavitation have been calculated to be maxima of 1000-2000 bar with temperatures of 4000-6000 K. Because of the transient nature of cavitation, direct measurement of the conditions generated during bubble collapse is difficult. Suslick^{2,13,14,15} has used comparisons with the known temperature behaviour of chemical reactions to probe the conditions and found experimentally temperatures of ~5000 K. Other evidence includes that of sonoluminescence (see page 29) induced in alkanes which is the same as that arising from their combustion at high temperatures and also other reactions which normally occur at several thousand Kelvin being carried out via sonication. molecular and continuum emission spectra

Another effect of cavitation occurs when bubbles are formed near a solid surface, where collapse is no longer spherical and jets of liquid are formed which strike the surface at speeds of upto 100 ms⁻¹. This can result in the increase of mass transfer at the surface, the removal of oxides and cleaning of the surface².

1.3 Factors Affecting Cavitation

Most effects of ultrasound can be attributed to cavitation, so the effect of changes in reaction conditions can usually be related to their effect upon the process of cavitation. The main factors which affect cavitation are ultrasonic frequency, intensity, the presence of dissolved gases, the properties of the solvent and temperature.

It has been found that increasing the ultrasonic frequency decreases the likelihood of cavitation. This is explained by the bubble having less time to grow and collapse at higher frequencies¹⁶. In general, sonochemical activity rises with increasing intensity. However, an indefinite increase is limited by the material stability of the transducer, decoupling with the medium and a large number of bubbles (causing a transmission barrier).

Gases with high solubilities decrease the intensity of the cavitation and lower the cavitation threshold. The more soluble the gas, the more gas enters the

cavitation bubble therefore cushioning bubble collapse and lowering the sonochemical effects. This can be shown by the equation:

$$P_{\max} = P \left\{ \frac{P_m (\gamma - 1)}{P} \right\}^{\gamma/(\gamma - 1)} \quad (7)$$

where P is the pressure in the cavitation bubble at maximum diameter, P_m is the pressure in the liquid when the bubble collapses and γ is the ratio of the specific heats of the gas. The effects of both gas and vapour in the bubble can be represented in the above equation by replacing P with $P_v + P_g$ where P_v is the vapour pressure and P_g is the gas pressure in the bubble.

The cavitation threshold is reduced by gases with higher solubilities because they create more nucleation sites for cavity formation.

Changes in temperature affect the vapour pressure of the liquid and the surface tension. Unlike most other reactions, sonochemical reactions do not accelerate with increasing temperature. In fact most sonochemically assisted reactions proceed more efficiently at lower temperatures. This is because an increase in temperature raises the vapour pressure and lowers the surface tension, so any cavitation bubbles formed contain more vapour. This means that bubble collapse will be cushioned and hence its effects lessened.

Solvents with high densities, viscosities and surface tensions generally give a higher threshold for cavitation, but greater effects are observed upon cavitation taking place. This is because viscous liquids with high surface tensions will have greater cohesive forces which need to be overcome to create cavities. The vapour pressure of the solvent is an important factor affecting cavitation. Solvents of high volatilities cause more solvent vapour to enter the cavitation bubbles, so cushioning bubble collapse.

Increasing the applied pressure increases both the intensity of bubble collapse and the cavitation threshold. As the pressure is increased, the cavities will become smaller due to surface tension forces, thus reducing cavitation.

1.4. History of the use of Ultrasound

The field of ultrasound was established in 1880 with the discovery of the piezoelectric effect by Curie. At this time work on ultrasound was conducted using mechanical methods of generation with one of the first examples being a whistle described by Galton in 1883 (figure 3) The frequency of the sound emitted from this whistle can be adjusted by moving the plunger⁶.

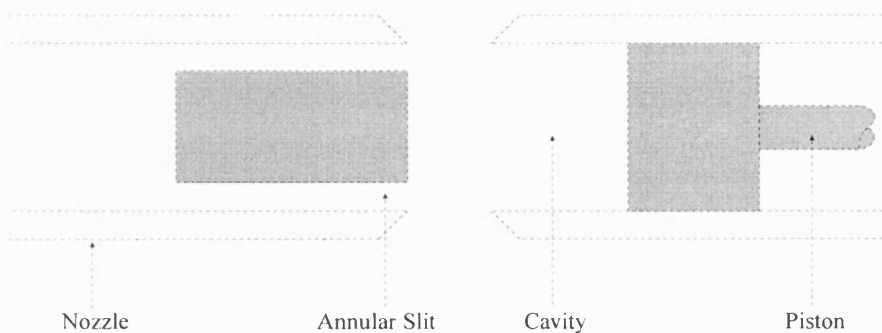


Figure 3. The Galton Whistle

Cavitation was first reported in 1895 in a report by Thornycroft and Barnaby¹⁷ when they described the results of an investigation into the poor speed of the torpedo boat destroyer, HMS Daring. It was found that a very low pressure was being developed behind the screw blades of the ship, resulting in cavities filled with air and water vapour. As well as reduced speed, a serious vibration of the stern was reported. The term "cavitation", attributed to a Mr. Froude, is also coined in the report. The problem was solved by altering the surface of the propeller, so decreasing its angular velocity and reducing the cavity formation. This discovery led to much research by the world's largest navies in understanding cavitation and bubble dynamics.

Early attempts to explain elements of bubble collapse were reported by Lord Rayleigh¹¹ in 1917 following interest from C. Parsons in cavitation behind screw propellers. The paper calculates the pressure developed during the collapse of a Spherical Cavity giving a result of 10,300 atmospheres or 68 tons per square inch.

The first actual application of ultrasonics in a fluid medium is attributed to Paul Langevin who became the first person to transmit sound waves in sea water. It has been suggested that he was encouraged to do this by a competition, started in 1912 following the Titanic disaster, to find a method of detecting icebergs. However, the first real commercial application of ultrasound was in detecting submarines, as a result of World War I. Electromagnetic waves were found to be ineffective in sea water, prompting research into acoustic waves. Langevin created the first underwater transducer which relied upon the piezoelectric effect in quartz crystals. The device was also used in depth measurement¹⁸.

Sonochemistry started making an appearance in 1927 when Loomis^{19,20} published two papers, "The Physical and Biological Effects of High Frequency Sound-Waves of Great Intensity" and "The Chemical Effects of High Frequency Sound Waves". In the first paper there are early descriptions of the effects of ultrasound on solids and liquids, and the formation of fogs and emulsions. They also described some biological effects, such as the rapid destruction of red blood cells, and the fatal effect on frogs and fish, although mice survived a 20 minute exposure! In the second of the two papers the research is more concentrated on chemistry with reports on the effects of ultrasound on metastable compounds such as nitrogen tri-iodide which exploded under sufficiently intense ultrasound! Also listed was the colour change of yellow mercuric iodide to red below 120⁰, the explosive discharge of superheated liquids (e.g. carbon tetrachloride), ultrasonic heating, degassing of liquids and the acceleration of chemical reactions such as the iodine "clock" reaction.

In 1933 whilst studying the bactericidal effects of intense audible sound, Flosdorf and Chambers²¹ discovered a variety of interesting chemical reactions. Egg albumin solutions at 30⁰C were found to coagulate almost immediately and sucrose in neutral solutions was hydrolysed to glucose approximately twice as fast at 5⁰C as it is ordinarily at the boiling point. Also, inorganic halides were found to oxidise to free halogen and the study was the first to report that the hydrolysis of esters is accelerated.

Also in 1933 Szent-Györgyi²² found that ultrasound depolymerised cane sugar and also highly polymerised substances such as starch and gum arabic. He

also found that irradiation of simpler compounds was not effective. The paper is ended with the statement, "It is hoped that ultrasonic radiation might contribute to the knowledge of the highly polymerised state and to the meaning of molecular weight of highly polymerised substances". Unfortunately his work was broken off due to lack of funds.

In 1935 Schultes and Frentzel ²³ reported the emission of light by ultrasonically irradiated water. From this it was proposed that sudden cavitation produces charge separation similar to that seen in lightning flashes. This theory was generally accepted at the time, but has since been superseded. The first patent ²⁴ utilising sonochemistry was in 1938 which claimed that the depolymerisation of solid, liquid, or gaseous hydrocarbons could be achieved at lower temperatures when subjected to ultrasonic waves.

Up until World War II quartz crystals along with magnetostrictive transducers were the main sources of ultrasound. During World War II extensive studies were made on new piezoelectric materials and in 1945 a major advance was made in the discovery of ceramic ferroelectrics. This resulted in much more ultrasonic research, due to the availability of reliable and reproducible ultrasonic sources.

During the 1950's Noltingk and Neppiras ^{25,26,27} worked on the theoretical aspects of ultrasound attempting to develop equations to describe the motion of a gas filled cavitation bubble in a liquid medium subjected to alternating pressure. This was later refined to also give the theoretical conditions for the appearance of cavitation. A lot of this work was an extension of Lord Rayleigh's treatment of cavitation in 1917, introducing alternating pressure rather than constant pressure. Noltingk and Neppiras also put forward the 'hot-spot' theory. Also during this period Griffing ^{28,29,30} realised that different dissolved gases can have an effect upon ultrasonic reactions and set about testing many gases.

As can be seen, sonochemistry has attracted interest for many years, although it was not until the 1980's that the subject became the focus of intense research.

1.4 Generation Of Ultrasound

1.5.1. The Piezoelectric Effect

Ultrasound generation was developed as early as 1880 when the piezoelectric effect was discovered by the Curies. But it is only since 1945 with the advances in electronic circuitry and transducer designs that ultrasonic equipment, particularly for power ultrasound, has become available. The most common method of generating ultrasound is by means of the piezoelectric effect of crystals such as quartz and ceramics such as lead zirconate titanate and barium titanate. The piezoelectric effect is the production of charges on the faces of a crystal as a result of applied pressure. The opposite of this effect, that is applying electrical charge to the crystal faces, to force the crystal to expand and contract is used to produce ultrasound.

1.5.2. Equipment For Power Ultrasound

There are two basic methods for applying ultrasound to a reaction or process³¹. One is a low intensity system, this is an ultrasonic cleaning bath, which is basically a liquid-filled tank which has multiple transducers fixed to its base and walls (see figure 4a). The other method is to use a probe system (see figure 4b). For both systems most commercial companies manufacture devices which operate at 20-50 kHz.

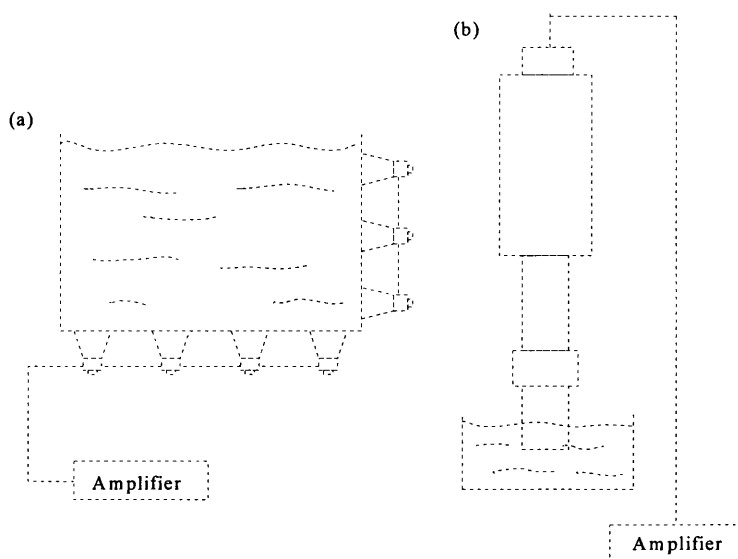


Figure 4.(a) Ultrasonic Bath and (b) Horn Systems.

The ultrasonic bath is the most accessible and simpler of the two. However this system does have limitations. These are:

- 1) Temperature control is a problem as the bath warms up during use. Addition of ice can help, but this will alter the power transmitted to the reaction vessel.
- 2) The efficiency and overall power generated by the bath depends upon the size and where the reaction vessel is positioned.
- 3) Comparison of results is difficult as ultrasonic baths do not all operate at the same frequency.

The sonic horn system is generally preferred in research as it is possible to achieve greater vibrational amplitudes, greater energy densities and there is a greater degree of control on the energy density in a test sample. However, prolonged use results in erosion of the probe tip which can cause contamination of the reaction mixture with metallic particles. Also, horn systems can only operate at one frequency.

Nearly all transducers used in ultrasonic systems are based upon the prestressed piezoelectric design. In these, a number of piezoelectric elements (usually 2-4) are bolted between a pair of metal end masses. In a typical transducer, two piezo elements are positioned near to a point of maximum stress in a half wave assembly. The assembly is then clamped together with a high tensile bolt which causes the ceramics to be in compression at maximum transducer displacement (Figure 5).

The vibrating motion generated by the transducer is usually too low for practical use and so it is necessary to magnify it. This is the function of the horn. These are usually half a wavelength long, although they can be designed in multiples of half a wavelength.

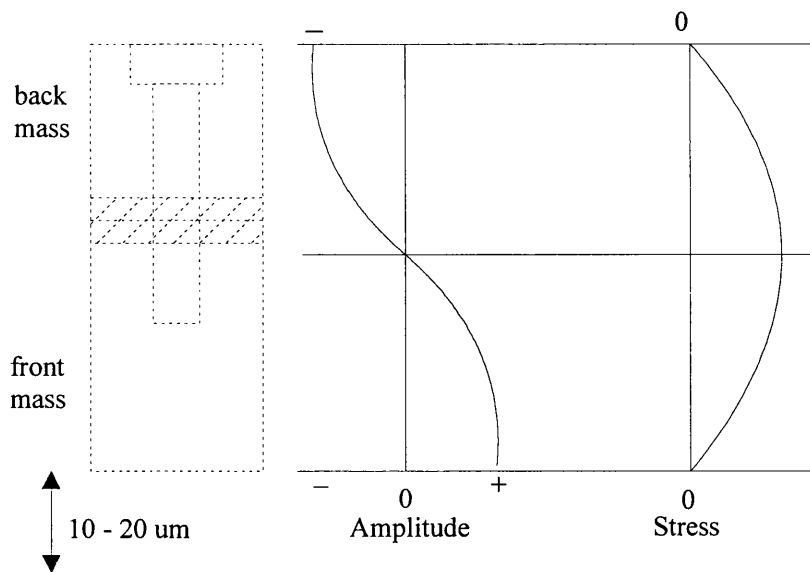


Figure 5. Typical Transducer Construction

The best materials for horn construction are titanium alloys, as they have high dynamic fatigue strength, low acoustic loss, resistance to cavitation erosion and chemical inertness.

The intensity of the ultrasound delivered by a horn system can be altered by either altering the power input or changing the size of the tip. A modification of the reaction vessel, such as the Rosett cell (Figure 6a) allows the reaction to be mixed and cooled by the propulsion of the liquid around the tubes. Another modification, a slight indentation at the base of the reaction vessel can allow mixing by dispersing the sonic waves as they are reflected from the base (Figure 6b).

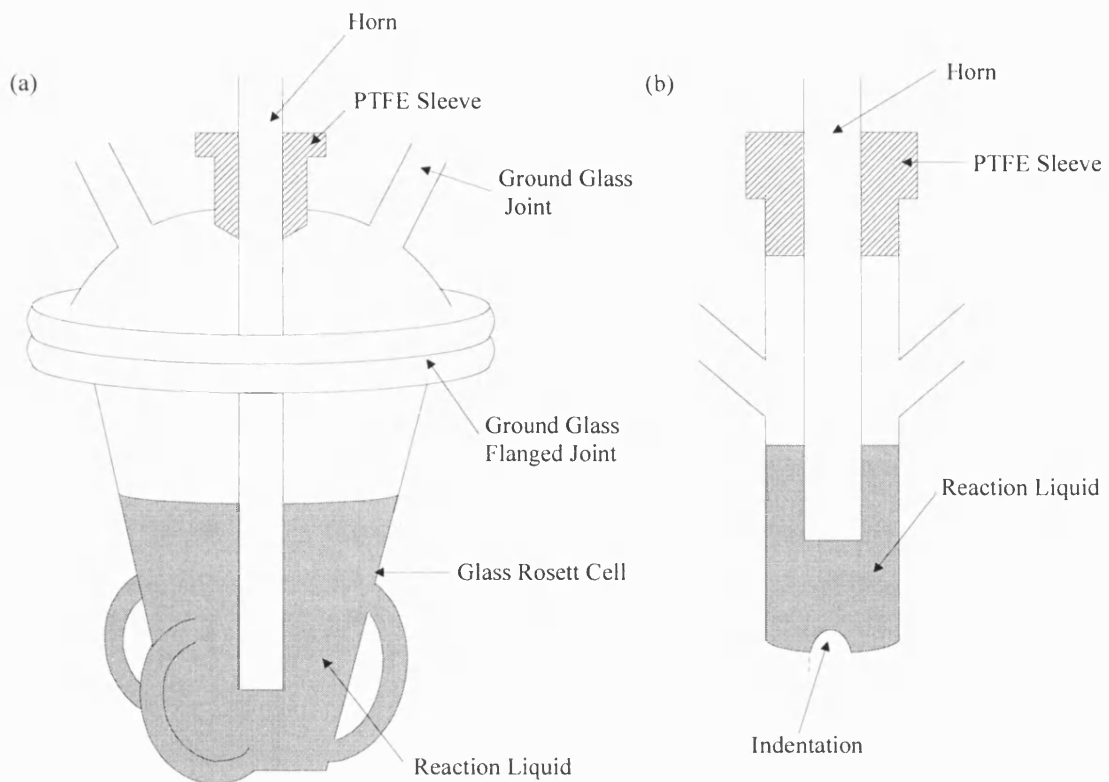


Figure 6. (a) Rosett Cell and (b) Indented Reaction Vessel.

1.6. Industrial Applications of Ultrasound

Ultrasound is used in many areas of industry and medicine. Examples of these uses are:

1.6.1 Ultrasonic Welding

This is used in industry for the welding or riveting of plastic mouldings for the consumer market. An ultrasonic welder consists of a generator producing an alternating frequency of around 20 kHz which supplies a transducer which converts the electrical energy into mechanical energy. A shaped horn transmits the vibrations (typically 50-100 μm in amplitude) to a shaped die pushing the two pieces to be welded together.

Ultrasonic welding is usually used on rigid amorphous thermoplastics. This is because they are most suitable for welding as the ultrasonic vibrations can

travel through the bulk plastic of the component to reach the joint. More flexible and crystalline polymers rapidly absorb (attenuate) the ultrasound as it passes through the material, so this type of plastic is generally only welded in thin films. It is important that the vibrational energy is transmitted only to the joint and not the body of the material, as any warming of the bulk material can lead to the release of internal moulding stresses and so produce distortion.

Thermoplastics have two major advantages which make them ideal for ultrasonic welding. These are their low thermal conductivities and melting / softening temperatures of between 100 and 200⁰C. Due to the low thermal conductivity of thermoplastics as soon as the ultrasonic power is switched off the substrate becomes a heat sink, giving rapid cooling of the newly formed joint. A major advantage of ultrasonic welding is that it gives high joint strengths, reaching 90-98% of the original material strength. Examples of the use of ultrasonic welding include welding the hinge of spectacles to the plastic frame, the rear reflector cluster on cars usually has its lens welded into place and the brass screw in a 13 amp plug is normally welded into place.

For polymer pairs which are incompatible, however, the success of direct welding is limited. This is solved by using ultrasonic welding to melt studs of polymer that are moulded into one of the parts and which protrude from holes in the other part (a process called staking). This process has the disadvantages of the stresses being concentrated at the studs and that bond lines are often visible because staking tends to create sink marks on the reverse side of the part.

Ultrasonic welding is not just restricted to plastics, metals may also be welded. For this the ultrasonic motion must be lateral rather than vertical so that frictional heating is induced between the two surfaces to be welded. An application of this is in the welding of aluminium, which is difficult by normal methods due to the presence of an oxide layer around the metal. With ultrasonic welding the oxide layer is easily broken up and absorbed within the metal surrounding the weld.

1.6.2. Ultrasonic Cleaning

Another major application of ultrasound is in ultrasonic cleaning. Commercial ultrasonic cleaners operate at a frequency range of 20-60 kHz and with a power of 25-2500W. They are usually stainless steel tanks with a capacity of 2-200 l, although much larger cleaning "baths" can be made for special purposes. Ultrasonic cleaning can be used for both delicate and large items. For example microcomponents for computers can be cleaned, other examples include engine blocks, jewellery and medical instruments. Practically all materials which are sound reflective can be cleaned (e.g. metal, glass, ceramics) sound absorbing materials such as rubber are cleaned less efficiently.

One of the more publicised uses of ultrasonic cleaning was in the cleaning of the huge amount of artefacts (some 17000 or so) recovered from the wreck of the Mary Rose. Normally each item would have to have been individually soaked and rinsed. Instead a specially constructed ultrasonic cleaning bath was used. This also solved another major problem in cleaning the items. This is the removal of iron deposits from organic materials, which can lead to deterioration, as the iron can stain and prevent penetration of preservative. Ultrasonic cleaning is very effective at removing these deposits and can also be used to improve preservative penetration.

The ultrasonic cleaning effect is caused by cavitation effects such as microjets, shock waves, temperature and pressure. In addition to the ultrasonic effects, external heating may be applied, also detergents, solvents and pH control may be used. The advantages of this technique are that complex items (e.g. surgical equipment) containing irregular shapes, crevices and inner surfaces may be easily cleaned; less solvent may be needed and it is easy to scale up.

1.6.3. Engineering Applications

Engineering uses include ultrasonic machining, abrasive jet machining, drilling and cutting and metal tube drawing. Ultrasonic machining was developed due to the increasing use of hard, brittle materials and the need to machine them accurately. Examples of its use are in the machining of carbides, stainless steel,

ceramics and glass. The process consists of a cutting tool operating at around 20 kHz in an abrasive slurry (usually containing silicon carbide, boron carbide or alumina).

Abrasive jet machining is used to cut hard, brittle materials (germanium, silicon, mica, glass and ceramics) in a wide variety of cutting, deburring and cleaning operations. This process is somewhat like sand blasting, except that the abrasive is much finer with a much more controlled cutting action. Ultrasonic drilling and cutting is used by the aerospace industry for the drilling of carbide tungsten blades and the cutting of complex carbon fibre shapes out of fibre sheets. Another use is in the production of three dimensional engraved glass which can easily be produced by a shaped ultrasonic tool.

Improvements in the cold drawing of metal tubing has been accomplished when the die to be used is subjected to radial ultrasonic vibrations of 20 kHz. This technique has been applied to stainless steel and gives much larger reductions in size per pass, greatly reduced draw pressures and a better finish than that obtained using conventional methods.

1.6.4. Chemical Engineering Applications

Uses of ultrasound in chemical engineering include solid dispersion, filtration, crystallisation and degassing of liquids. Agglomerates of solid particles can be broken down and dispersed in liquids using power ultrasound. An example of this is in the use of an ultrasonic homogeniser which is used to prepare plastic resins.

Filtration can be assisted by the application of ultrasound. Sonication in the region of the filter reduces the occurrence of clogging which is a common problem and also increases filtration rates. In the process of crystallisation, ultrasound, when applied to a saturated solution, has the effect of producing smaller and more uniform crystals than obtained from conventional methods. This is thought to be due to the larger number of nucleation sites created by cavitation and the formation of more seeds as solid agglomerates are sonically dispersed.

The degassing of liquids is achieved rapidly upon application of ultrasound. This has potential for use in the soft drinks and beer industries. For

example ultrasound could be used to speed up the filling of bottles on a production line by eliminating the initial froth as the fizzy liquid is poured in.

1.6.5. Medical Uses

Ultrasound is used widely in medicine^{32,33} for diagnostic purposes. Low power (milliwatts), high frequency ultrasound is used to provide a non invasive technique for scanning the human body. One of the better known uses is in foetal imaging. Also it is used for the continuous and non-hazardous visualising of the position of needles and surgical instruments as they are used within the body. In the medical use of ultrasound, high frequency acoustic pulses are propagated in straight lines and scattered as they encounter various boundaries within tissues. Reflected pulses are detected at the skin surface. The lapse of time between launching and receiving the returned pulse is proportional to the depth of the reflecting tissue. Signals also vary in strength, or amplitude, depending on the features of the reflecting structures.

There have, however, always been concerns about the potentially damaging effects that might be induced by ultrasound, particularly for foetal imaging. Fortunately, ultrasonic imaging has been proved to be amongst the safest diagnostic tools used in modern medicine. Although it must be noted that when used at sufficiently high intensities, high frequency ultrasound can induce high temperatures and mechanical activity in human tissue. This gives it the potential to treat various medical conditions.

Thermal effects are caused by part of the ultrasonic energy being absorbed by the tissue and converted to heat. Ultrasound will kill all types of tissue within a few seconds if temperatures of 60-70⁰C are achieved. If the amplitude is sufficiently high cavitation is observed. Cavitation often leads to blood vessel damage, which is undesirable, also the formation of bubbles can reflect the ultrasonic waves back to the transducer. The reflected sound creates a heated zone at the focus of the transducer, producing an area of dead tissue called a lesion where it was not intended.

The first ultrasonic surgery performed on a large number of patients was to treat glaucoma, in which the pressure inside the eye increases, damaging the optic

nerve. However, laser treatment is now used in preference due to its ease of use. Focused high-intensity ultrasound is now commonly used to treat benign prostatic hyperplasia and it is also believed that ultrasound may be of use in the treatment of prostate cancer.

High-intensity ultrasound is also used in the destruction of kidney stones. This treatment relies upon the mechanical break up of the stones by single pulse shock waves, causing cavitation, into particles small enough to be excreted normally. This process, which is rapid and non-invasive, replaces the need for surgery. Power ultrasound is used in the treatment of sporting injuries, particularly strains and tennis elbow.

Small ultrasonic probes are used in dentistry which operate at 25 kHz. Attachments allow them to be used for cleaning and polishing teeth, drilling and root canal work. For cleaning the dentist will use a vibrating tip which is used to sonicate a fine spray of air, water and sodium carbonate. This spray when projected against the tooth surface has been found to have a cleaning / polishing effect which is also much less abrasive than the technique it replaced, which is grinding with pumice stone. The same implement can be used, with a selection of hook shaped tools, for descaling of the teeth. If a straight diamond tip is used in conjunction with an abrasive slurry then it can be used for drilling.

1.7. Research In Ultrasound

Much work has been carried out on ultrasound in chemistry, especially over the last twenty years or so, with the topics ranging from the basic understanding of the processes involved in sonication to the application of ultrasound for significantly increasing reaction rates.

1.7.1. Basic Understanding

Prominent researchers in this field include Margulis and Suslick. Such research centres on the phenomenon of cavitation. Noltingk and Neppiras^{25,26,27} put forward the 'Hot Spot' theory which suggests that hot spots are formed upon the collapse of cavitation bubbles. Suslick^{2,13,14,15} experimentally found these hot

spots to have temperatures of ~ 5000 K, pressures of ~ 1800 atm, and cooling rates in excess of 10^{10} Ks⁻¹. Suslick's research has since moved on to use these extreme conditions to form nanostructured metals, alloys and carbides¹⁶.

However, Margulis^{34,35} insists that the hot spot theory is inadequate, and has put forward his own 'electrical theory'. In this he states that the hot spot theory cannot explain many experimental dependencies of rates of sonochemical reactions and sonoluminescence flux in terms of the temperature of a liquid (near the boiling point), the hydrostatic pressure, the amplitude of sound pressure or the viscosity of liquid (especially high viscosity). The electrical theory attempts to explain this. This theory concerns the dipole distribution in a solvent around a cavitation bubble. It has been shown that during sonication large electrical fields of 10^{11} Vm⁻¹ are generated which are large enough to cause chemical bonds to break and therefore cause chemical activity. The major difference being that for the hot spot theory the initial major thermal effects in the collapsing cavitation bubble are the molecule-molecule shocks. For the electrical theory there are electron-molecule shocks. This, in principle, is the most important difference and leads to explanations to the areas which the hot-spot theory fails to cover.

1.7.2. Single Bubble Sonoluminescence

Sonoluminescence^{36,37,38,39} is the transformation of sound (ultrasound) into light by the non-linear pulsations of a gas bubble trapped in a fluid. In 1990 Gaitan and Crum⁴⁰ showed that a single air bubble can levitate in a standing acoustic wave set-up in sufficiently degassed water until light is emitted when the acoustic stress is increased. Much research is now being carried out into this phenomenon. Once a bubble has been placed in a sound field, the successive rarefactions and compressions cause it to pulsate rapidly. During rarefaction the bubble expands, with the following compression phase causing the bubble to collapse. The collapse reaches supersonic speed and is stopped only when the gas contained within the bubble is compressed to its van der Waals radius. At this moment a flash of light is emitted, "sonoluminescence".

These light pulses are on a very short time scale (less than 50 picoseconds), typically containing 10^5 - 10^7 photons emitted uniformly in all

directions. The time scale is such that sonoluminescence is the only way to produce such short flashes of light without using a laser. The peculiar properties of sonoluminescence have led to much debate on the nature of cavitation collapse. Especially as the generally accepted hot-spot theory fails to explain single bubble sonoluminescence.

1.7.3. Ultrasound in Heterogeneous Systems

The use of ultrasound to enhance the reactivity of metals in heterogeneous systems ^{1,41,42,43} leading to the improved preparation of a wide variety of substances, as well as the synthesis of novel compounds, is increasingly widespread. Rate enhancements of more than tenfold are common, yields are improved and by-products avoided. These ultrasonically assisted reactions are now common, especially for those involving reactive metals such as Mg, Li, and Zn. Good examples of these reactions include the Barbier reaction investigated by Luche ⁴⁴.

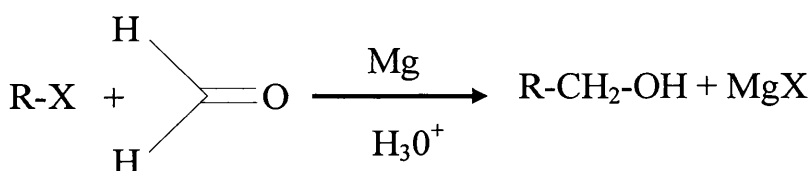


Figure 7. Barbier Reaction

In this reaction alkyl halides, carbonyl compounds and magnesium react in a one step process to produce an alcohol (figure 7). The reaction proceeds only if the alkyl halides possess good leaving groups. If lithium is used rather than magnesium the reaction proceeds faster and less reactive alkyl halides may be used. With lithium and ultrasound the Barbier reaction is improved considerably, side reactions are minimised and even benzyl and allyl halides, which usually lead to Wurtz-coupling, give good yields. With the sonicated reaction the rate increases as the temperature decreases. As described earlier this is because increased temperature increases the vapour pressure, so cushioning cavitation collapse. However, with this reaction it has been found that when the temperature

falls below a certain point the opposite effect is observed, which is that the rate of reaction decreases with decreasing temperature. This is thought to be due to the increased viscosity of the solvent at lower temperatures, which will decrease the intensity of bubble collapse. The Barbier reaction, like any reaction that involves the production of organolithium agents, proceeds only if the metal surface contains defects, where the lithium atoms are exposed, so making it possible for single electron transfers to individual carbon-halogen bonds in the organic halides. Sonication of the reaction accelerates the formation of these defects, and therefore increases the amount of radical anions, which increases the rate of reaction.

Ultrasound also influences the Reformatsky reaction in which a β -hydroxyester is synthesised by reacting a α -haloester with metallic zinc and a carbonyl compound. The haloester and zinc form an ester enolate, which reacts with the carbonyl to give the β -hydroxyester (figure 8).

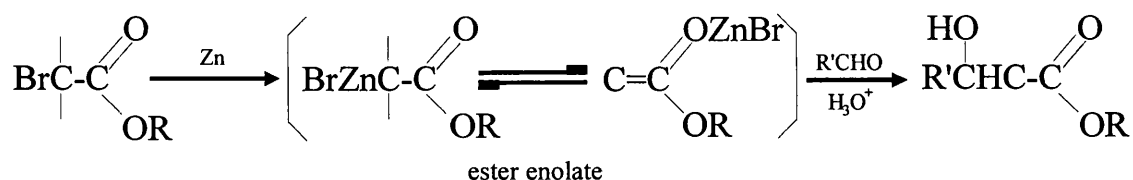


Figure 8. Reformatsky Reaction and Formation of Enolate

The Reformatsky reaction between trifluoroacetaldehyde and ethyl-2-bromopropionate was examined by Kitazume⁴⁵ and co-workers. The geometry of the starting enolate determines which stereoisomer is formed (figure 8). The (*Z*) enolate gives the syn isomer and the (*E*) enolate gives the anti isomer. The transition state for the (*E*) isomer has a lower energy than that of the (*Z*) isomer. Under normal conditions the products are racemic, which means that the reaction is under both thermodynamic and kinetic control. The application of ultrasound alters this result, favouring the production of anti isomer (73% anti, 27% syn). This means that the reaction is influenced more by kinetic factors when sonicated.

This observation may lead to the development of stereoselective preparations of β -hydroxyesters.

Also it has been demonstrated that ultrasound switches the main pathway from aromatic electrophilic to aliphatic nucleophilic substitution in the reaction between benzyl bromide, toluene, potassium cyanide and alumina (figure 9).

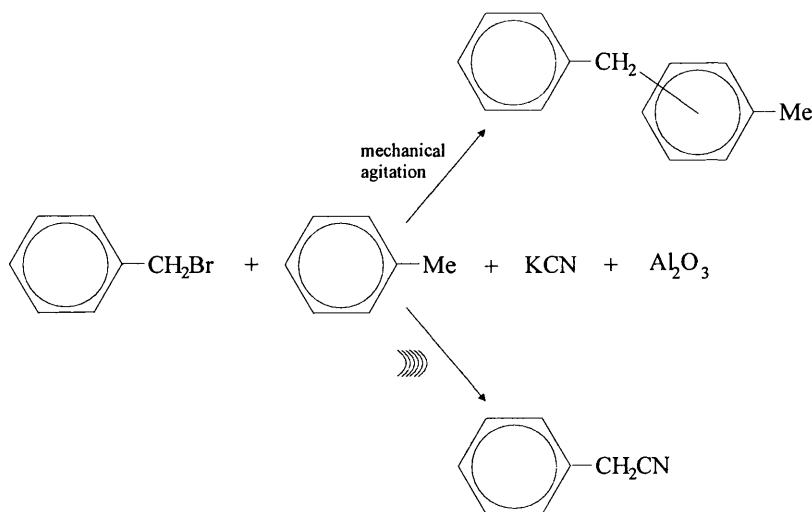


Figure 9. Sonochemical Switching

In the non-sonicated reaction, alumina catalyses the Friedel-Crafts substitution between benzyl bromide and toluene with a yield of 75%. But when the system is sonicated, the S_N2 reaction between benzyl bromide and KCN predominates and gives a 71% product yield. It is thought that increases the interaction between KCN and alumina, resulting in the neutralising of the acid sites on the alumina. The basic sites on alumina then catalyse the slow reaction between benzyl bromide and KCN.

Koenig⁴⁶ and co-workers have demonstrated that the formation of the diphosphine is accelerated under ultrasonic irradiation (Figure 10). The yield of the silent reaction (with stirring) is 22% at 20⁰C. The yield of the sonochemical reaction is 65% at 5⁰C.

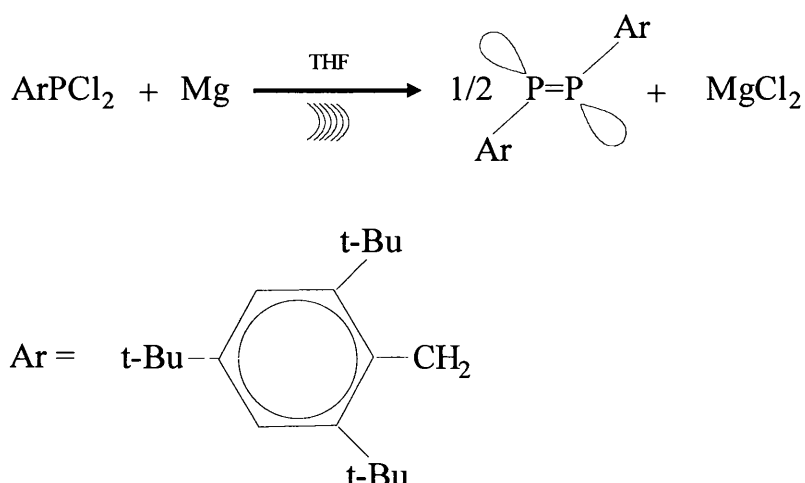


Figure 10. Formation Of Diphosphine

Also the reaction yield decreases with temperature for the silent reaction whereas it increases until it reaches an optimum at 5⁰C for the ultrasonically assisted reaction.

Carboxylic ester groups can be reduced to alcohol groups by zinc borohydride under ultrasonic irradiation. This reaction does not proceed without ultrasound. Also the reaction is selective towards aliphatic ester groups while aromatic groups are not affected. The addition of an electron transfer agent, N,N-dimethylaniline, to the mixture enhances the reaction to the point where even the aromatic compounds are reduced by zinc borohydride.

Alkenes may be synthesised by the dehydrohalogenation of properly substituted acetyl halides or by the dehalogenation of α -haloacetyl halides, but it is difficult to obtain a good yield of ketenes which are substituted with bulky groups. The use of ultrasound gives yields between 86 and 90% compared to the usual less than 10% yields.

1.7.4. Decomposition of Metal Carbonyls

Suslick et al ^{14,16,42} have prepared stable ferromagnetic colloids using high intensity ultrasound to decompose volatile organometallic compounds. The colloids formed are superparamagnetic. Colloids of ferromagnetic materials are of special interest due to their many important technological applications as ferrofluids. Ferrofluids find uses in information storage media, audio

reproduction, magnetic refrigeration and magnetic sealing. Commercial magnetic fluids are produced by extensive milling of magnetite (Fe_3O_4) in ball mills for several weeks in the presence of surfactants producing a very broad particle distribution. Whereas the colloids formed using ultrasound have narrow size distributions and are synthesised much easier.

Using sonoluminescence as a spectroscopic probe of iron pentacarbonyl decomposition, Suslick estimated temperatures of >5000 K and pressures of approximately 1700 atm for the hotspot at cavitation during a period of less than 100ns.

1.7.5. Sonication of metals

During sonication of metals or solids, microjets and shock waves resulting from cavitation collapse impinge upon the surface causing surface cleaning, particle size reduction, inter-particle collisions, defects and erosion. Sonication of soft metals with hard oxides causes the metal to change shape damaging the oxide layer e.g. Al, Li, Na. For hard metals the surface is not plastically deformed, but the surface is still activated by cavitation effects due to the low cohesion of the oxide layer. Very small particles can collide, causing agglomeration and even fusion due to the extreme temperatures encountered.

A well investigated area is the sonication of ordinary commercial Nickel^{42,43} to obtain highly active metal powder. Irradiation with ultrasound can increase the catalytic activity dramatically, even reaching that of Raney Nickel. After ultrasonic irradiation, changes in the surface morphology have been observed. The surface is smoothed by removal of crystallites and the oxide layer is not present. For mixtures of metals molten 'necks' can be observed between two different metal particles. Suslick⁴⁷ found that for iron and tin the 'neck' is an alloy of the two metals, suggesting that the collision possessed enough energy to melt the metals.

1.7.6. Ultrasonic degradation of water contaminants

There are several mechanisms by which pollutants in water may be degraded. Any compounds entering cavitation bubbles would be destroyed by the

harsh conditions found there, in the vicinity of bubbles the compounds will react with radicals formed whilst others may be oxidised by the peroxide formed as a result of H₂O sonication. Amongst the pollutants receiving most attention are chlorinated hydrocarbons, in particular polychlorinated biphenyls (PCBs), perchloroethylene and carbon tetrachloride. These chemicals have been shown to be toxic and present in the environment, having been detected in waterways, wildlife, and soil.

Luche et al ⁴⁸ have worked on the degradation of pentachlorophenolate (PCP) showing that sonication cleaves the carbon-chlorine bond and, when the solution is air-saturated, mineralisation of the PCP to CO₂. The PCP disappearance was also marked by a decrease in toxicity of the water to a strain of green algae. Price et al ⁴⁹, have investigated the effect of ultrasound upon a range of aromatic compounds including chlorobenzene and dichlorobenzene showing that the compounds were degraded and consumed after approximately 45 minutes at 39 Wcm⁻². Greater than 99% destruction rates for carbon tetrachloride have been reported by Huang ⁵⁰. Johnston and Hocking⁵¹ have combined ultrasonics with photocatalytic waste treatment to destroy contaminants. It was found that ultrasound also improved the efficiency of the photocatalytic process as well as destroying pollutants.

2.0. ULTRASOUND AND POLYMERS

2.1. Polymer Degradation

When a high molecular weight polymer in solution is subjected to sonication the basic effect is a reduction in molecular weight (fig 11). This effect is one of the main principles underlying this project. This reduction in molecular weight, or degradation, is non-random and the breakage of the polymer chains occurs statistically near the middle of the chain. The degradation effects can be used to modify polymers in a number of ways. First, the molecular weight dependence means that the higher molecular weight chains are, generally, removed faster giving narrower more uniform molecular weight distributions.

This can improve both the processing parameters and the material and physical properties of the final polymer.

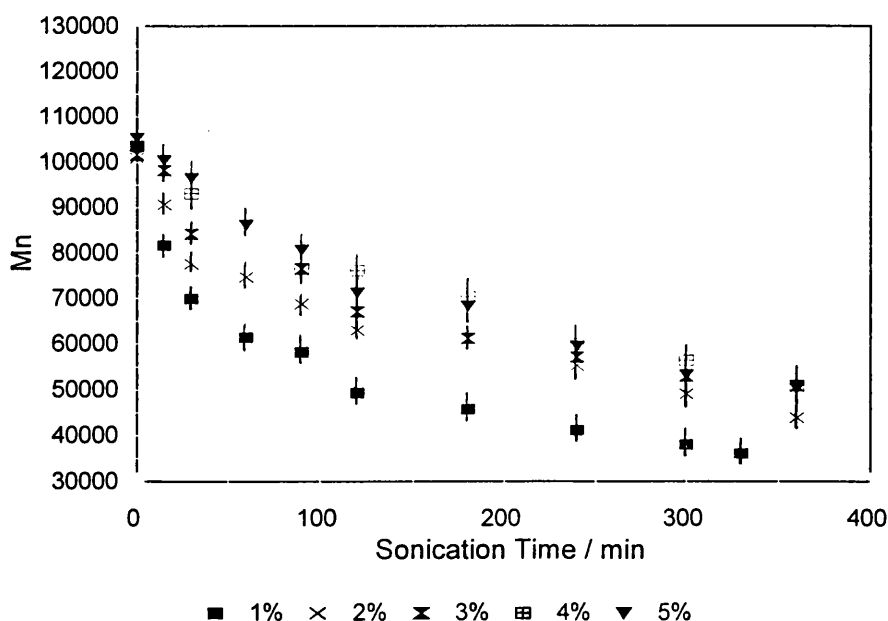


Figure 11. Example Of Ultrasonic Degradation: Plot Of Mn (Number Average Molecular Weight) vs Sonication Time For 1 to 5 % Polystyrene in Toluene, 10 Watts, 25⁰C. *Source: Author's Research*

2.1.1. Mechanism of degradation

A number of mechanisms have been suggested to account for the degradation, and a large amount of evidence point to effects accompanying cavitation. No depolymerisation occurs in solutions that have been degassed to prevent cavitation or when sonicated at intensities below those required to produce sonication. Oxidative fission was ruled out as being responsible by working in an atmosphere of nitrogen and obtaining the same rate of breakdown as that found under air.

However, the actual effect of cavitation which causes this to occur is subject to debate. Possibilities have included: 1) thermal effects at collapsing bubbles, 2) hydrodynamic forces due to shock waves generated by bubble collapse i.e. transient cavitation, 3) shear stresses at resonating bubbles i.e. stable cavitation.

The first of these has been discounted due to the observed absence of monomer even after very long sonication times, which is the usual product of thermal degradation. Direct thermal degradation by the temperatures found at cavitation collapse seems to play only a small part, as this process would be random, unlike the non-random scission found via ultrasound.

a) Shock wave degradation

Cavitation collapse is thought to create large hydrodynamic pressures and velocity gradients in the surrounding liquid. This produces intense field flows of solvent molecules towards the implosion site, which will carry some polymer chains along with it leading to large stresses within the polymer molecule capable of breaking a C-C bond. A relatively simple model was put forward by Thomas⁵² in which the end of the polymer chain nearest the collapsing bubble moves faster than the side oriented away, elongating the chain until the stresses become too large and the polymer molecule cleaves. The mathematical development showed that the stresses would be greatest at the centre of the chain with a linear dependence of the degradation rate on the molecular weight. Assumptions of this model included that the polymer was essentially a string of beads and that the

concentration of the polymer in solution was so low as to discount the possibility of chain entanglement or overlap.

A further development of this theory was proposed by Okuyama and Hirose⁵³ who suggested that the stress forces only acted on areas of the chain, extending and stretching them whilst the remainder of the molecule remains relatively undisturbed (see figure 12 below). This model gave an expression for the limiting degree of polymerisation after infinite sonication time with calculations for both stable and transient cavitation. From this it was calculated that the limiting degree of polymerisation for a stable cavity was far greater than experimental predictions, whereas for transient cavities the results were in agreement. As such it was concluded that the degradation occurred about transient cavities.

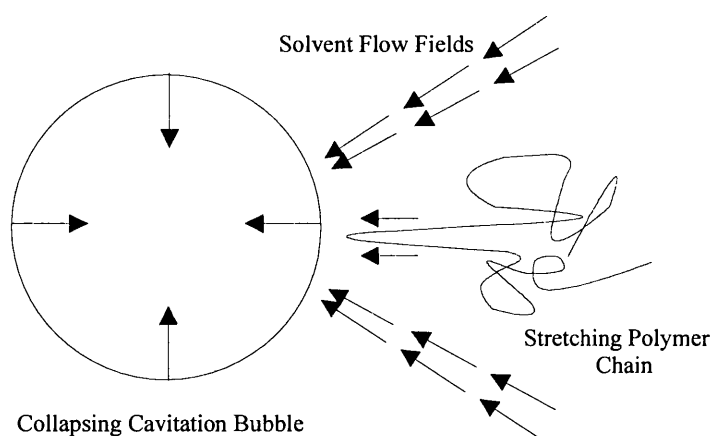


Figure 12. Diagram showing part of a polymer chain stretching out due to solvent flow towards a collapsing bubble (from ref 68).

A further hydrodynamic effect caused by cavitation is the large shock wave created at the end of cavitation collapse. It was suggested by Gooberman⁵⁴ that shock waves travel outwards from the implosion site rapidly crossing the polymer chain and creating large stresses in the molecule. These stresses would be greatest at the centre of the chain, although due to the large number of possible conformations not all chains will break in the middle. This treatment predicted the effect of ultrasonic intensity on limiting molecular weight in agreement with

experiments, with calculated stresses of the order capable of causing chain cleavage.

b) Shear Degradation

It is well known that polymer degradation can occur when polymer solutions are subjected to hydrodynamic shear such as being forced through a narrow capillary or being rapidly stirred⁵⁵. The processes involved have proved difficult to quantify, but nevertheless attempts have been made.

Harrington and Zimm⁵⁶ showed that the critical stress was different in various solvents. They degraded polystyrene in various solvents reporting ranges of results for thermodynamically 'good' to 'poor' solvents. The shear stresses created by cavitation are thought to arise from the movement of solvent molecules around resonating bubbles. In order to investigate this process, Hughes and Nyborg⁵⁷ designed apparatus to simulate resonating bubbles without causing cavitation collapse, through the use of a needle vibrating at very high frequencies but at low power. A variety of suspensions of bacteria and erythrocytes were subjected to this treatment. In each case the cell wall/membranes were broken releasing the contents. Shearing effects produced in the eddy currents around the needle tip were given as the most likely explanation for these results.

From this, it appears that shear stresses are capable of causing polymer degradation without the presence of cavitation collapse. Although there is no clear agreement as to which of the effects best explains the experimental observations, the generally accepted proposal is that a combination of the above causes the degradation.

The degradative^{34,58-65} effects of ultrasound are more efficient for higher molecular weight polymers. There is also a limiting value of molecular weight below which degradation is not apparent. This would support the above theories, as longer polymer chains would break more easily than short chains.

2.1.2 Factors affecting ultrasonic degradation

There are various experimental conditions, which affect ultrasonic degradation, these include temperature, solvent concentration, solvent properties, dissolved gases and ultrasound intensity (see Below).

- External Temperature - Bubble collapse is less violent with increasing temperature as solvent vapour pressure is increased, causing more vapour to enter the cavitation bubble which cushions its collapse. This reduces the forces in the liquid and so decreases degradation.
- Frequency - An optimum frequency⁶⁶ at which cavitation intensity, and therefore degradation, attains a maximum past which degradation decreases with increasing frequency.
- Dissolved Gas - Increasing amounts of dissolved gas lower the intensity of shock waves from cavitation as the gases can enter the cavitation bubble and cushion its collapse.
- Intensity - Increasing intensity increases the rate and extent of degradation, although there is an upper limit due to transducer thresholds, decoupling with the medium and large numbers of bubbles acting as sound barriers.
- Solvent - For solvents with low surface tensions and viscosities cavitation occurs more readily. Also the higher the vapour pressure, the

less violent is the bubble collapse and so the degradative effect is less.

- Molecular Mass
- For larger initial molecular mass polymers the degree of degradation and the rate is greater. Also there is a threshold value under which there is no degradation.

The degradation of polymers by ultrasound has a number of applications in polymer processing, such as the removal of high molecular weight, or as an alternative approach to controlling the rate of polymerisation. A recent paper has been published by Nguyen⁶⁷, discusses the kinetics of ultrasonic degradation and compares this to the kinetics of elongational flow degradation. The system used was polystyrene in decalin. The conclusion finds that many of the phenomena found during ultrasonic degradation can be rationalised from the findings of elongational flow degradation.

Studies by Price et al⁶⁸ on the ultrasonic degradation of polystyrene show that extensive control over the molecular mass and polydispersity of the polymer can be achieved by variation of the reaction parameters (intensity, temperature, concentration, solvent).

2.1.3. Kinetics of ultrasonic polymer degradation

The aim of studying the kinetics of polymer degradation is to characterise the process in terms of a rate constant, k . However, the physical nature of polymer molecules makes the definition of the rate equation difficult. The solution degradation process consists of a mixture of polymer chain lengths undergoing parallel reactions, so that a precise solution would be to have a large number of rate equations and therefore many rate constants.

Numerous attempts at proposing rate equations for polymer degradation have been made, of which the first was by Schmid⁶⁹ and was applied to a monodisperse polymer sample. He proposed that the degradation rate, dx/dt , (where x is the number of chain breaks per unit time) of a polymer with a degree

of polymerisation (dp) at time t , P_t , is proportional to the chain fraction whose dp is greater than the limiting dp , P_{lim} . This is represented by

$$dx/dt = 0 \quad \text{for } P_t < P_{lim}$$

and

$$dx/dt = k(P_t - P_{lim}) \quad \text{for } P_t > P_{lim}$$

(8)

Therefore, the chain is undegraded if it is shorter than the limiting molecular weight, whereas longer chains will degrade at a rate proportional to the chain length above the limiting value. Conversion of the dp to molecular weight and integration of equation 8 gives the Schmid rate equation:

$$M_{lim}/M_t + \ln(1 - M_{lim}/M_t) = -k/c(M_{lim}/M_0)^2 t + M_{lim}/M_i + \ln(1 - M_{lim}/M_i) \quad (9)$$

where M_t , M_i , M_{lim} and M_0 are the molecular weights at time t , the initial molecular weight, the limiting molecular weight and the monomer molecular weight, respectively, and c is the solution concentration in base moles (or moles of monomer) per unit volume. A plot of the left hand side of equation 9 against t should give a straight line with a gradient of $k(M_{lim}/M_0)^2/c$ from which k may be calculated. However the model does not take into account the variation in molecular weights during the degradation.

Ovenall et al^{70,71} following earlier work by Henglein⁷² suggested a different model, which gave a more accurate equation than Schmid for the rate of bond breaking,

$$\ln(1/M_{lim} - 1/M_t) = \ln(1/M_{lim} - 1/M_0) - k(M_{lim}/cM_0)t \quad (10)$$

A plot of $\ln(1/M_{lim} - 1/M_t)$ against t gives a graph with a gradient of $-k/c(M_{lim}/M_0)$ from which k may be calculated. This equation was based on results from Henglein's experiments using DPPH (2,2-diphenyl-1-picrylhydrazyl) as a radical scavenger to follow the ultrasonic degradation of PMMA.

Other rate models include those of Fujiwara⁷³, which gives a rate of mechanical degradation, and also Sato, and Nalepa⁷⁴ whose model assumes a random degradation process, although ultrasonic degradation is non-random.

2.1.4. Products of polymer chain degradation

A covalent bond can cleave in one of two ways, either homolytically, with one electron from the bond going to both fragments, creating radicals, or heterolytically, with both electrons going to one fragment giving a negative ion (both electrons) and a positive ion (no electrons). This is the case for polymer chain scission (breaking of the covalent C-C backbone).

Homolytic cleavage, in which two macroradicals are formed, is the most common chain cleavage observed during ultrasonic degradation. Henglein⁷² showed evidence for the presence of radicals by the trapping of the radicals using 2,2-diphenyl-1-picrylhydrazyl (DPPH). Direct evidence has also come from the use of electron paramagnetic resonance spectroscopy (EPR or ESR) which detects the spin properties of unpaired radical electrons⁷⁵. Examples of polymers which cleave in this way include polystyrene and polypropylene (see figure 13 below).

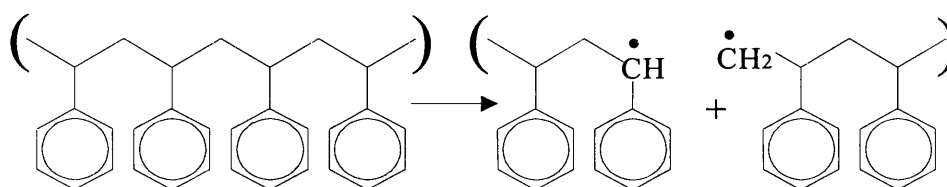


Figure 13. Homolytic Cleavage of Polystyrene

Heterolytic bond cleavage, in which two macromolecular ions are formed, has been studied in solutions of poly(dimethylsiloxane) (PDMS) in methanol by Thomas and De Vries⁷⁶. When the sonication was carried out in the presence of radioactive ¹⁴C-labelled methanol, they found that the radioactivity was incorporated into the polymer, whereas this did not occur upon sonication of polystyrene or upon refluxing of PDMS solutions. Methanol, being a strong nucleophile, reacts rapidly with carbonium and siliconium ions due to the heterolytic cleavage of the Si-O bond. From this it was suggested that during sonication an ion pair was formed followed by a stabilisation reaction with a

strong nucleophile (e.g. water or methanol), or alternatively, in the absence of methanol or similar nucleophile, a disproportionation reaction may occur (figure 14 below).

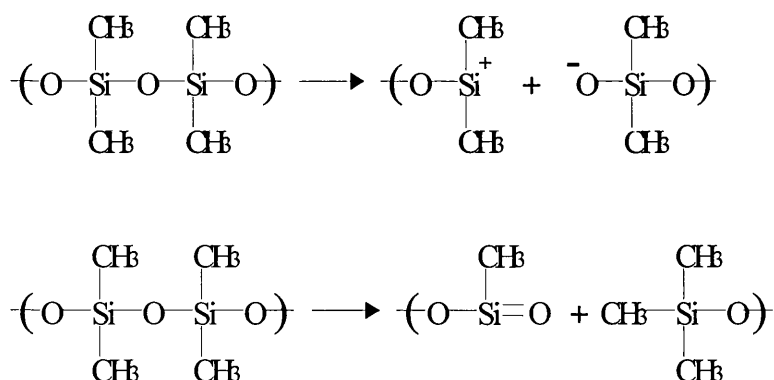


Figure 14. Heterolytic Cleavage of PDMS, above: formation of ion pair.

below: disproportionation

2.2. Polymer Synthesis

One of the effects of cavitation is the production of radicals^{2,30,34,50,81} from decomposition of the solvent and other dissolved species. These are then capable of initiating polymerisation of monomers. Polymerisation can be induced, for some polymers, in just the pure, dry monomer⁷⁷⁻⁷⁹. Examples of polymers which may be produced include polystyrene, PMMA, Poly(vinylpyrrolidone) and Poly(vinylcarbazole). High molecular weight polymers formed by this process are then subject to the degradation described earlier. An advantage of this form of polymerisation is that initiators and high starting temperatures are avoided, although as this is carried out at lower temperatures the propagation steps are slower. A consequence of this is that there are differences in polydispersity and tacticity as compared to the thermal methods. Variation of the conditions for sonication of monomers can be used to synthesise polymers with different tacticities⁷⁹.

Copolymers may also be produced by ultrasound^{58,80,81}. The primary result from chain cleavage is a macromolecular radical which can react with a

second species. The macro-radical from one polymer, if formed in the presence of a polymerisable monomer, can initiate the polymerisation of a second monomer in solution leading to the formation of block copolymers. Previous work⁹⁸ used this technique to form *in situ* copolymers of polystyrene-polybutadiene and polystyrene-poly(methyl phenyl silane). The results of the compatibilisation could be clearly seen from electron micrographs, which showed the absence of phase separation in the compatibilised system as compared to a non sonicated homopolymer mixture where phase separation was obviously present. Sonication of a mixture of two polymers also gives rise to block copolymers (see page 50). For this to occur the two homopolymers must both possess molecular weights above the limiting values expected from their ultrasonic degradation. Addition of a radical scavenging compound to a sonicated polymer solution leads to end-functionalised polymers or copolymer, e.g. to the introduction of a fluorescent group⁴. Following this strategy, polymers with modified properties (solubility, elasticity, thermal behaviour, etc.) or for special uses can be obtained.

Ultrasound can give enhanced yields and rates of reactions in polymerisations. An example is the Ziegler-Natta^{35,58} process by which high-density polyethylene, polypropylene and other polyolefins are produced using a mixed metal catalyst. This reaction gives polymer chains where the substituents are regularly arranged on the chain. For this reaction molecular weight control is difficult and samples of very wide weight distribution are often formed. The application of ultrasound to this synthesis speeds the reaction, keeps the stereospecificity and gives more uniform molecular weights. The preparation of polysilanes^{35,58,82} is another example, where conventional methods use Wurtz coupling of dichlorodiorganosilanes with molten sodium give irreproducible results, low yields, and, usually, a bimodal distribution of molecular weights. Under ultrasound polysilanes of narrow distributions are formed and variation in the ultrasound intensity can be used to control the polydispersity of the polymer. Polysiloxanes can also be prepared with ultrasound. The usual procedure for formation of PDMS is a cationic ring-opening reaction of the cyclic tetramer, catalysed by a small amount of acid. Under ultrasound this reaction is accelerated twofold, with similar yields and higher molecular weights. Heusinger et al⁸³ have

carried out experiments on the polymerisation of glucose in aqueous solution using ultrasound.

Ultrasound has also been applied to emulsion and suspension polymerisations.. Work by Grieser⁸⁹ et al used ultrasound as an initiator in the synthesis of butyl acrylate/vinyl acetate copolymer Latex. This technique was used to polymerise oil in water emulsions of monomeric species at 30⁰C in the absence of any added chemical initiators. The ultrasound forms radicals which induce polymerisation. Effects include more rapid formation of emulsions and control over particle size

Some research has also been carried out on ring opening and organometallic catalysis based polymerisations under ultrasound. An interesting development is that of a possible new route for the production of C₆₀ by ultrasound⁸⁴. Katoh et al have analysed the products of benzene sonication using FAB mass spectroscopy, among the products small amounts of C₆₀ were identified.

3. COMPATIBILISATION OF POLYMERS

3.1. Polymer-Polymer Thermodynamics

A major part of the work undertaken for this project concerns the compatibilisation of immiscible polymer pairs. Most polymer pairs are incompatible, a fact which is explained by thermodynamic considerations. This section aims to give the basic background as to why this is so. Before polymer-polymer thermodynamics^{85,86} is discussed it is useful to review some basic solution thermodynamics in order to establish a reference point for comparison.

3.1.1. The Ideal Solution

An ideal solution is formed when two components mix to give a free energy change that is determined completely by the entropy gained by each component due to the extra degrees of freedom created by solvation (an example is CCl₄ and cyclohexane). The entropy is termed the combinatorial entropy, which for systems of equal sized molecules, is given by:

$$\Delta S^M = -k(x_1 \ln x_1 + x_2 \ln x_2) \quad (11)$$

where ΔS^M is the combinatorial entropy, k the Boltzmann constant and x_i the mole fraction of component i . For an ideal solution there is no change in volume on mixing, so ΔH^M , the enthalpy of mixing, is zero.

Because of the relationship:

$$\Delta G = \Delta H - T\Delta S \quad \Delta H = 0, \text{ ideal} \quad (12)$$

the components forming an ideal solution will always be completely miscible.

3.1.2 The Regular Solution

The idea of the regular solution is that even if molecules in the solution interact, either favourably or unfavourably, they will be so jostled by their kinetic energy that the combination of positions available to each molecule will be the same as if the solution were ideal. Therefore the entropy of a regular solution will be the same as that of an ideal solution.

In the regular solution the free energy of mixing is the ideal value ($-T\Delta S^M$) plus a term for the enthalpy, which is no longer zero. This enthalpy term can be developed in terms of an exchange energy w :

$$w = 1/2\varepsilon_{11} + 1/(2\varepsilon_{22} - \varepsilon_{12}) \quad (13)$$

where ε_{ij} is the energy of a contact between components i and j . As the mixing must be random in order to have ideal entropy, the total enthalpy is given by:

$$\Delta H^M = zwx_1x_2 \quad (14)$$

where z is a coordination number. The free energy of mixing is thus given by combining (11) and (14) to give:

$$\Delta G^M = zwx_1x_2 + kT(x_1\ln x_1 + x_2\ln x_2) \quad (15)$$

3.1.3 Polymer-Solvent Systems

For high molecular weight mixtures with low molecular weight solvents the solvent pressure is found to be far lower than expected, using the above free energy relation using mole fractions. To solve this problem the mole fraction or, molecule/ molecule interchangeability needs to be replaced by a sort of fraction characteristic of chain molecular systems. For this, the concept of a lattice is used. The sites of the lattice represent the exchangeable units for the calculation of entropy. The polymer molecule can occupy many adjacent sites of the lattice. The

diagram below (fig 15) is useful in understanding the ideas involved in this topic, especially when discussing polymers.

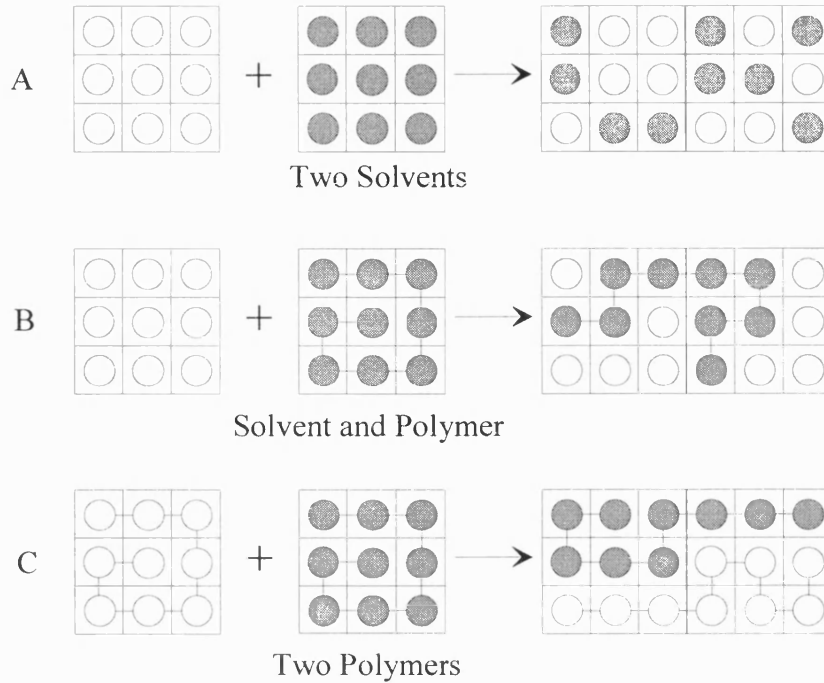


Figure 15. Schematic illustration of the numbers of possible arrangements in a small molecule mixture (A), a polymer solution (B), and a polymer mixture (C). The polymer chains each contain nine segments of the size of solvent molecules.

Taking into account that the polymer segment must have at least two adjacent sites occupied by polymer segments yields the Flory-Huggins expression for the entropy of mixing of polymer with solvent:

$$\Delta S^M = -k(N_1 \ln \phi_1 + N_2 \ln \phi_2) \quad (16)$$

In the above equation the volume fraction has replaced the mole fractions in the natural log terms of the ideal entropy of mixing contained in Eq.(11). The enthalpy of mixing must also be modified, because it is the segments of the polymer molecule which interact. The number of polymer occupied lattice sites is N_2 times the ratio of the size of the polymer chain to that of the solvent, i.e.,

V_2/V_1 . This is the equivalent of saying that the lattice size is determined by the solvent, and the polymer occupies the lattice (see fig. 15). The enthalpy is obtained from Eq.(14) by substituting:

$$\phi_2 \text{ for } x_2, \quad \phi_1 \text{ for } x_1, \quad \text{and } (N_2V_2)/V_1 \text{ for } N_2$$

to give:

$$\Delta H^M = (N_1 + N_2V_2/V_1)zw\phi_1\phi_2 \quad (17)$$

In the above, z should be reduced as the polymer segment has some surface blocked by the rest of the polymer chain.

So, the free energy of mixing becomes:

$$\Delta G^M = kT(N_1 + N_2V_2/V_1)[\phi_1\ln\phi_1 + \phi_2(V_1/V_2)\ln\phi_2 + zw\phi_1\phi_2/kT] \quad (18)$$

and is written in this form because the term in the square brackets is identifiable with the free energy per lattice site (kT units). The free energy per unit volume can be determined by dividing both sides of equation (18) by $N_1V_1 + N_2V_2$, which is the total volume V :

$$\Delta G^M/V = kT[\phi_1/V_1\ln\phi_1 + \phi_2/V_2 + zw\phi_1\phi_2/V_1kT] \quad (19)$$

3.1.4 Polymer-Polymer Systems

For these systems the lattice concept is not rejected, although it is more difficult to use as a lattice of “solvent” size without leaving vacant sites, because both polymers must retain their chain character. To explain these systems, the Flory Huggins equation (16) is written in terms of an interacting segment volume V_s . This neatly preserves the interaction energy w at about the same value. So:

$$\Delta H^M = Vz\phi_1\phi_2/V_s, \quad \& \quad \Delta S^M = -k(N_1\ln\phi_1 + N_2\ln\phi_2)$$

combine to give the free energy on a volume basis:

$$\Delta G^M/V = + kT[\phi_1/V_1\ln\phi_1 + \phi_2/V_2\ln\phi_2] + zw/V_s \phi_1\phi_2 \quad (20)$$

Now, the combinatorial entropy is decreased in magnitude because of the polymer volume V_i and that it makes a negligible contribution to ΔG^M . This leads to it being difficult to achieve a negative ΔG^M . V_s can also be quite large as the polymer chain connectivity leads to the exclusion of neighbouring chains (so increasing volume), unless organisation is allowed i.e. polymer-polymer interactions.

3.1.5 Polymer Incompatibility

The reason why most polymer mixtures are not usually miscible is apparent from simple thermodynamic considerations. For example, a requirement for miscibility is that ΔG^M , the free energy of mixing, must be negative:

$$\Delta G^M = \Delta H^M - T\Delta S^M < 0 \quad (21)$$

Where ΔH^M is the enthalpy of mixing, ΔS^M the entropy of mixing and T the absolute temperature.

From Flory Huggins lattice Theory:

$$\Delta S^M = -R(N_1 \ln \phi_1 + N_2 \ln \phi_2) \quad (22)$$

Where N_i is the number of moles of component i , ϕ_i is the volume fraction of component i and R is the gas constant.

For non-polar molecules the enthalpy of mixing is expected to be unfavourable (i.e. negative). This combination of low ΔS^M and unfavourable ΔH^M leads to most polymer mixtures to be immiscible.

3.2 Compatibilisation Of Polymer Mixtures

Blending of polymers represents one of the most cost-effective ways to improve material properties. This also means that it has the potential to be a reliable and cheap way to recycle them. Unfortunately most polymers are immiscible and the number of known miscible systems is small. Blends of immiscible polymers obtained by simple melt mixing show generally poorer ultimate properties than their individual constituents. These immiscible blends are characterised by a two-phase morphology, a thin interface and poor physical and chemical interactions across the phase boundaries.

The poor properties of these blends can be overcome by stabilising the phase structure by bond formation (physical or chemical) at the interface. This is known as compatibilisation and leads to finer phase structure, enhanced interfacial adhesion and, hence, improved material properties. Block or graft copolymers⁸⁷⁻⁹² have been utilised to this end. The copolymers segregate at the interface and thus act as an emulsifier, reducing interfacial tension so ensuring a finer dispersion during melt blending. However, although the addition of copolymers is an effective method of compatibilising immiscible polymer blends, they have disadvantages such as difficulty in their synthesis. Since most block copolymers are in the microphase-separated state at mixing temperatures, they have high viscosities, making it difficult to disperse them near the interface between two phases. Also, added block copolymers may stay in a homopolymer phase as micelles rather than move to the interface, decreasing the efficiency of the whole process.

An alternative to adding copolymers separately, is the *in situ* formation of compatibilising agents⁹³⁻⁹⁷. In situ formed compatibilisers are obtained by blending suitable functionalised polymers, which react in the melt and form chemical bonds between the constituents.

3.2.1 Ultrasonic Compatibilisation

A potentially easier method is the use of ultrasound to create copolymers^{98,99} *in situ*. The action of ultrasound causes cleavage of organic polymers to create macromolecular radicals. If two polymers are present the radicals formed can combine to form block copolymers, which will then act as compatibilisers between the two phases. This is illustrated in figure 16.

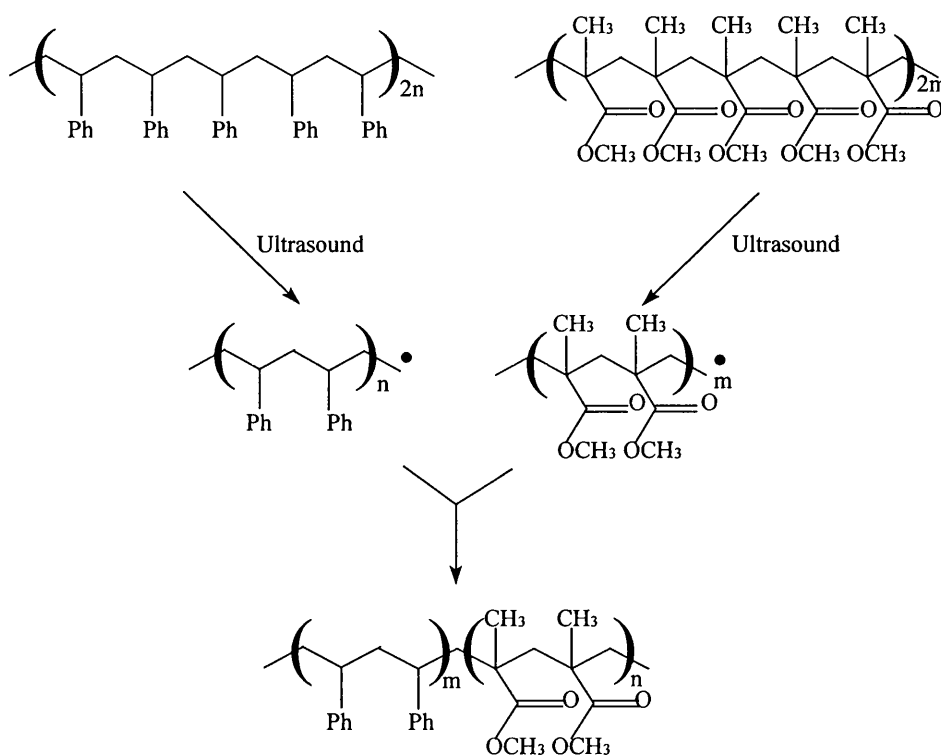


Figure 16. Diagram showing ultrasonic reaction scheme producing copolymers for polystyrene/poly(methylmethacrylate).

3.3. Some Current Research in Polymer Compatibilisation

Most research in this area revolves around the synthesis of block copolymers for specific polymer pairs. It must be noted that much research centres

on the production of novel block copolymers for their properties alone and not for compatibilisation.

Reactive extrusion, where polymer pairs are reacted with a compatibilising agent during the extrusion process, is a widely used method for compatibilisation, especially for the production of block copolymers. An example of this is in the work of Macosko et al ¹⁰⁵ who used premade block copolymers to compatibilise poly(methylmethacrylate) (PMMA) and polystyrene (PS). The copolymer used was diblock PS/PMMA which was added to the polymer mixture and then mixed in via melting in an extruder. Also making use of addition of copolymers, Chang ⁹¹ used styrene-glycidyl methacrylate for the *in situ* compatibilisation of poly(butylene terephthalate) (PBT) and poly(2,6-dimethyl-1,4-phenylene oxide) (PPO) ⁹³ and of PBT and polyamide 6 ¹⁰⁶. The results of the study claimed that the resulting blends had improved processability, impact strength, phase stability and tensile properties. Other research in this area includes that of Kim et al ⁹⁵ and of Jo et al ⁹⁴ both of whom used an *in situ* compatibiliser which formed grafts between polymer pairs. The compatibiliser used in Kim's work was polystyrene-glycidyl methacrylate (GMA) which formed grafts with PE and PBT. Jo used maleic anhydride as the graft, attaching it to PS which was then compatibilised with polyamide 6. The formation of the copolymers during melt mixing was followed using spectroscopic analyses. GMA has also been used as a graft to poly(propylene) (PP) in compatibilisation of PP/Polycarbonate (PC) ¹⁰⁷. Horák et al ⁹⁶ have used melt mixing in an extruder to obtain HIPS/PP blends which were compatibilised with the introduction of styrene-butadiene block copolymers. SEM photos show improved miscibility of the polymers with mechanical tests verifying this

A different compatibilising method, which also makes use of extrusion techniques, is one-step reactive extrusion. One step reactive extrusion is the functionalisation of a polymer with a desired functional group and the subsequent interfacial reaction of this functionalised polymer with a second polymer, with the whole operation being carried out in a single extrusion process. In the work carried out by Hu et al ¹⁰⁸ compatibilisation of PP/PBT ¹⁰⁹ was achieved via this method. Three monomers, acrylic acid, maleic anhydride, and glycidyl

methacrylate, which are all reactive towards the carboxylic and/or hydroxyl groups at the chain ends of the PBT were melt grafted on to the PP by free radical reactions. A comparative study showed that GMA was the most effective graft.

Investigation into the structure-property relationships of highly structured graft copolymers by Pfeiffer and Rabeony⁸⁸, concluded that blending the graft copolymers they used into their respective homopolymer pairs results in mechanical property enhancements which are dependent upon the molecular characteristics of the graft copolymer e.g. the number of grafts per chain. Similar results were shown by D'Orazio¹¹⁰ et al in their work on PS/PP graft copolymers and the resultant blends.

An interesting use of compatibilisation techniques is the compatibilisation of liquid crystalline materials with non-liquid crystalline polymers. Lub et al⁹² synthesised AB block copolymers consisting of a non-crystalline chain poly(isobutyl vinyl ether) and a chiral liquid crystalline block. This combination gave rise to interesting effects on the properties, with the resulting copolymer showing the ferroelectric chiral smectic C mesophase at room temperature with low viscosities and low birefringance, due to the presence of the non-liquid crystalline chain. Maganini et al¹¹¹ have also published in this area, looking into the synthesis of PET-LCP copolymers for compatibilising PET/LCP blends.

As stated earlier the synthesis of the block copolymers required for these studies, is the subject of many researchers. Some researchers have used group transfer polymerisation (GTP) to create block copolymers. Recent examples include those of 3 methacycloxypropyl-pentamethyl-disiloxane and *tert*-butyl methacrylate block copolymers⁸⁹ and of zwitterionic methacrylate block copolymers⁹⁰. GTP is used as it gives synthesis of methacrylate copolymers of controlled structure and narrow molecular mass distribution. Another method is ring opening metathesis polymerisation (ROMP)^{87,91}. Anionic synthesis is commonly used, examples include synthesis of ABC triblock copolymers of PS/PBMS/PMMA¹¹².

The use of ultrasound to induce compatibilisation has so far only been achieved in very dilute solutions (1%) in work by Price and West⁹⁸. In their study compatibilisers were made *in situ* by the creation of macroradicals from ultrasonic

degradation (see page 35) which initiated the polymerisation of a second monomer in solution. By varying the concentration of the monomer it was found that control of the block lengths was gained. Polymer systems studied using this technique were PS-polybutadiene and PS-poly(methyl phenyl silane).

4.0. POLYMER RECYCLING

Polymers are being used more and more in everyday aspects of life, yet their re-use and disposal, particularly for thermosets is still a problem¹¹³⁻¹¹⁶. The recycling processes include industrial operations in which secondary materials are reprocessed and / or monomers recovered for further polymerisation; such processes are termed secondary and tertiary recycling. The major three uses of polymeric materials in the most developed countries are packaging and transportation, with the construction industry^{117,118} third.

Polymers can be roughly divided into two groups, thermosets and thermoplastics. Thermosets are plastics that once formed or moulded cannot be reshaped by heat and so cannot be recycled easily. Thermoplastics can be re-melted and reshaped, and so can, in principle, easily be recycled. The majority of thermoplastics can be classified as commodity plastics, these are cheap and produced in large quantities. Examples include polypropylene (PP), polystyrene (PS), polyethylene (PE) and polyethylene terephthalate (PET). These plastics are used in such applications as disposable packaging, agricultural and architectural coverings and also some engineering uses. The throwaway character of these plastics makes them a major target of any recycling campaign.

Thermoplastics can be collected and re-used in further products, although the collection and separation of these plastics is a costly process. Problems included in separating polymers are the huge number of polymers in use, copolymers and coextruded plastics and the use of several polymers in different components. Other problems involved in plastics recycling include degradation during polymer reprocessing and lifetime, different melting points and polymer incompatibility. In particular the degradation of plastics after several reprocessings can lead to a drastic reduction of the plastics mechanical properties.

4.0.1 Polymer Recycling in The Automotive Industry

Currently, the recycling technology used in the automotive industry^{119,120} is capable of recycling about 75% of the weight of scrap vehicles. This is one of

the highest recovery rates in any sector of industry. The recovery of materials from scrap vehicles, however, is generally limited to metals, such as steel, iron, aluminium, copper and zinc. The polymer content is usually dumped as landfill. This problem is set to grow as more manufacturers increase the amount and variety of polymers used in vehicle construction. Although this is, in terms of fuel consumption, a good thing as the vehicles become progressively lighter and more efficient, it is creating a problem which until recently wasn't receiving much attention. Solutions include cutting down on the number of different polymers used and labelling them clearly to aid recycling, removal of large plastic components, such as bumpers, on scrapping. Recent research has also suggested that some of the polymer waste can be pyrolysed and incorporated into concrete¹¹⁹, in some cases enhancing the concrete's properties.

4.0.2 Polymer Recycling in Europe

Four million tonnes of plastics waste was recovered in Europe in 1995^{122,123}, this is equivalent to 26 percent of the total plastic waste. Although actual material recycling amounted to only 9.2 per cent of plastics waste, with the remaining 16.8 percent being energy recovery. Plastics recovery has grown from 3.3 million tonnes in 1993. Of the 4 million tonnes recovered in 1995, almost 100,000 tonnes was reclaimed by turning the plastic back into basic chemicals (feedstock recycling).

Post user packaging recycling improved in 1995 towards the target of 15 percent set by the EC for 2001. Incineration of plastics without energy recovery decreased by 5.8 percent. Of the estimated 16,056,000 tonnes of plastic waste in 1995, agriculture accounted for 293,000 tonnes, construction 841,000 tonnes, the automotive sector 888,000 tonnes, distribution and industry 3,083,000 tonnes, electrical/electronics industry 812,000 tonnes and municipal 10,139,000 tonnes¹²².

A total of 11,354,000 tonnes went to landfill, energy was recovered from 2,698,000 tonnes and 1,222,000 tonnes was mechanically recycled. Plastics represented 8 percent of household waste, that is approximately 10 million tonnes out of 130 million tonnes. By comparison glass was 9 percent, metal 5 percent and

paper and board 27 percent¹²². Organic products and miscellaneous (including ashes, dust and textiles) made up the remainder.

Plastics in household waste have the following ratios¹²²: PP 18.5 percent; LDPE 23 percent; HDPE 17.3 percent; PVC 10.7 percent PS 12.3 percent; PET 8.5 percent; other materials 9.7 percent.

4.1 Methods Of Recycling Plastics

4.1.1. Mixed Waste

Dirty and mixed plastic¹²⁰ waste can be used to manufacture products with acceptable properties. The incompatibility of different polymers is overcome by using compatibilisers and stabilisers. The usual method is to crush, wash and separate the fractions e.g. by their different densities using a hydrocyclone. After this process they can be re-melted and formed. The number of different types of plastics in the mixture, however, should not be too large, so as to keep separating expenditure low.

Another solution is to design products which can use a mixture of polymer types. This results in far less expensive sorting and collection systems and eliminates the problem of classifying the polymers for separation. Unfortunately, products created from mixed polymers do not maintain consistent properties due to varying concentrations of different polymers. Also the costs of the stabilisers and compatibilisers can be too high for the product obtained.

4.1.2. Pyrolysis

The chemical bonds holding polymer chains together break if subjected to high temperatures. The temperature will vary according to the strength of the chains which is determined by the individual molecular structure (figure 17 below). The following applies:

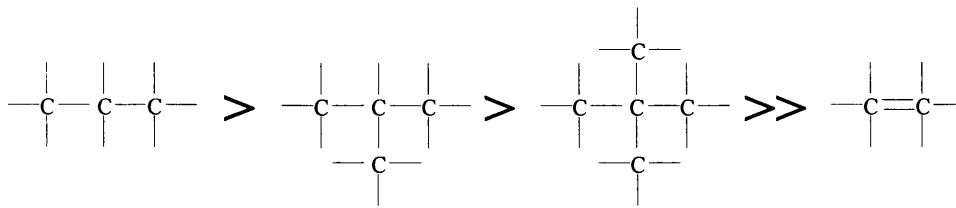


Figure 17: Polymer chain strength

Chain splitting generally starts at 200⁰C. Polymer pyrolysis is carried out under vacuum, where as the temperature rises, low molecular weight molecules are generated. In most pilot plants, a pyrolytic gas is used as the heat energy carrier, at temperatures of up to 1000⁰C. For the production of high quality hydrocarbons and valuable oils from plastic waste, the plants must operate at temperatures of approximately 700⁰C^{113,114,121}. This method is particularly suited to recover certain monomers, e.g. styrene from relatively pure polystyrene waste¹¹³. However a pilot plant in Hamburg has been built specifically to deal with co-mingled post-user plastic waste with a capacity of 10-40 kg/hr¹¹⁴.

4.1.3. Hydrolysis

This makes use of the fact that polycondensation, which is use in the production of polyamides and polyesters, is an equilibrium reaction. This means that at high temperatures the presence, or not, of water will determine whether the polymer chains are composed or decomposed. If, at high temperatures, a polycondensate comes into contact with water, then it decomposes into its original monomers. This method is used in the recycling of polyurethane foams to give polyols and di-isocyanates¹¹³.

4.1.4 Hydrogenation

In this method high pressures and temperatures of up to 500⁰C are used. The plastics are ground to a fine powder, dispersed in used oil to form a mash and then pressed into high-pressure cell¹¹³. Due to the hydrogen present the polymers are split and reduced to oil and coke. This technique is of particular advantage, because, of all known techniques hydrogenation is the one which least damages the molecules, so allowing the easy generation of new macromolecules. In

addition a synthetic oil is obtained (Syncrude) which refineries can use as a raw material.

4.1.5. Other Depolymerization Methods

Depolymerization methods are a way of restoring almost full engineering properties to the recycled product. Processes to achieve this include selective dissolution and flash devolatilisation, which uses xylene to dissolve mixtures of PVC, PS, PE, and PE into separate streams. Also there are chemical routes to convert one polymer into another, such as PET which can be converted by three steps into polyols used in polyurethane foams. Endo et al¹²⁵ have proposed a reversible depolymerisation method, where a bifunctional monomer is used to create a curing-depolymerisation system between the monomer and polymer. The direction of this reaction can be controlled by simply altering the conditions.

4.1.6. Incineration

This is really a technique for recycling the energy content of plastic materials as they are nearly all flammable. In addition to providing energy, this method reduces the volume of waste down to around 10%. The slag created can bond heavy metals in a non-elutable way. This can then be used for construction purposes. Special furnaces capable of generating vitrified slag¹¹³ must be used as any organic waste, unless perfectly mineralised by safe incineration will be a hazard in the long run, as organic waste keeps reacting in refuse pits. Using pure oxygen in the incineration process gives more efficient incineration, and so allows smaller furnaces to be used. In addition, some toxic compounds in the exhaust fumes are destroyed due to the high temperatures generated (up to 1600⁰C). This method¹²⁶ has various drawbacks, these are; high plant cost, sorting costs, potential pollution, the need to be large scale and also adverse public conception leading to a political barrier in establishing incinerator plants. The bonuses include energy generation, already available technology and its high efficiency for sterilisation (important in medicinal uses for example).

4.1.7. Composite Materials

Thermoset composites are another problem for recycling^{124,122}. As well as not being able to remelt and remould a thermoset, composites only contain a proportion of polymeric material, around 30% for glass reinforced plastics, with the bulk of the material being fibre reinforcement and particulate fillers. Also scrap material from end of life applications is likely to be contaminated. There are main methods for recycling thermoset composites. The first of these is regrinding to produce particulate and fibrous materials for use as fillers or reinforcing agents in new composite materials. Only relatively uncontaminated materials can be treated this way. Up to about 20% of recyclate can be added to new composites without causing significant deterioration in properties.

The second method is chemical recycling in which the polymer is reduced to a chemical feedstock, via pyrolysis or similar methods. This method is commonly used in the automobile industry¹²³ to recycle the many reinforced polymers, such as sheet moulding compound, used in automotive applications. The final method is combustion, which recovers the energy content of the materials, although a use for the large amounts of incombustible fillers remaining after combustion needs to be found to make this viable.

4.1.8. Biodegradation

Various forms of degradation can be used for polymer waste disposal. The most environmentally compatible is biodegradation^{126,128}. Many plastics are used as protective coatings, structures and packagings. They are designed and manufactured to resist environmental degradation, including biodegradation. So most of the current large volumes of polymers are not biodegradable and so biodegradation as a means of disposal will only become widespread when new biodegradable polymers and facilities for biodegradation become available. If biodegradation can be controlled and useful products obtained, they become bioconversion or biorecycling processes. Some of the promising approaches to new useful biodegradable polymers are biopolymers, modified biopolymers and blends. Examples include poly-R-3-hydroxyalkanoates which are energy storage

materials for bacteria, cellulose acetates and blends of starch and degradable polymers.

4.1.9. Landfill

Other than being recycled, most waste polymers will eventually end up in a landfill site ¹²⁹⁻¹³¹. Obviously the space in landfill sites is not infinite and eventually this form of disposal will become very costly and difficult. Also most landfills are not designed to photodegrade or biodegrade solid waste. This is due to the fact that for these processes to occur sunlight or humidity is required. In most landfill sites neither of these two conditions are given.

Most of the plastic waste which is disposed of in landfills is from packaging and non-durable consumer goods; it is estimated that this source of plastic waste is six times greater than that from automotive waste. Even so, this is a small fraction of the total solid waste accounting for about 7.5% by weight. But, on a volume basis, after compacting in landfills, the fraction of plastics is about 20%! In an uncompacted state, the volume of plastics would be about a third.

In the U.K landfill dominates the municipal waste industry, accounting for in excess of 80% of all treatment and disposal. This contrasts with several other European countries where alternative practices including recycling, composting and incineration play more important roles. The majority of active landfill sites in England will be infilled and returned to agricultural or recreational use within the next 15 years. Landfill use has decreased over the last 5 years. The industry is aware of the government's attempts at discouraging the use of landfill, and cited the landfill tax and general recycling policy as being the main reasons for this change of emphasis.

4.1.11. Rubber Reclamation

Rubber reclamation involves the regeneration of the rubber through the devulcanization process to restore the elasticity of the rubber. This 'reclaimed' rubber can only be used for low quality applications, as its physical properties are not as good as the virgin rubber. In rubber reclamation of waste tyres the tyre is first cut along the edge tread manually or mechanically. The carcass is then

divided into the tyre face and the fibre layer portions. The tyre face is used for producing the reclaimed rubber. The tyre side portion is used for stamping the bottom parts of sandals or in making tyres for agricultural and other uses. The fibre portion is further sub-divided into three layers and then cut into strips for other applications, such as a substitute for the springs in sofas.

4.1.12. Other

Research suggests it is possible to use waste tyre rubber in asphalt pavement¹³². Asphalt paving is made up of mineral aggregate held together by asphalt cement, a residue of petroleum. There are two general methods for using tyre rubber in asphalt mixes. In asphalt rubber concrete, ground tyre rubber is mixed with asphalt cement, for use as a binder for the mineral aggregate particles in the mix. Tyre rubber may also be used in the production of rubber modified asphalt concrete. In this, ground rubber chips replace some of the mineral aggregate.

Other research includes the production of activated carbon¹³³ upon pyrolysis of tyres, thereby making a more valuable end product, and the use of ultrasound to devulcanize rubbers. A recent development by Isayev et al¹³⁴⁻¹⁴¹ incorporates an ultrasonic horn into the die of an extruder, so enabling continuous sonication of an extruded melt, this process is claimed to devulcanize the rubber to a partial extent. Ultrasound is also being studied for its potential in identification and characterisation of reclaimed and recycled polymers by ultrasound attenuation analysis¹⁴².

4.2. Economic Considerations For Polymer Recycling

Environmental pressure has created legislative rulings, regulations and appealed to individual and business guilt to promote recycling of not only plastics but also many materials, such as glass, paper, aluminium etc. Unfortunately, markets for collected waste have been much slower in developing. This has led to the situation where recycled waste polymers are more expensive than virgin polymers. For newspaper recycling there has even been a glut in the market of

recycled paper. For businesses setting on a recycling scheme the incentives have to weighed against the disincentives, many of which are economic (see below):

<u>Incentives</u>	<u>Disincentives</u>
Green Image	Competition from virgin products
Legislative incentives	Regulatory restrictions
Customer/community goodwill	Lack Of Markets
Regulations	Lack of Interest
	Transport Logistics
	Competition from other recycling methods

Collection and separation ¹⁴³ of plastics prior to recycling can be expensive, for heavily mixed plastics these alone can be more than the cost of buying new polymers. Landfill is still a cheaper option, although the cost of this is rising steeply, due to government regulations aimed at encouraging recycling. If long transport distances are involved, this again will increase costs, therefore most successful recycling operations are locally-based.

The recycling of plastics, like other waste problems, is subject to the laws of economics ¹⁴⁴⁻¹⁴⁶ i.e. polymer recycling needs to be market-driven. Those willing to venture their capital on recycling must ultimately be able to generate a viable business. Recycling should be encouraged, but not if the advantages gained are minimal and too costly to support.

4.3. Overview

From the preceding chapters it can be seen that the knowledge and use of ultrasound is becoming, if not already so, an established part of chemistry and industry as a whole. When applied to polymers the degradative effect and subsequent production of macroradicals can be used to create block copolymers. This could potentially be of great use in helping solve the growing polymer

recycling problem and also be used to create useful new materials. As can be seen from chapter 4 the recycling of polymers is an ongoing problem, and although many techniques are being applied to this, there is still no easy solution, especially when the laws of economics are taken into account. The use of ultrasonic compatibilisation in recycling could remove much of the need for the costly process of sorting waste polymer streams prior to treatment as is the case with many recycling techniques.

When applied to mixes of virgin homopolymers there is also the potential to create new and novel materials by combination and enhancement of the original polymer's properties.

5.0 Experimental Introduction

During the course of this project a variety of analytical techniques has been used to obtain data from the polymers under study. The following pages give a basic introduction to each of these.

5.1 Gel Permeation Chromatography

Gel Permeation Chromatography (GPC) gives measurements of molecular weight averages and polydispersities. It is also known as size exclusion chromatography. Separation of molecules via size occurs in a packed column full of rigid beads (e.g. cross linked polystyrene, pore size $10\text{-}10^5$ nm). As the dissolved polymer flows past the beads, small molecules can enter the pores, so slowing down their flow along the column. Larger molecules cannot enter the pores and so flow further along the column. This means that large molecules are eluted first from the column, small molecules last. A schematic is shown below.

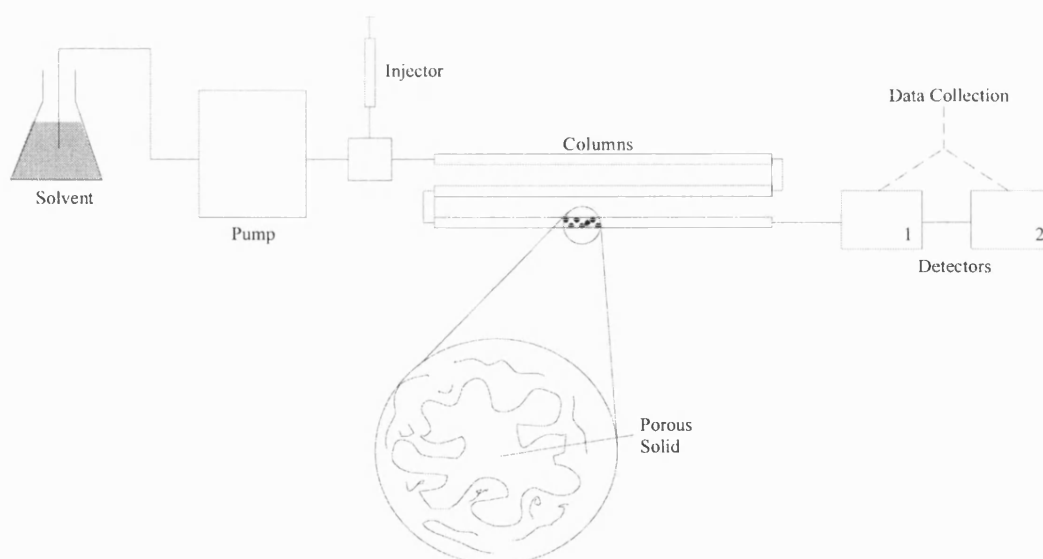


Figure 18: Schematic of a GPC System.

The detectors used are normally non-destructive, enabling the collection of eluted samples if necessary. The main detector used is the differential refractometer which measures the difference in refractive index between the common effluent and a pure solvent reference. Also UV/Vis detectors may be used. As GPC is a secondary method of analysis, it requires calibration with known standards.

For calibration in this case commercially available standards of polystyrene were used, which have accurately known molecular weights and very narrow distributions. Any time that solvents were changed or repairs carried out the GPC was re-calibrated.

From GPC analysis, results are acquired in the form of concentration vs retention time from which number average molecular weights (\bar{M}_n) and weight average molecular weights (\bar{M}_w) are derived. Since a distribution of molecular weights exists in any finite sample of polymer, the experimental measurement of molecular weight can give only an average value. The type of average depends on the nature of the method used. If you consider a polymer with a large but finite number of species, N_i , w_i , and M_i will be the number of molecules, mass and molecular weight, respectively, of the i th species. X_i designates any arbitrary property of the species. So,

$$w_i = N_i M_i / N_{Av} \quad (23)$$

where N_{Av} is Avogadro's number.

Number averages are worked out as follows (a bar over the symbol represents the average), with the number averages identified by the subscript n:

$$\bar{X}_n \equiv \sum_i N_i X_i / \sum_i N_i \quad (24)$$

$$\bar{M}_n \equiv \sum_i N_i M_i / \sum_i N_i \quad (25)$$

where \bar{X}_n and \bar{M}_n are the number average value of property X and number average molecular weight, respectively. In these formulas, N_i , can be replaced by

any quantity that is proportional to number of molecules, for example, by number of moles, molarity or molality.

Substituting equation (23) into equations (24) and (25) gives an alternative definition of the number averages:

$$\bar{X} \equiv \frac{\sum_i w_i X_i / M_i}{\sum_i N_i} \quad (26)$$

$$\bar{M}_n \equiv \frac{\sum_i w_i}{\sum_i w_i / M_i} \quad (27)$$

For typical polymers the \bar{M}_n lies near the peak of the weight distribution curve or the most probable molecular weight (figure 19).

For \bar{M}_w the mass of the polymer chains is averaged. Weight averages are defined as follows:

$$\bar{X}_w \equiv \sum_i w_i M_i / \sum_i w_i \quad (28)$$

and

$$\bar{M}_w \equiv \sum_i w_i M_i / \sum_i w_i \quad (29)$$

or alternatively,

$$\bar{X}_w \equiv \sum_i N_i M_i X_i / \sum_i N_i M_i \quad (30)$$

and

$$\bar{M}_w \equiv \sum_i N_i M_i^2 / \sum_i N_i M_i \quad (31)$$

The weight average molecular weight \bar{M}_w results from measurements of light scattering and sedimentation equilibrium. Heavy molecules are favoured in this averaging process. \bar{M}_w is equal to, or greater than, \bar{M}_n . The ratio of \bar{M}_w / \bar{M}_n can be used as a measure of the breadth of the molecular weight distribution. A polymer with only a single mass, and identical chain lengths would have an \bar{M}_w / \bar{M}_n of 1.

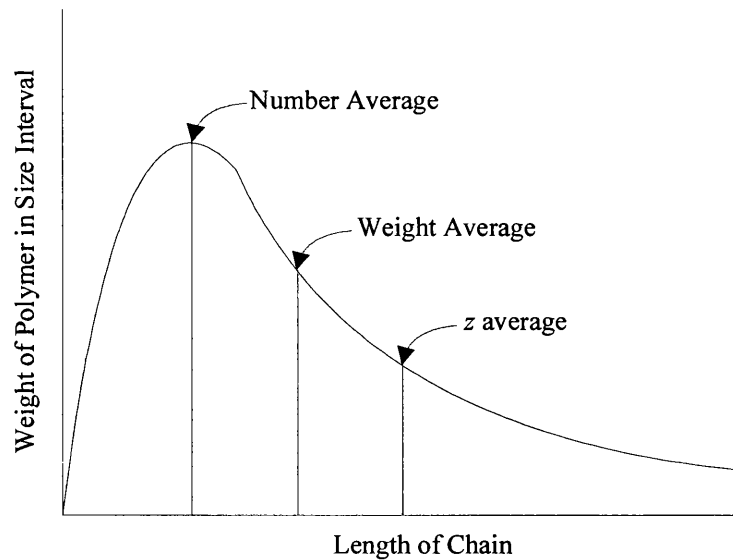


Figure 19. Example of Molecular Weight Distributions for a Typical Polymer

A large number of other averages may also be defined. One of these is the z average. This results from sedimentation equilibrium measurements in a centrifuge (z stands for centrifuge using the German *zentrifuge*) and is defined as

$$\bar{M}_z \equiv \frac{\sum_i N_i M_i^3}{\sum_i N_i M_i^2} \equiv \frac{\sum_i w_i M_i^2}{\sum_i w_i M_i} \quad (32)$$

or

$$\bar{X}_z \equiv \frac{\sum_i N_i M_i^2 X_i}{\sum_i N_i M_i^2} \equiv \frac{\sum_i w_i M_i X_i}{\sum_i w_i M_i} \quad (33)$$

5.2 Differential Scanning Calorimetry (DSC) & Dynamic Mechanical Thermal Analysis (DMTA)

Polymers, as with many common liquids, exhibit certain characteristics similar to a second-order transition upon supercooling to below their crystalline melting point. The viscous liquid (or rubbery material in the case of high molecular weight polymers) is transformed into a hard, glassy material upon passing through this transition. The temperature at which this occurs for any given polymer is termed the glass transition temperature (T_g). This change occurs due to the polymer chains no longer being able to undergo rotational movement about their ends i.e. there is no longer enough heat energy available to overcome

the energy barrier preventing this movement. As the polymer has lost a degree of freedom in movement it becomes the hard, glassy material mentioned earlier.

A commonly used method of determining miscibility in a polymer blend is through comparison of the glass transition (or transitions)^{98,99} in the blend against those of the unblended constituents. A miscible polymer blend should exhibit a single glass transition between those of the components, with a sharpness of transition similar to that of the components. In the case of borderline miscibility, the transition will broaden becoming two transitions as the miscibility lessens. The basic limitation of glass transition temperatures in determining miscibility is that for blends of polymers which have equal or similar (<20⁰C difference) T_g's it becomes difficult to achieve resolution of the two T_g's.

Differential Scanning Calorimetry (DSC) can be used to determine the glass transition of polymers. The DSC measures the amount of heat required to increase the sample temperature by a value ΔT over that required to heat a reference material by the same ΔT .

Dynamic Mechanical Thermal Analysis^{98,99} (DMTA) is another method of determining the T_g of a polymer sample. The technique usually applies a sinusoidal load to a sample (although other loading schedules could be used). When a sinusoidal stress is applied to a perfectly elastic solid the deformation (and hence the strain) occurs exactly in phase with the applied stress. A completely viscous material will respond with the deformation lagging 90⁰ behind the applied stress (see figure 20, overleaf).

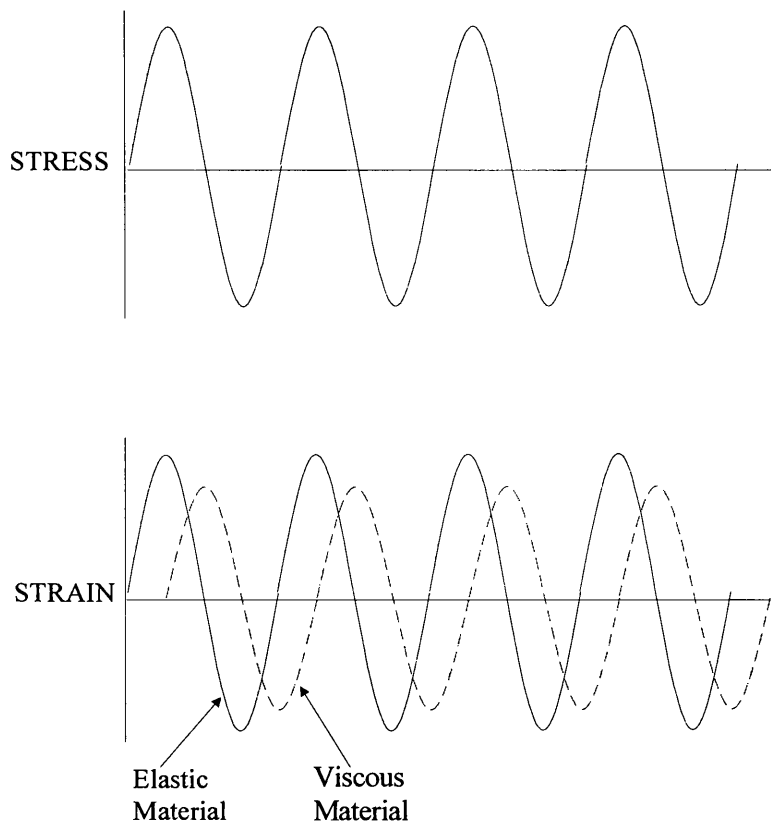


Figure 20: Schematic representation of the response of a perfectly elastic and perfectly viscous materials to an applied stress.

When a sinusoidal stress is applied to a viscoelastic material it will behave neither as a perfectly elastic nor as a perfectly viscous body and the resultant strain will lag behind the stress by some angle (the loss angle, T) where $T < 90^{\circ}$ (see figure 21, overleaf). The magnitude of the loss angle is dependent upon the amount of internal motion occurring in the same frequency range as the imposed stress.

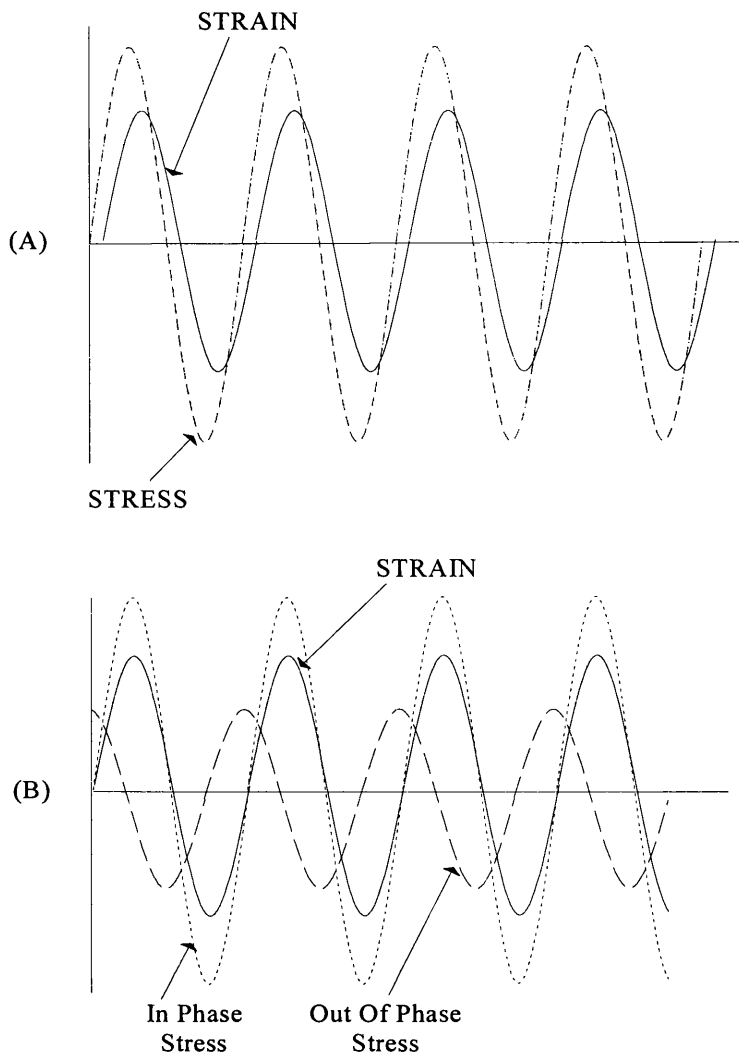


Figure 21: a) Schematic representation of the response of a viscoelastic material to an applied sinusoidal stress.
 b) Schematic representation of the resolution of the in (and out) of phase stress components

The complex dynamic modulus (E^*) is defined as:

$$E^* = \text{Stress Amplitude} / \text{Strain Amplitude} \quad (34)$$

The complex modulus, however, does not take into account the relative phases of the stress and strain components and it is therefore convenient to define the completely elastic and completely viscous components of the deformation so

overcoming this problem. These are the in phase or storage modulus (E') and the out of phase or loss modulus (E'') and are defined as:

$$E' = \text{Amplitude of In Phase Stress Component} / \text{Strain Amplitude} \quad (35)$$

and

$$E'' = \text{Amplitude of Out of Phase Stress Component} / \text{Strain Amplitude} \quad (36)$$

The storage moduli and loss moduli represent the elastic and viscous behaviour of the sample respectively. Their ratio (E''/E') defines the loss tangent, $\tan \delta$. The ability to measure both of these moduli enables the full characterisation of a viscoelastic material. At the glass transition a material goes from a frozen glassy state with limited mobility to a totally mobile system. The fall in modulus (E') is usually three orders of magnitude for an amorphous polymer. The onset of polymer motion is shown by large peaks in the values of E'' and $\tan \delta$. The determination of T_g in this method is direct i.e. material mechanical properties are measured by a mechanical response.

For this project the following experimental conditions were used for DSC and DMTA:

DSC :Heating rate of 10^0C per minute, liquid nitrogen cooling.

DMTA:(Polymer laboratories system) Heating rate of 10^0C per minute,
liquid nitrogen cooling, vibrational frequency 1Hz, single
cantilever
bending mode.

5.3 Scanning Electron Microscopy

Scanning Electron Microscopy (SEM) was used to view samples of polymer after compatibilisation experiments. A schematic of a SEM can be seen in figure 22 overleaf. The operating principles are as follows; electrons from a thermionic or field-emission cathode are accelerated by a voltage of 1-50kV between cathode and anode. The smallest beam cross section at the gun (the

crossover point on figure 22), with a diameter of the order of 10-50 μm for thermionic and 10-100 nm for field-emission guns, is demagnified by a two or three stage electron lens system, so that an electron probe of diameter 1-10 nm carrying an electron probe current of 10^{-10} - 10^{-12} A is formed at the specimen surface.

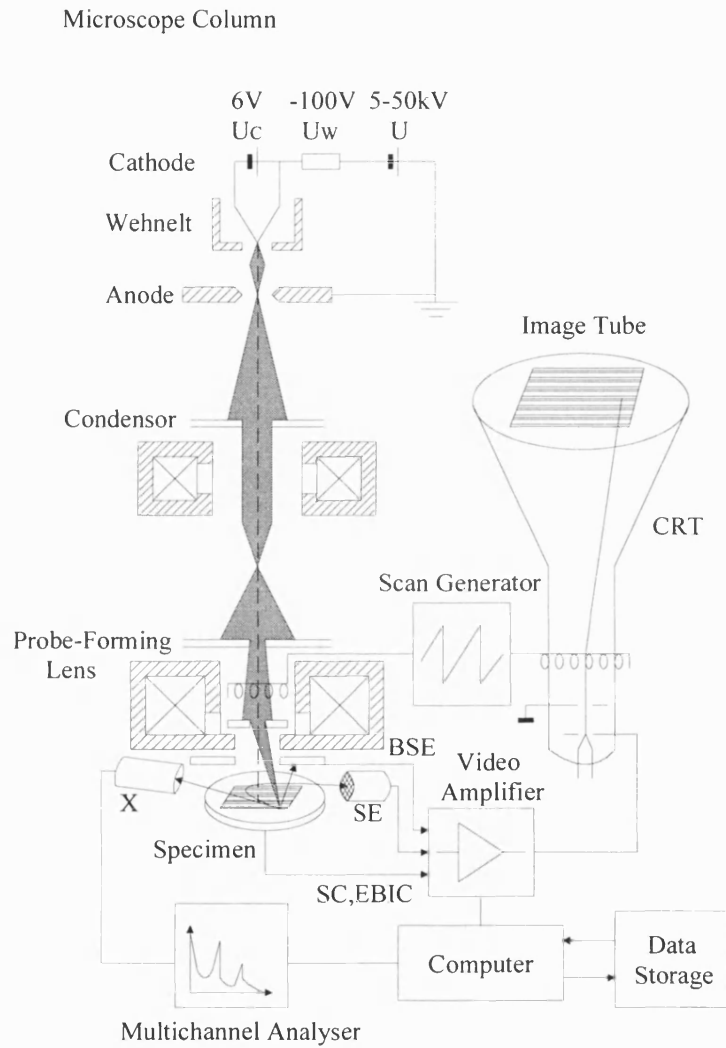


Figure 22: Scanning Electron Microscope (BSE = Backscattered Electrons, SE = Secondary Electrons, SC = Specimen Current, EBIC = Electron-Beam-Induced Current, X = X-Rays, CRT = Cathode Ray Tube)

The large depth of focus, the excellent contrast and straightforward preparation of solid specimens are the reasons for the success and widespread use of SEM in the imaging of surfaces over the past decades.

5.4 Experimental Methods

Most of the experiments carried out during this research project can be classified into the following groups; sonication of model solutions, ultrasonic compatibilisation of polymers in solution, polymer melt degradation using ultrasound, ultrasonic compatibilisation of polymer melts, ultrasonic degradation and compatibilisation of polymer melts under pressure (carried out at TWI). The basic methods are outlined on the following pages, with the results in the next section.

5.5 Sonication Of Model Solutions

e.g. Polystyrene/Toluene

Solutions of polystyrene (Aldrich, Mn~110,000, Mw~280,000) were prepared in toluene (Aldrich, HPLC grade). The concentrations studied were 1, 2, 3, 4, 5, 10 and 15 % by weight of polystyrene in toluene. Concentrations of greater than 15% were not studied as this was found to be the approximate limit of polystyrene solubility in toluene.

For each experiment 100 cm³ of each solution was placed in a water jacketed reaction vessel (figure 23) with the water at a thermostatically controlled 25⁰C. They were then sonicated for six hours 10 Watts, 19.9 kHz , with samples taken at regular intervals. These samples were then later analysed by GPC (see page 64).

Other polymers examined under similar conditions in this study were polyisoprene (Aldrich 97% *cis*, Mn~275,000), *cis* polybutadiene (Aldrich, Mn~180,000), and poly(vinyl chloride) (Aldrich, Mn~85,000). Each experiment was carried out across a range of concentrations

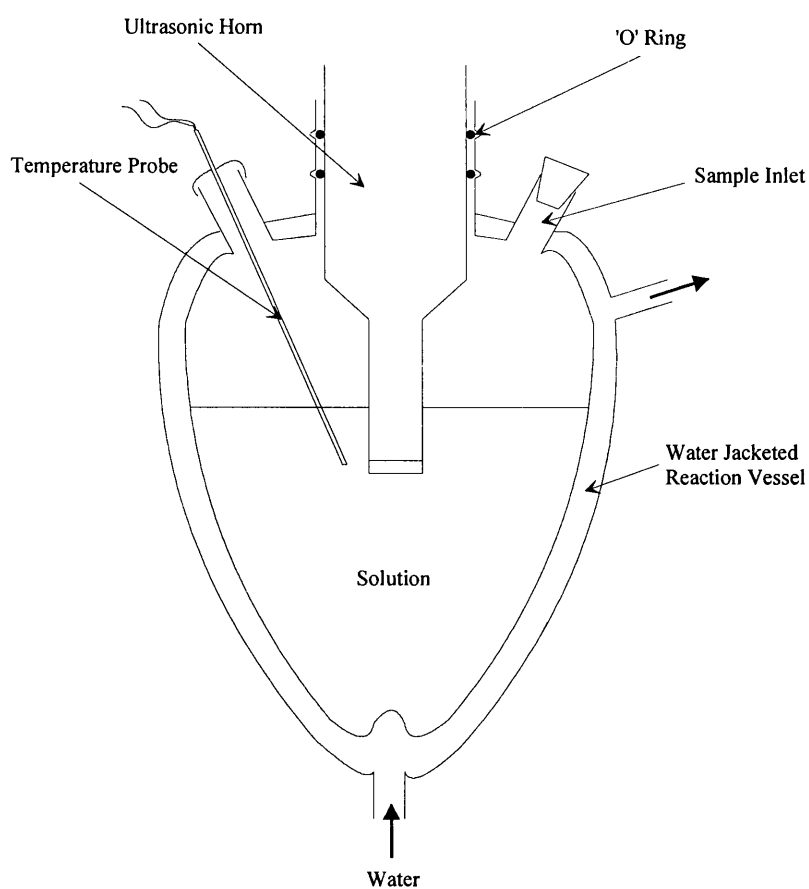


Figure 23. Apparatus For Solution Sonication.

5.6 Electron Microscope Study Of The Effects Of Ultrasound On Polymer Mixtures in Solution

Samples of sonicated polymer mixtures, non-sonicated polymer mixtures and separately sonicated homopolymers which were then later mixed were prepared for study by electron microscope.

Polymer Solutions Studied by Scanning Electron Microscope (SEM)

Polystyrene / Polyisoprene

Polystyrene / Poly(methylmethacrylate)

Polyethylene / Polypropylene

A film of each sample was prepared on aluminium discs, this was done by covering the plates surface with drops of polymer solution and then removing the solvent in a vacuum oven. The discs with polymer films were then sputter coated with a thin layer of gold. This was done as the electron microscope needs a conducting surface in order to give a picture.

These samples were then studied using either a JEOL T-330 or JEOL 6310 electron microscope and a number of photographs of the images were taken at a variety of magnifications using the in-built camera.

5.7 Sonication of Polymer Melts

Equipment to enable the sonication of polymer melts under vacuum conditions, so minimising any oxidative degradation, was designed and constructed. This consisted of a furnace, vacuum chamber (figure 24) and pump, and a furnace control box. The furnace consisted of a 90mm pyrex glass tube, sealed at one end, with 3.6m of $23.29 \Omega\text{m}^{-1}$ resistance wire tightly coiled around it. This was then set in furnace cement (Feb fire cement), insulated with rock wool and placed in an aluminium sleeve.

The vacuum chamber was a 10mm thick, 220mm tall, 105mm diameter glass tube, with a vacuum inlet and sample hole. The ends are sealed by 10mm thick aluminium disks with rubber vacuum seals. The top aluminium disk has a hole to allow an ultrasonic horn to be inserted into the system which is sealed with a rubber 'o' ring around the antinode of the horn. Also the appropriate wiring is fed through the top disk.

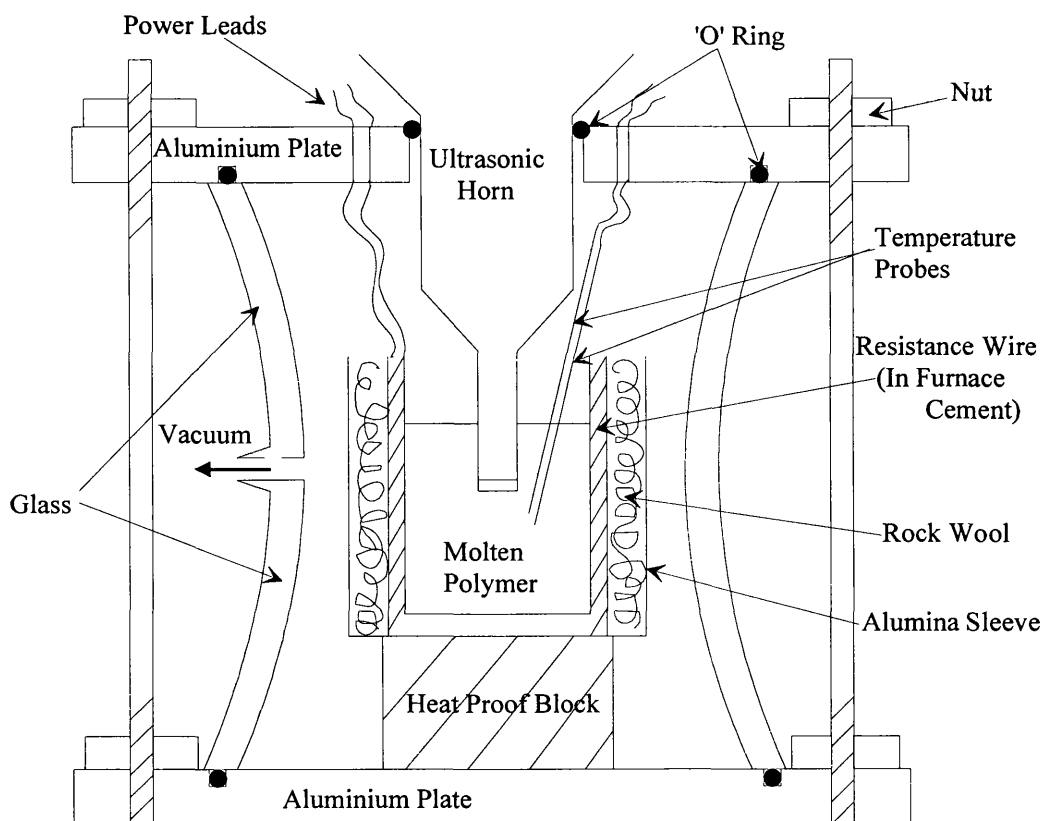


Figure 24. Furnace and Vacuum Chamber

The electronic controls consist of a temperature controller (Omron multi-temperature range) with a thermocouple probe and an independent digital thermometer with thermocouple probe. As the temperature controller sent out low voltage signals, a relay was required to work the furnace as it was designed to work with a mains supply. The various components were mounted on a metal plate and encased in an aluminium box.

The ultrasonic horn used was purchased from Sonic Systems (Isle Brewers, UK). This was a 500 W device which also came with an electronic operating box which gave continuous readings of transmitted intensity and frequency. The horn was been installed in a sound proofed box.

5.8 Polymer Melt Degradation

One of the aims of this project was to investigate the behaviour of molten polymers when subjected to ultrasonic irradiation. To do this, a furnace and controller were designed and constructed which enabled the experiments to be carried out under controlled conditions (see previous page).

The polymer was placed inside a aluminium foil lined furnace which in turn was placed inside a vacuum chamber. A sonic probe and temperature probes were then placed in position so as to be in the polystyrene. The system was then evacuated and the temperature of the furnace brought to above that of the polymer's melting range. Once a constant temperature was achieved the sonic horn was switched on.

After a set time the horn was turned off, as was the furnace. The vacuum was removed and the horn and temperature probes pulled out of the soft polymer before it set. The polymer pellet was wrapped in foil for GPC analysis later. Samples of the polymer were taken from the area directly below the ultrasonic horn tip in each case, and then analysed via GPC. It was hoped that the number average molecular mass (M_n) would drop further for the sonicated samples than for the non-sonicated ones. For GPC 0.1g of polymer was dissolved in 10ml of solvent. These experiments were then also repeated without ultrasound, i.e. the samples were heated for the same length of time. This was done in order to show that thermal degradation was not the main cause of any degradation observed.

One of the main practical considerations was the removal of the polymer from the furnace at the end of the experiment. Also, the original coiled wire furnace design was liable to burning out causing damage to the expensive solid state relay and so it was necessary to add electronic protection in the form of semi-conductor fuses and a voltage dependent resistor across the relay. It was found that the furnace could be made more reliable by encasing all the coiled resistance wire in cement i.e. the connection was buried in the cement casing, so that no resistance wire protruded out of the furnace.

5.9 Polymer Melt Compatibilisation

The procedure for a mixed polymer was the same, except that the polymers need to be mixed together thoroughly. In order to obtain a good mix the polymers were dissolved together in a mutual solvent and then the solvent was removed by placing the solution on a large watch glass and putting it in a vacuum oven. The resulting polymer film was then crushed and placed in the furnace.

These experiments were then also repeated without ultrasound, i.e. the samples were heated for the same length of time. This was done in order to show that thermal degradation was not the main cause of any degradation observed.

In relation to the compatibilisation studies the next step for the sonicated (and non-sonicated) polymer mixtures was to cast a film from them and study them under the electron microscope to see if blending occurred in the melt.

5.10 SEM of Polymer Melts

Two methods were used to prepare the samples obtained from polymer melt compatibilisation studies. At first the samples were dissolved in a mutual solvent and then cast onto an aluminium planchette. A different, preferred approach was later used, which was to simply glue the solid polymer onto the planchettes prior to sputter coating. As SEM only looks at the surface of the sample the glue was not seen and the need for solvent was removed. It was found that the gold coating had to be relatively thick in order to prevent the polymer samples from burning under the electron beam. This was especially the case for samples containing poly(methylmethacrylate).

5.11 Sonication of Polymer Melt Systems Under Pressure

In order to maximise coupling between the ultrasonic horn and polymer melt, it was decided that using a pressurised system may be of use. As we did not have the facilities for this at Bath, use was made of a Branson sonic welding machine at TWI (The Welding Institute, Cambridge). To enable this a reaction vessel was designed.

TWI possessed an ultrasonic welding machine, which had a hydraulic attachment to the sonic horn. A reaction chamber was designed to hold the polymer in a molten state under pressure (figure 25) and was constructed at Bath. This consisted of an aluminium furnace, heated by two cartridge heaters connected to an electronic temperature controller.

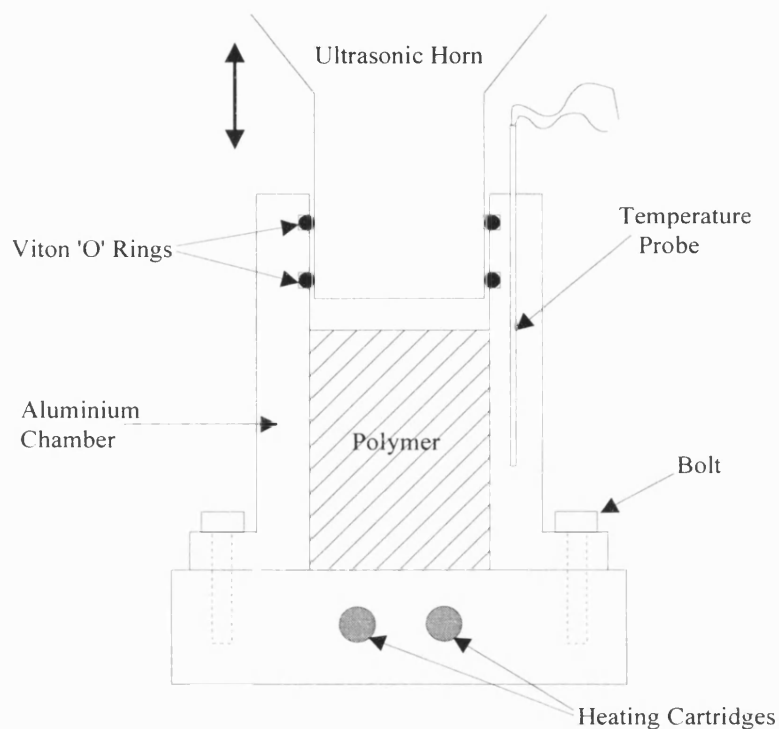


Figure 25. Aluminium Furnace design

During the first experiments it was observed that the polymer charred due exposure to oxygen, so for the following experiments the equipment was housed in a sealed polyethylene-covered frame filled with nitrogen (figure 26). This effectively dealt with the charring problem.

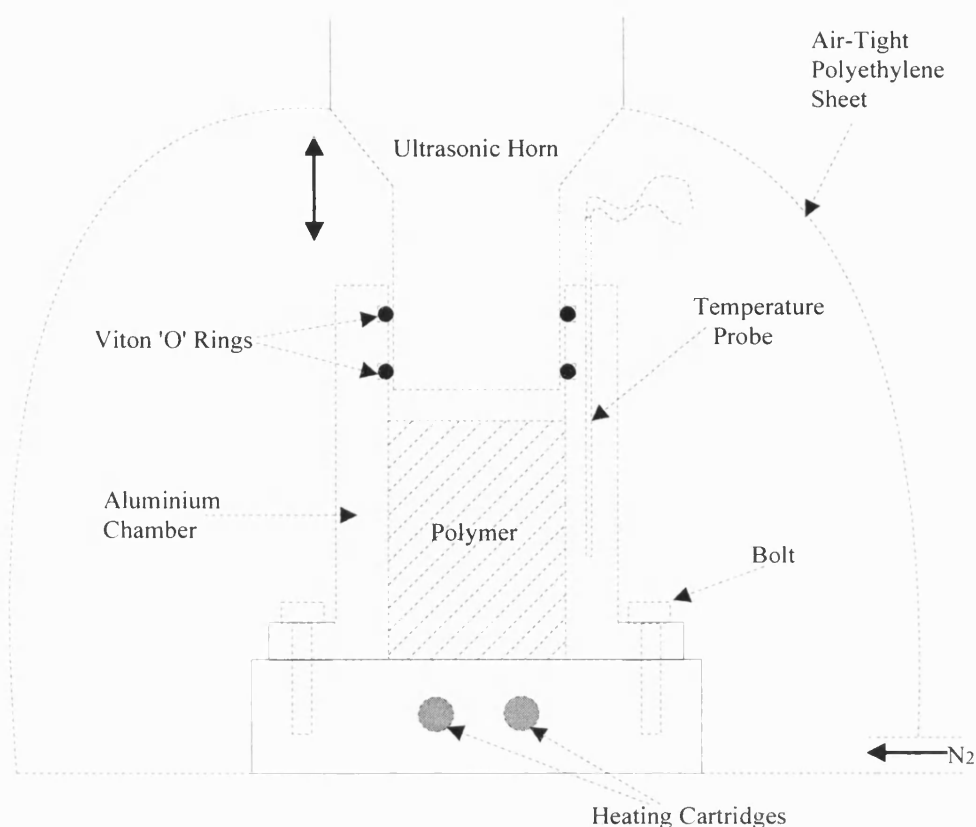


Figure 26. Equipment design used at TWI with N₂ atmosphere

Work was carried out using a Branson Ultrasonic Welder. Polymer samples were melted, in a nitrogen atmosphere, at 240-250⁰C (depending on polymer) in an aluminium furnace (see figures 25,26). A furnace extension was also made to see if any effect could be seen further away from the horn. The following polymers were investigated.

Polyethylene

Polyethylene / polypropylene 1:1

Polyethylene / poly(vinylidifluoride) 1:1

Polystyrene

Poly(methylmethacrylate)

The polystyrene and poly(methylmethacrylate) samples were analysed by GPC analysis.

5.12 Sonication of Poly(methylmethacrylate) / Silica layers

In order to ensure that mixing was occurring and discover where the mixing action of ultrasound was greatest the following experiment was devised. Layers of poly(methylmethacrylate) and silica were arranged in a furnace. This was then heated to 240⁰C under vacuum and then sonicated for one hour. The contents were then allowed to solidify before removing the horn and temperature probes. The resulting solid cylinder was then cut in half vertically to show the mixing effects of ultrasound on a polymer melt i.e. the layers should be broken up.

5.13 Materials used in study

The following chemicals were used as part of this work:

Polystyrene	(Aldrich, Mn~110,000, Mw~280,000, Tg-100 ⁰ C)
Poly(methylmethacrylate)	(Aldrich, Mn~150,000, Mw~290,000, Tg-105 ⁰ C)
Polyisoprene	(Aldrich 97% <i>cis</i> , Mn~275,000, Tg-73 ⁰ C)
<i>cis</i> Polybutadiene	(Aldrich, Mn~180,000, Tg-85 ⁰ C)
Poly(vinylchloride)	(Aldrich, Mn~85,000, Mw~200,000, Tg-40 ⁰ C)
Polyethylene	(Aldrich, LDPE, Mn~ 100,000, Tg-120 ⁰ C)
Polypropylene	(Aldrich, Mn~150,000, Tg-10 ⁰ C)
Poly(vinylidifluoride)	(TWI-sponsors material)
Toluene	(Aldrich, HPLC grade)
Tetrahydrofuran	(Aldrich, HPLC grade)

6.0. RESULTS

6.1. Ultrasonic Degradation of Polymers in Solution

The first experiments upon commencing this project were to carry out polymer degradation in solution of a range of polymers. It was already known that polystyrene gave the characteristic degradation curve (see figure 11, page 36) at low concentrations, but this had not been tested at higher concentrations of 10 and 15%. Solution degradation of polybutadiene and polyisoprene had also not been investigated before, and interesting results were obtained (see discussion on page 90 and conclusions). For each homopolymer degradation extra results are presented in which the results have been inserted into the Schmid equation and the resulting graph plotted. The aim of the Schmid treatment is to characterise the process in terms of a rate constant, k , from the Schmid equation below:

$$M_{lim}/M_t + \ln(1 - M_{lim}/M_t) = -k/c (M_{lim}/M_o)^2 t + M_{lim}/M_t + \ln(1 - M_{lim}/M_t) \quad (37)$$

where M_t , M_i and M_o are the molecular weights at time t , initially and of monomer respectively, c is the concentration of the solution in base moles (or moles of repeat unit) per unit volume and M_{lim} is the limiting low molecular weight after degradation. For the graphs, $-[M_{lim}/M_t + \ln(M_{lim}/M_t)]$ vs time was plotted. The slope of the graph allows the calculation of k . This treatment and a further development of it by Ovenall are presented more fully in section 2.13, page 41.

Presented in this chapter are plots of M_n vs time sonicated for a selection of polymers at a range of concentrations. Alongside these the Schmid and, where appropriate, the Ovenall plots are also shown.

6.1.1. Polystyrene/Toluene

Solutions of polystyrene (Aldrich) were prepared in toluene (Aldrich, HPLC grade). The concentrations studied were 1, 2, 3, 4, 5, 10 and 15 % by weight of polystyrene in toluene. Concentrations of greater than 15% were not studied, as this was found to be the approximate limit of polystyrene solubility in

toluene. The solutions were sonicated (19.9 kHz, 10 W) in a water-jacketed reaction vessel (see page 77) at 25⁰C. The resulting degradation plot, polydispersities and accompanying Schmid plot are shown below:

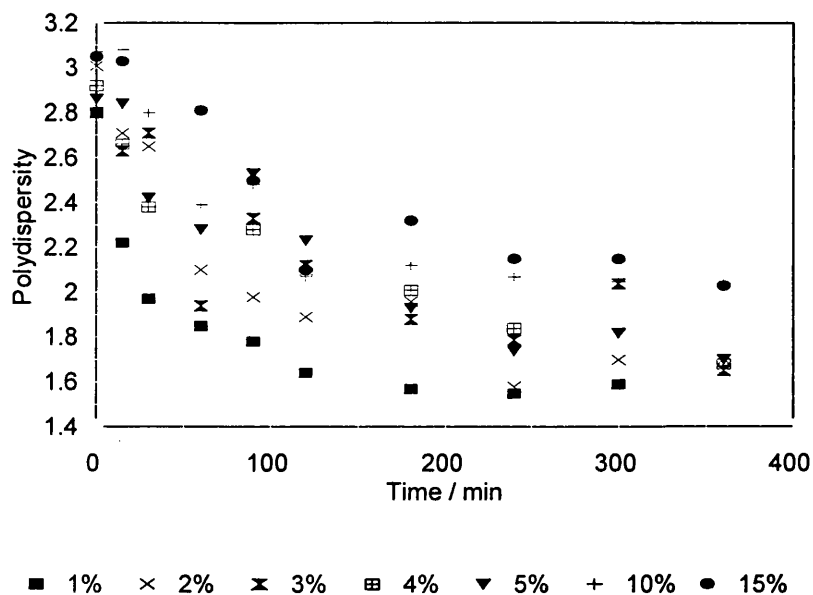


Figure 27: Polydispersity vs Sonication Time for Polystyrene Solutions.

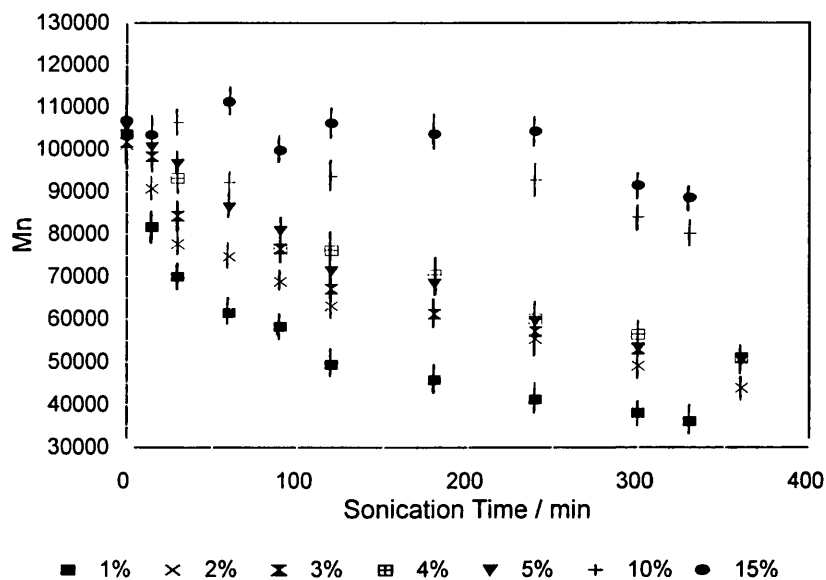


Figure 28. M_n vs Sonication Time For Polystyrene Solutions

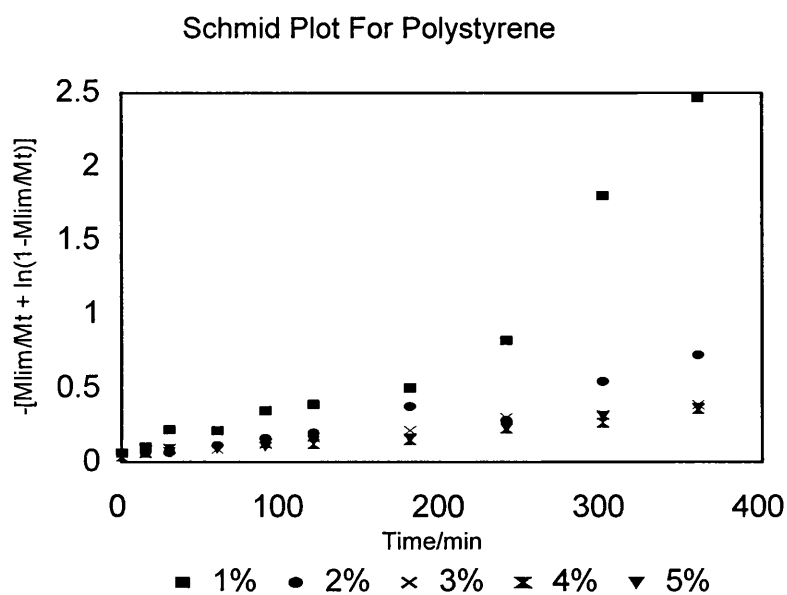


Figure 29: Schmid Plot for Polystyrene Solutions

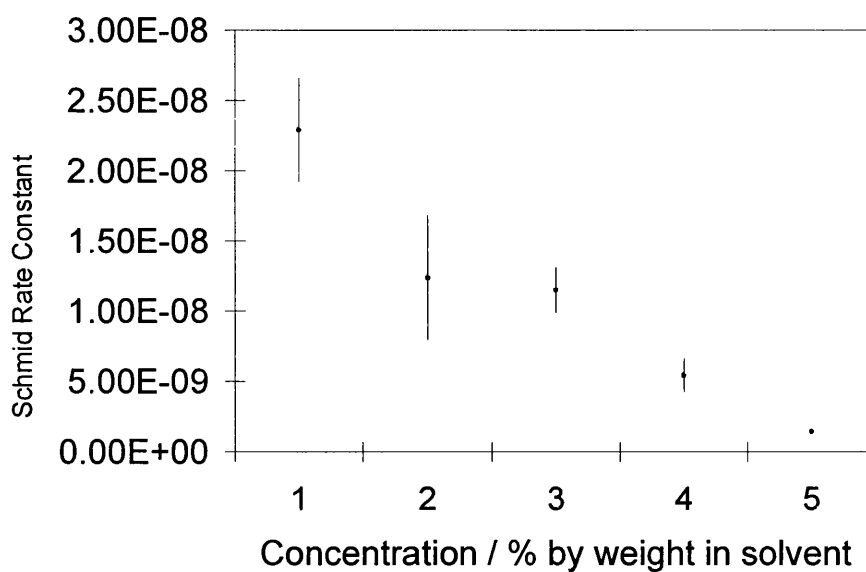


Figure 30: Plot of k (Schmid rate constant) vs Concentration of Polystyrene in Toluene (with 95% confidence intervals)

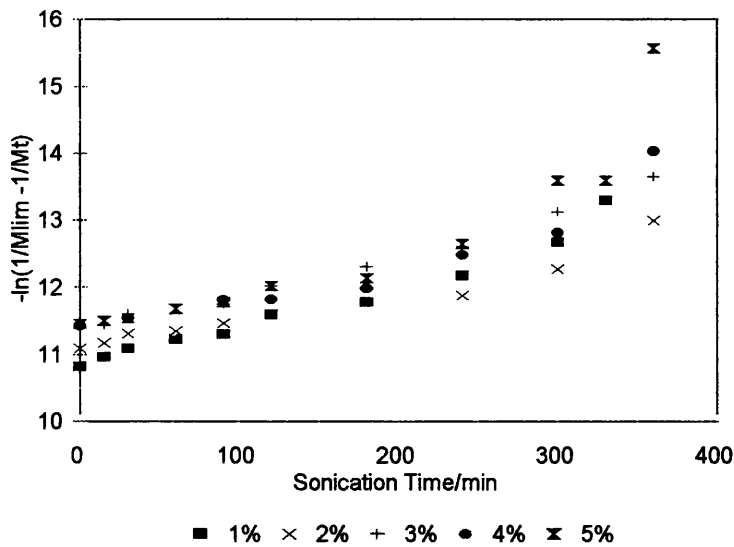


Figure 31: Overall Plot for Polystyrene Solutions.

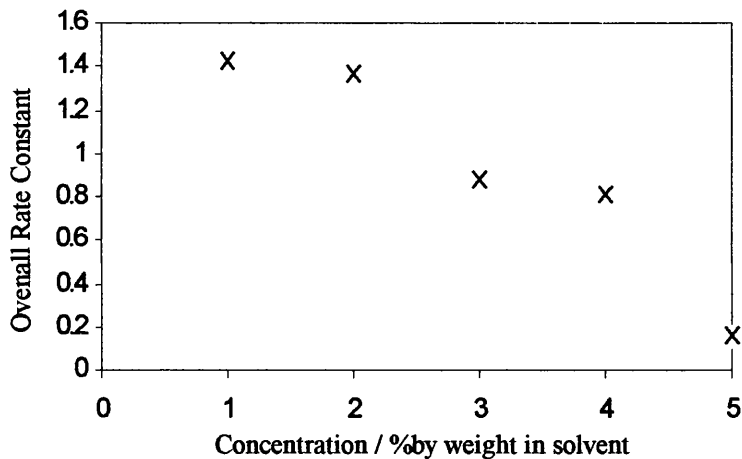


Figure 32: Plot of k (Overall rate constant) vs Concentration of Polystyrene in Toluene

From the above graphs, the expected degradation curve (investigated previously by Price and West⁹⁸) was seen for low concentrations (1-5%). A shallower curve is seen for 10 & 15%, as predicted from comparison of the 1 and 5% curves (5% is shallower). The low drop in M_n for 10 and 15% suggests that conditions for cavitation are becoming increasingly difficult at higher viscosities. The increased viscosity at higher concentrations (10 & 15%) leads to poor mixing and therefore uneven sonication of the solution, this would explain the observed

increases in M_n at high concentrations as the sonication proceeds. The results at these concentrations would then be affected by which part of the solution the sample came from. However, as some degradation has still occurred, it may still be possible to achieve the project aim of degrading and ultimately compatibilising polymer mixtures in a viscous melt.

The Schmid treatment works well for lower concentrations but begins to break down for the 4% plot and above at around 200 mins sonication time. The 10 and 15% results did not give any meaningful results via the Schmid equation and have been omitted. Reasons for this and suggestions on how it may be overcome are discussed at the end of this section. The plot of k vs concentration (plotted using the first 120 mins data from the Schmid graph) shows that the rate decreases with concentration, this is as expected as the viscosity increase will lessen the effect of cavitation. Again, this is discussed more fully at the end of the chapter.

The Overall plot shows a better fit for longer sonication periods than the Schmid treatment, and a plot of k vs concentration also shows a decrease in degradation rate at increasing concentrations.

6.1.2. Cis Polybutadiene/Toluene

Solutions of *cis*-polybutadiene (Aldrich) were prepared in toluene. The concentrations used were 0.5, 1 and 2% by weight of *cis*-polybutadiene in toluene. At 2% the solutions were extremely viscous. The method of sonication was the same as for polystyrene (page 85). The results are shown below (figure 29).

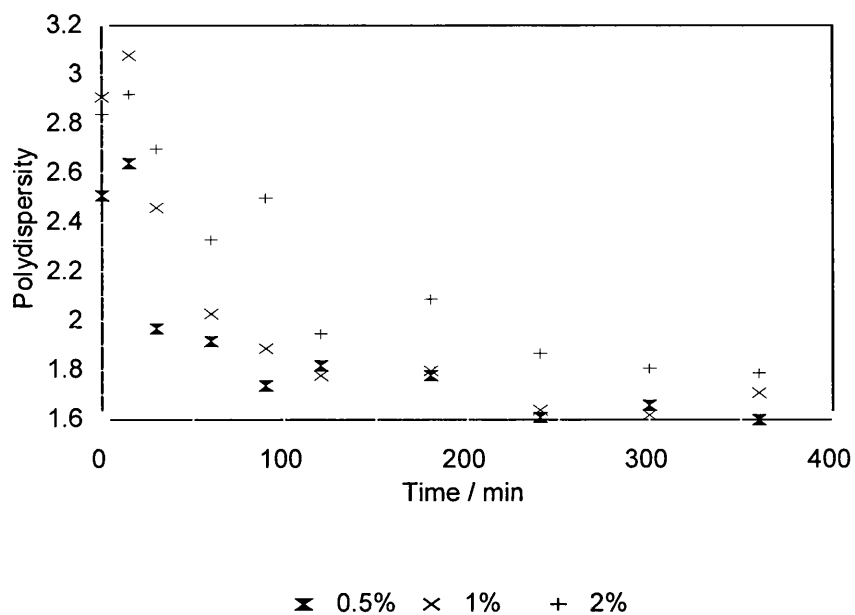


Figure 33: Polydispersity vs Sonication Time for Polybutadiene Solutions

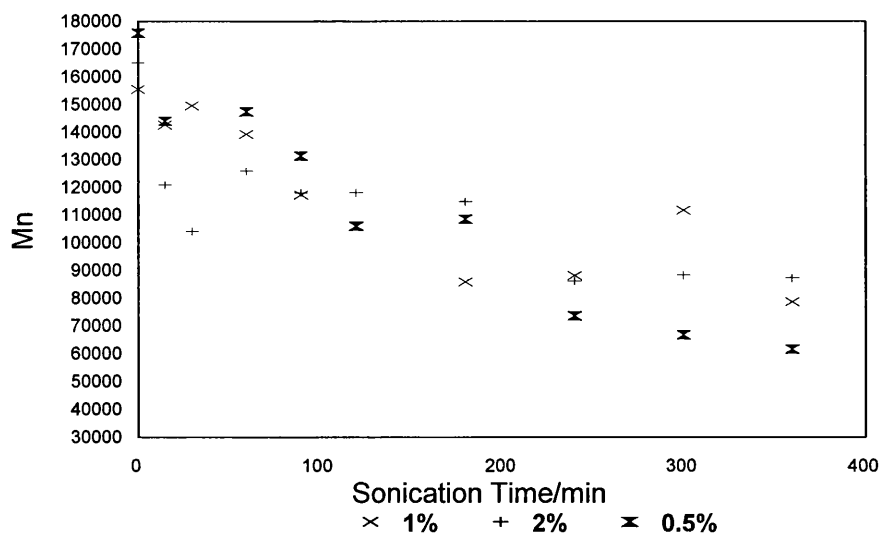


Figure 34. . M_n vs Sonication Time Polybutadiene Solutions.

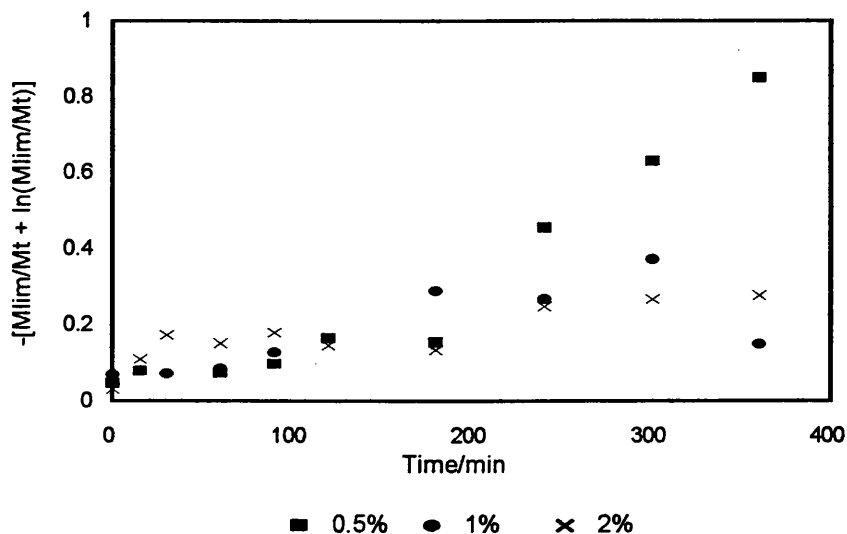


Fig.35: Schmid Plot for *cis*-polybutadiene Solutions

Repeated experiments showed that this polymer does not give the usual degradation curve. In fact, the polymer actually seems to increase in molecular weight at some points during sonication. An explanation for this would be the occurrence of chain branch formation across the polymeric double bond. This would proceed as shown in Figure 36 below:

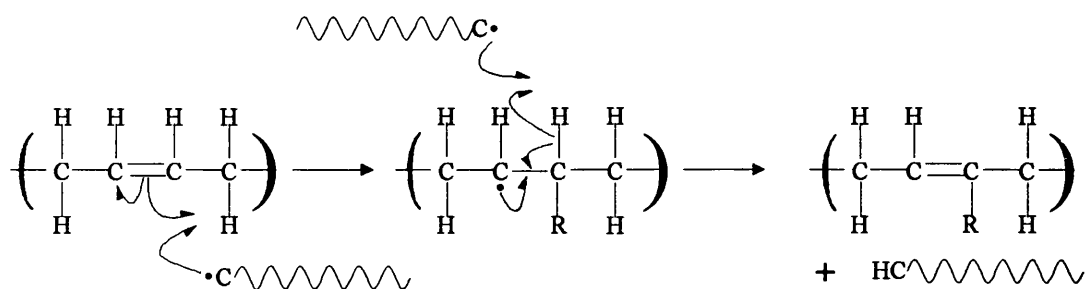


Figure 36: Suggested Mechanism for Polybutadiene Chain Branch Formation.

In this approach, macroradicals created by ultrasonic cleavage (see Chapter 2, page 36) attack a polybutadiene molecule across a double bond along the polymer backbone. This leads to a branch at one of the former double bond

carbon atoms and a radical at the other carbon atom. This radical then reacts with another macroradical, reforming the double bond and losing a hydrogen atom to the approaching macroradical in the process. Direct radical/radical reaction is unlikely as the presence of the first branch would hinder this process.

In order to test this idea, the sonicated polymer (and non-sonicated for comparison) were analysed by NMR (proton and ^{13}C) spectroscopy, by which method any chain branched carbon atoms in the polymer would be shown. What was seen was the presence of a non-protonated sp^2 carbon peak in the ^{13}C spectra of the sonicated polybutadiene. This peak appears shifted to the left of the protonated sp^2 carbon peak (the other carbon in the double bond) as the absence of protons has a deshielding effect. This carbon peak, shown at 133 ppm, is removed when viewing the 135 DEPT spectra (which only leaves the protonated carbons in the spectra) and is also absent in the non-sonicated solution. The NMR spectra for both sonicated and non-sonicated polybutadiene solutions are shown overleaf (figs.37 & 38).

The Schmid plots are disordered, failing to give a straight line from which k may be calculated. This is due to the very erratic degradation plot gained from polybutadiene. As such, a plot of the Schmid rate constant vs concentration was not possible in this case.

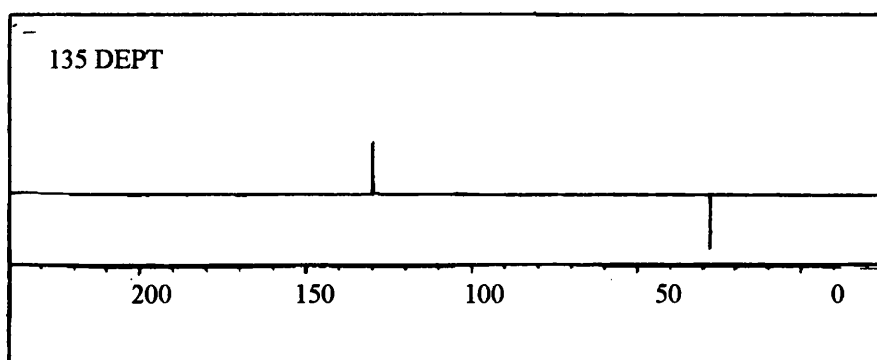
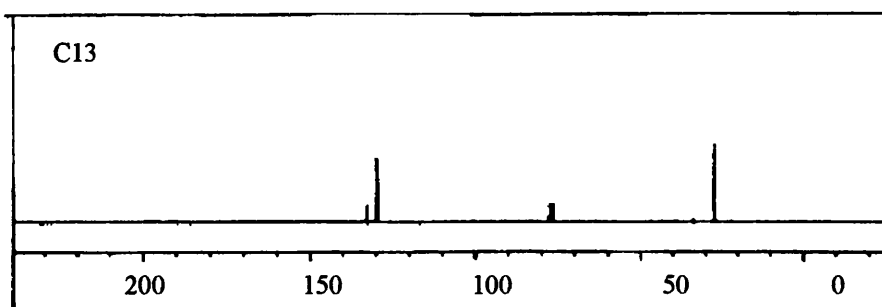
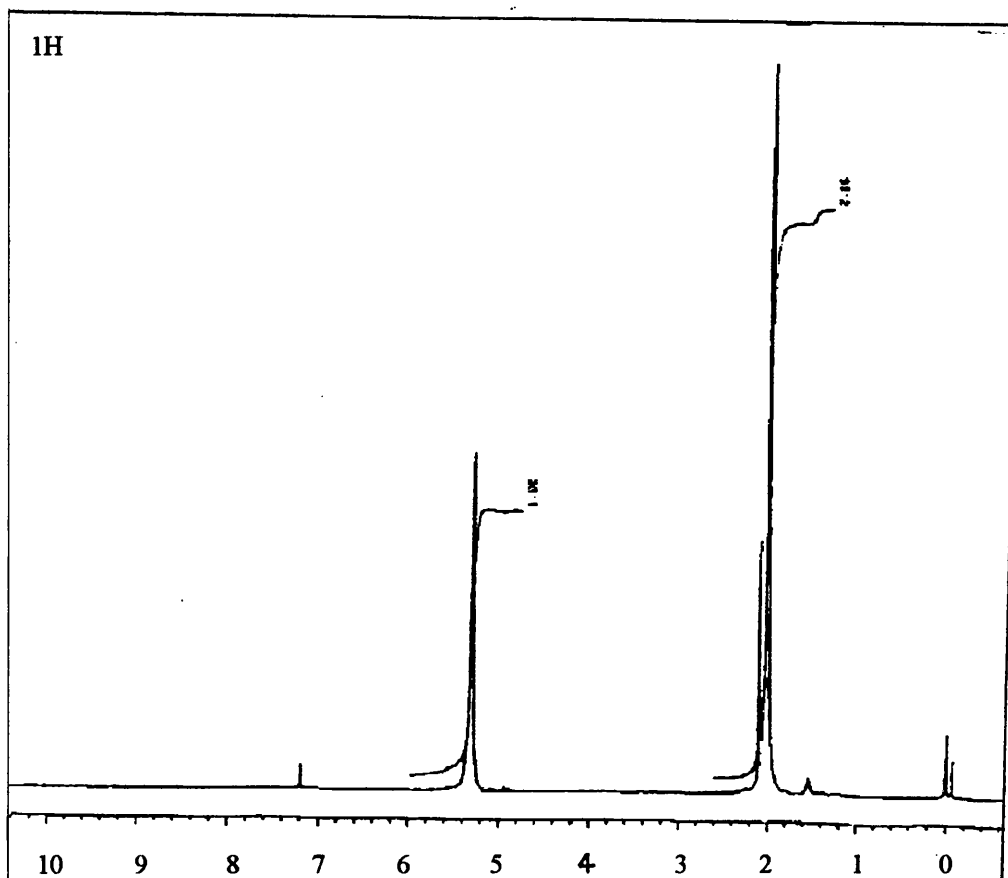


Figure 37: Proton and ¹³C spectra for sonicated polybutadiene solution

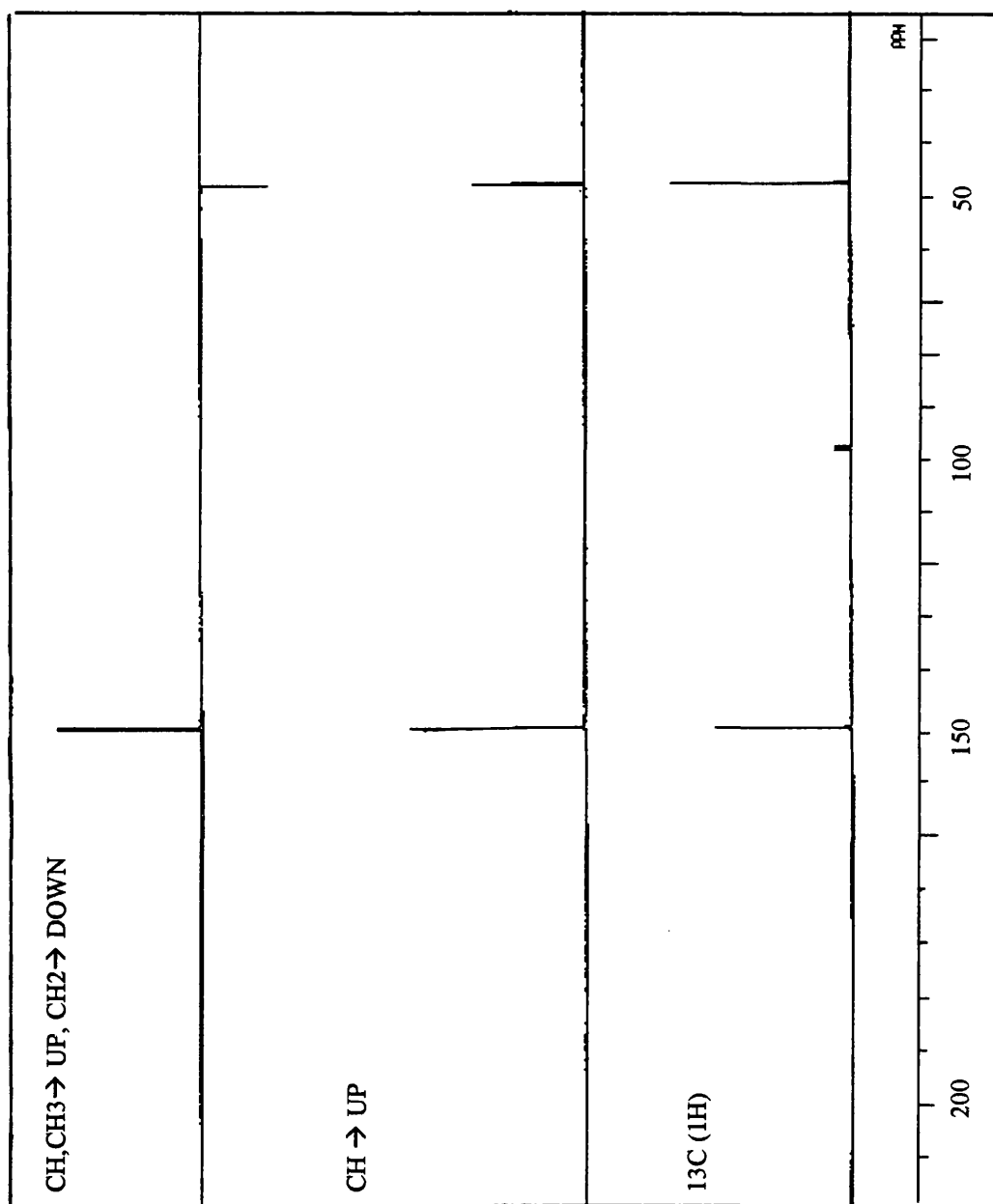


Figure 38: ^{13}C spectra for non-sonicated polybutadiene solution

6.1.3. Poly(isoprene)/toluene

Solutions of *cis* polyisoprene (Aldrich 97% *cis*) in toluene were prepared. The concentrations used were 0.5, 1, 2, and 3%. The method of sonication was the same as described earlier. The results are shown in figures 39 and 40.

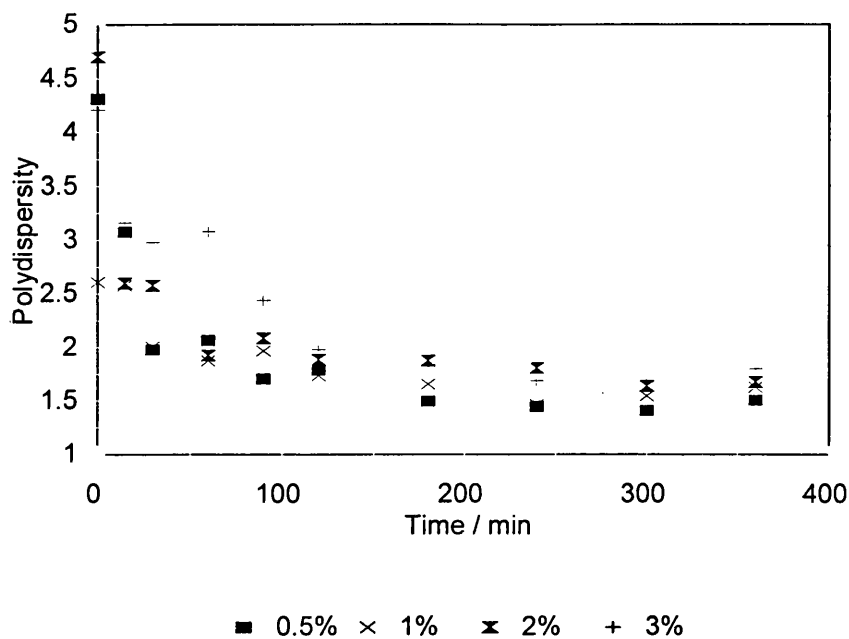


Figure 39: Polydispersities vs Sonication Time for Polyisoprene Solutions

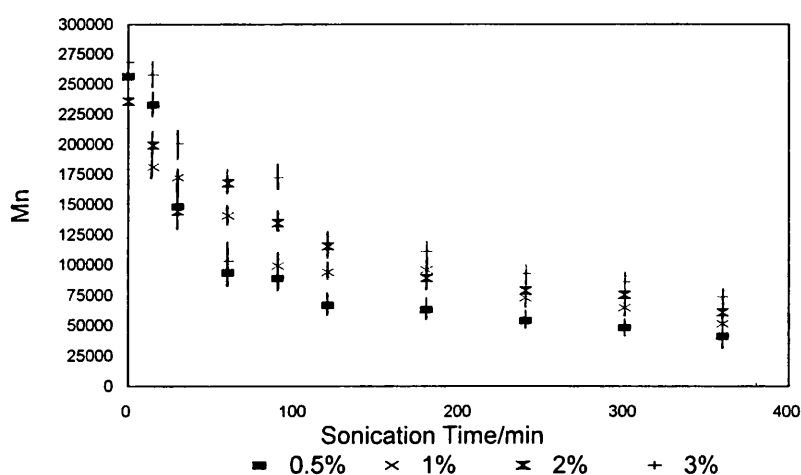


Figure 40. Mn vs Sonication Time For Polyisoprene Solutions

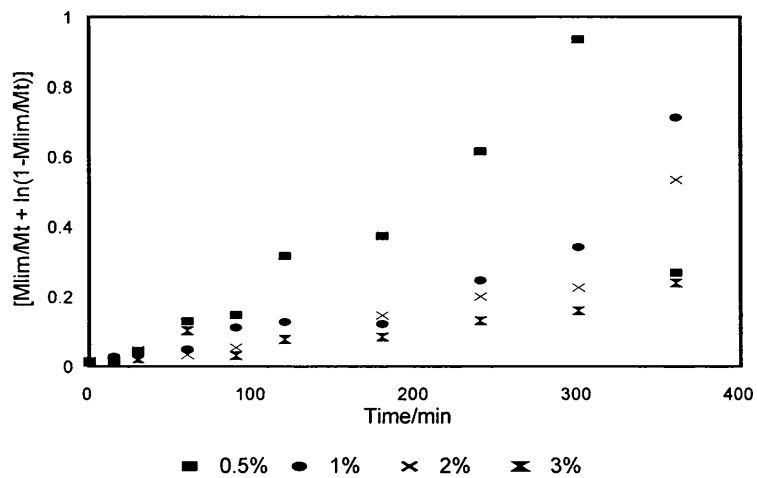


Figure 41: Schmid Plot for Polyisoprene Solutions

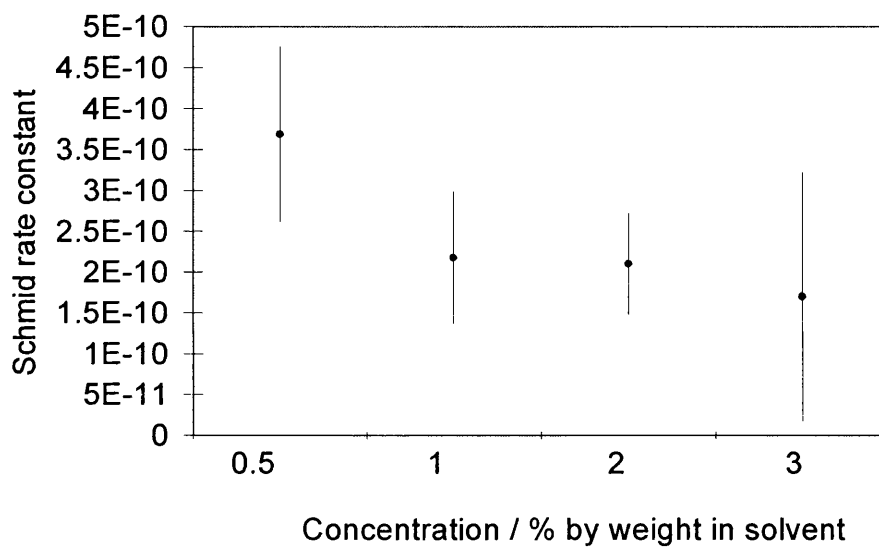


Figure 42: Plot of k (Schmid rate constant) vs concentration of polyisoprene in toluene (with 95% confidence intervals)

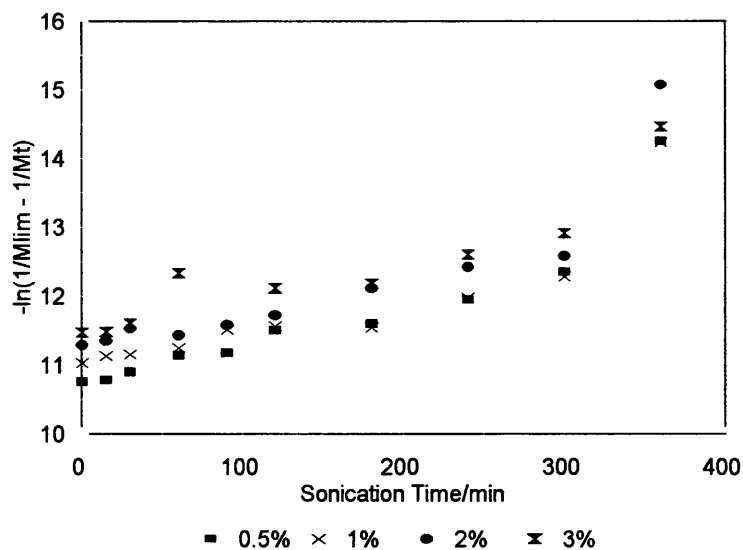


Figure 43: Overall Plot for Polyisoprene Solutions.

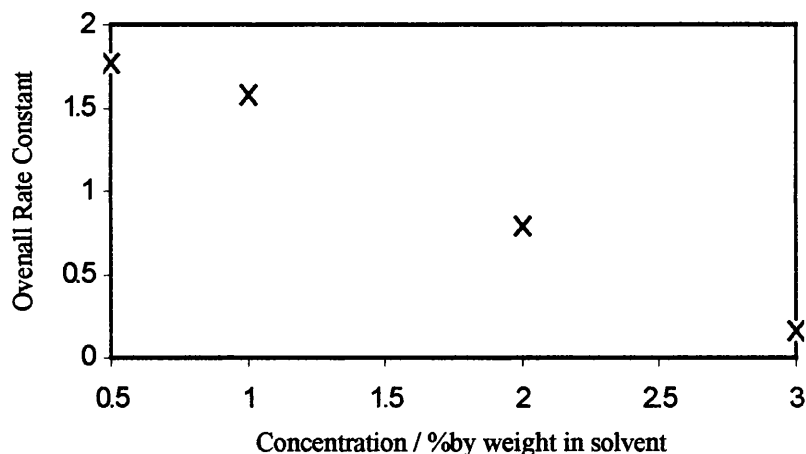


Figure 44: Plot of k (Overall rate constant) vs Concentration of Polyisoprene in Toluene

These results are very similar to those for polystyrene, with the expected curved degradation plot, with lower concentrations degrading faster and all eventually reaching a common limiting value (approximately 50,000). Again the Overall plot shows a better fit than the Schmid treatment with both plots of k vs concentration showing a decrease in rate with increasing concentration. Comparison with the rate vs concentration plots for polystyrene show that

polyisoprene degrades at a lower overall rate. This is most likely because of the higher viscosity of polyisoprene, which will decrease the effects of cavitation.

6.1.4. PVC/Tetrahydrofuran

A 1% solution of PVC in THF was prepared and sonicated for 6 hours with samples taken regularly. The samples were then analysed via GPC. The results are displayed below.

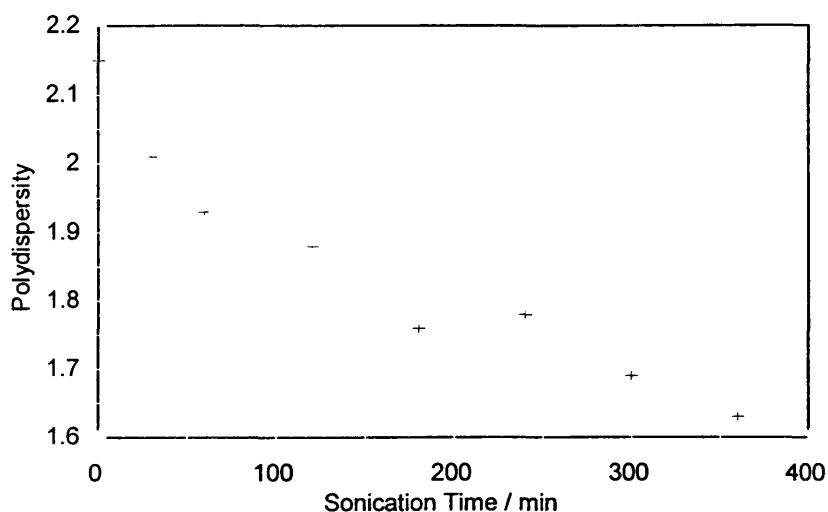


Figure 45: Polydispersities vs Sonication Time For Poly(vinylchloride) Solutions.

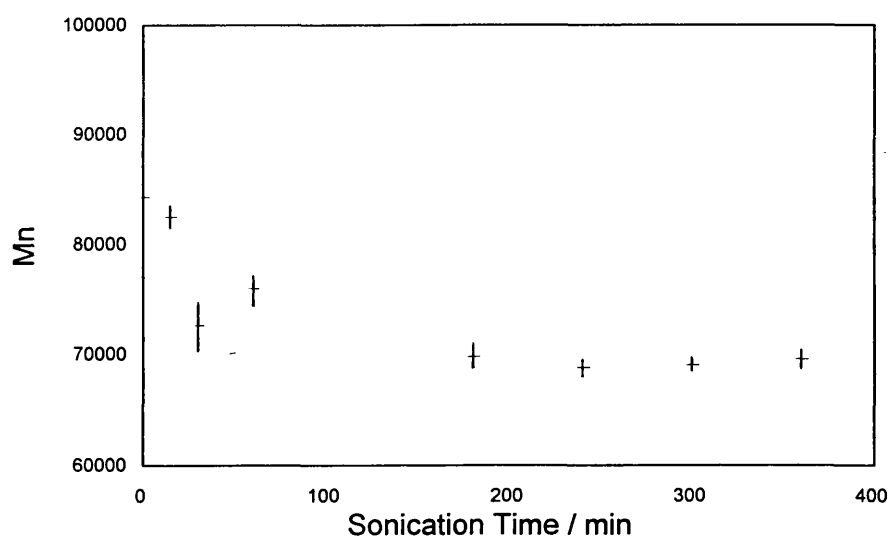


Figure 46. Mn vs Sonication Time For 1% Poly(vinylchloride) Solution.

PVC gives the typical curved degradation plot, with a limiting M_n value of around 68000.

6.3 Section Discussion

The degradation plots obtained for the 1-5% polystyrene solutions were as expected, showing an initial sharp fall, followed by gradual reduction in molecular mass to a minimum. Also the lower the concentration of the solution the faster it degrades. The reasons for these trends are that large chains are broken first with the ultrasound having no effect on chains with a weight below around 35000.

At higher concentrations (10-15%) the plots are more erratic. It was thought that the high viscosities of these solutions may cause this. The polymer content of these solutions, especially the 15%, was close to the physical limit of the amount it is possible to dissolve in toluene. It is possible that the high viscosities of the solutions are preventing adequate mixing, and so some areas of the solution are subjected to different amounts of sonication to others. This, is shown in chapter 8, in the sonication of viscous poly(dimethylsiloxane), where dead spaces (areas of no mixing) can be seen.

The results for all solutions of *cis*-polybutadiene gave extremely erratic graphs, which cannot be explained by the effects of viscosity alone. In fact, actual increases in M_n occur in places. Repetition of these experiments gave the same, erratic, results. The nature of the polymer itself with its double bonds present is causing these effects, with chain branching and back-biting reactions occurring across the double bonds along the polymer chain which explains the increases in M_n . To prove that this was the case, samples of the polybutadiene solution (sonicated and non-sonicated) were analysed by NMR. The ^{13}C NMR (figure 32) showed a peak denoting an unprotonated sp^2 carbon in the polymer. This could only be present if the reaction mechanism shown on page 91 is occurring.

The solutions of polyisoprene were similar in viscosity to the *cis*-polybutadiene solutions, yet almost perfect degradation curves were obtained. Although, again, the most erratic plot of all the polyisoprene results was from the most viscous (3%), showing that there is a decreased mixing effect.

Poly(vinylchloride) degrades in solution, giving the characteristic degradation plot. The various polymer degradation results displayed here are sufficient to show that the use of ultrasound on polymer solutions will cause a reduction in M_n for most polymers. This work has also reinforced earlier work⁶⁸; which suggests that the effectiveness of this technique is reliant upon viscosity/concentration and sonication time, by showing this effect in a variety of different polymers.

The plot of k vs concentration for polystyrene shows a lowering of the rate with increasing concentration. This is because at low concentrations, the polymer chains are relatively free from contact with other polymer chains, so as cavitation occurs the polymers are readily stretched and broken by the intense shear gradients formed. As the concentration increases, the effect of the shear gradients is diminished as the large volume of polymer chains will hinder the flow of polymers towards the cavitation site so lessening the effect. The net result is that polymers near the bubble site will still be degraded, but the range of the shock wave will be smaller, so reducing the overall reduction in molecular weight and the rate.

The Schmid plots for these polymers show the limitations of this equation for deriving kinetic schemes. Schmid plots applied to these polymers are linear, at first, as expected, but this trend breaks down after around 200 mins. This is because there are a number of problems with this treatment. One of which is the derivation assumes an initially monodisperse polymer so that the initial distribution of molecular weights, and the variation in weights caused by degradation are not taken into account. Various other treatments exist including equations by Fujiwara and also by Ovenall. Treatment of the results using the Ovenall equation lead to better results than those for the Schmid treatment, and give a determination of the rate constant using all the points on the graph, not just the first half of the experiment.

Comparison of the polystyrene and polyisoprene rate constant vs concentration plots (both Schmid and Ovenall) show a linear drop in rate vs concentration for all the graphs and a greater overall rate of degradation for polystyrene. This is probably because polyisoprene was much more viscous in solution than the equivalent weight of polystyrene. As already stated, increasing

viscosity will decrease cavitation, so the degradation rate will be less for the more viscous solution.

The results shown in this chapter lay the basic groundwork for the rest of the project by showing that the use of ultrasound does cause reduction in molecular weight in a variety of polymers. It is important that this was illustrated as the compatibilisation technique relies upon the occurrence of this reaction.

7.0. Electron Microscope Study Of The Effects Of Ultrasound On

Solutions Containing Two Polymer Species

In order to show that the ultrasonic compatibilisation theory (page 52) was viable, pairs of polymers, which had already been shown to degrade in solution, were mixed in a mutual solvent and sonicated (page 77). The effects of this sonication were observed by scanning electron microscopy (SEM), where it was expected that the evidence of polymer phase separation would be less for the sonicated examples. If this was the case then the next step was to sonicate molten polymers.

7.0.1 Polystyrene/Polyisoprene 1:1

The following were prepared for study by SEM:

Polystyrene / polyisoprene mixture (1% each by weight in toluene)

Polystyrene (1% by weight in toluene)

Polyisoprene (1% by weight in toluene)

The single polymer solutions were sonicated separately and then mixed. Samples for SEM were prepared as described on page 78.

The sonicated together results show little evidence of any phase separation of the polymers. For both the unsonicated and sonicated separately polymer mixes, the SEMs show clear evidence of phase separation, this is shown by the appearance of distinctly different regions (circular areas) on the SEM images. From the SEM results it can be seen that the polymer mix becomes more homogenous when the polymers are sonicated together rather than mixed after sonication, indicating an in-situ reaction creating copolymers which compatibilise the polymer-polymer mix.

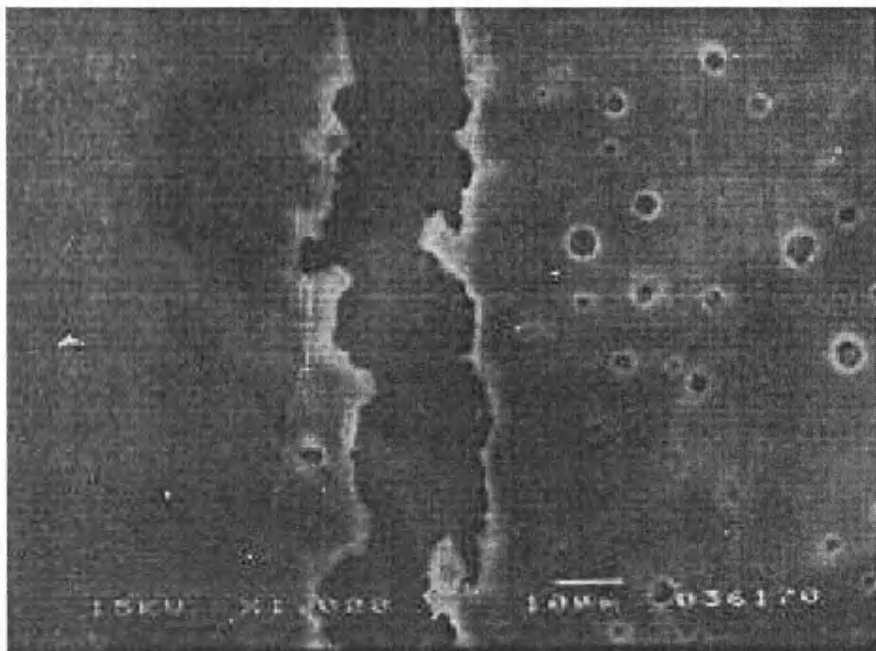


Figure 47: PIP/PS, 1:1, prior to sonication

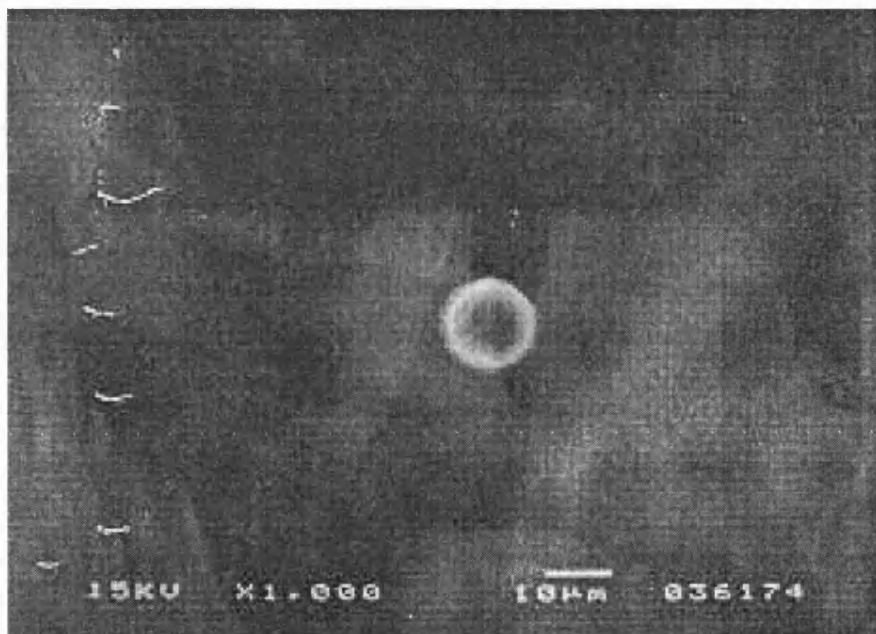


Figure 48: PIP/PS, 1:1, sonicated separately for 6 hours prior to mixing



Figure 49: PIP/PS, 1:1, sonicated together for 6 hours

7.0.2. *Polystyrene/Polymethylmethacrylate in tetrahydrofuran*

Polystyrene (PS) and Polymethylmethacrylate (PMMA) were sonicated (19.8 kHz, 10 W), in tetrahydrofuran (1% by weight solution) both separately and mixed together. The separately sonicated solutions were mixed together after sonication as described earlier. Results were obtained by SEM, which show no difference between any of the samples. This failure of compatibilisation was surprising, and the next step was to try again using a different solvent, in order to rule out any effect due to tetrahydrofuran.

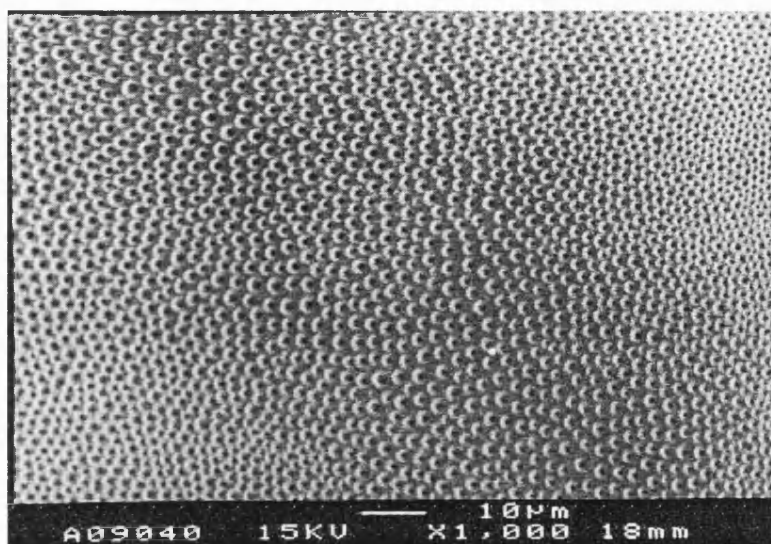


Figure 50: PMMA/PS 1:1 Before Sonication in THF, mag x1,000

The above photograph, as with all the SEM results shown for this polymer pair, shows one polymer phase in which are many separate globular arrangements of the other polymer. As this picture shows a 50/50 mixture, there is no way of knowing which polymer is which. Achieving magnifications of much greater than x2,000 was extremely difficult, as this focuses the microscope's electron beam on a much smaller area leading to 'burning' of the polymer film. The black areas in the middle of many of the globular structures are caused by this process. However, the net result is still obvious, the two polymers are still separated.

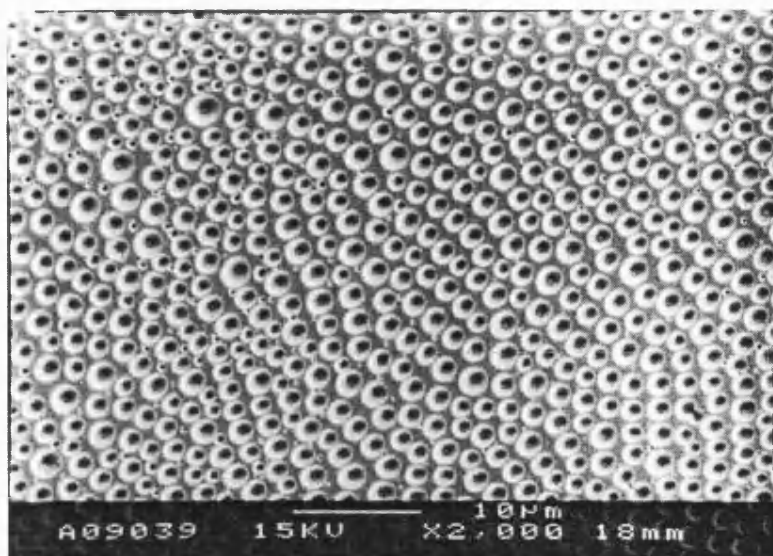


Figure 51: PMMA/PS 1:1 Before Sonication in THF, mag x2,000

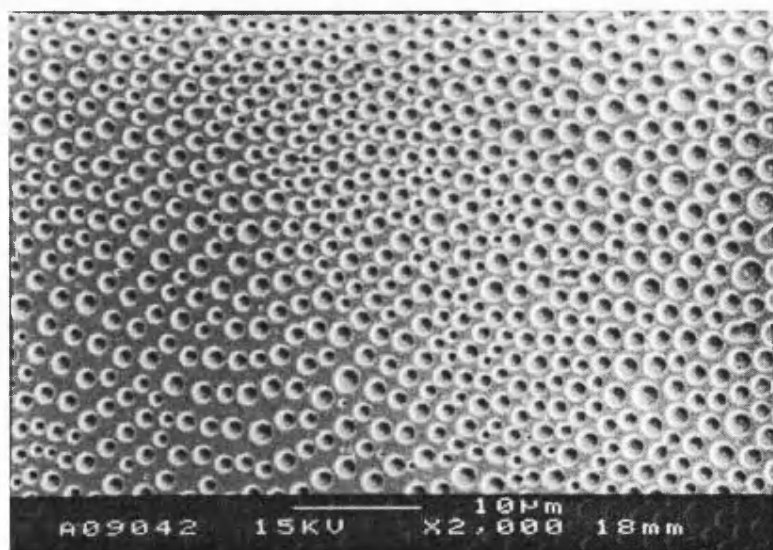


Figure 52: PMMA/PS 1:1 sonicated for 1hr in THF, mag x2,000

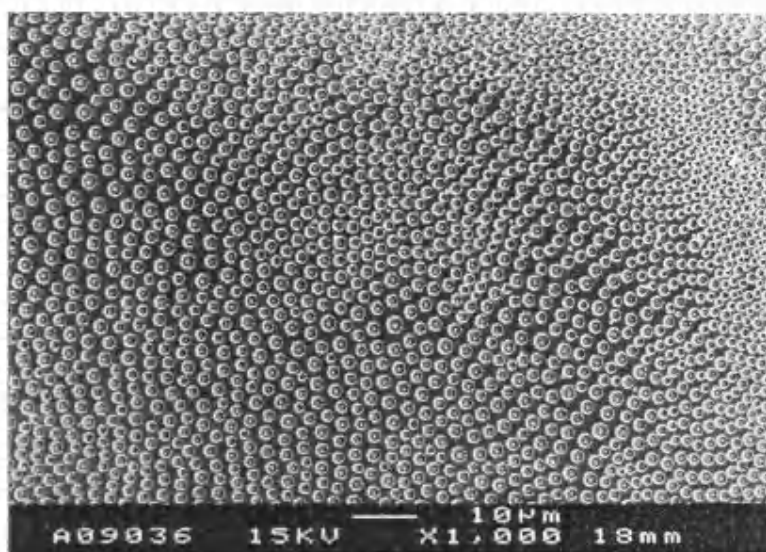


Figure 53: PMMA/PS 1:1 sonicated for 3hrs in THF, mag x1,000

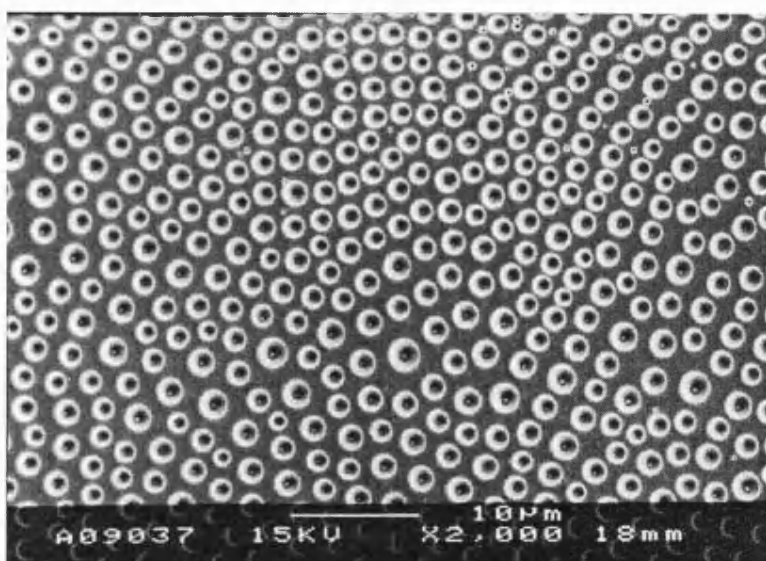


Figure 54: PMMA/PS 1:1 sonicated for 3hrs in THF, mag x2,000

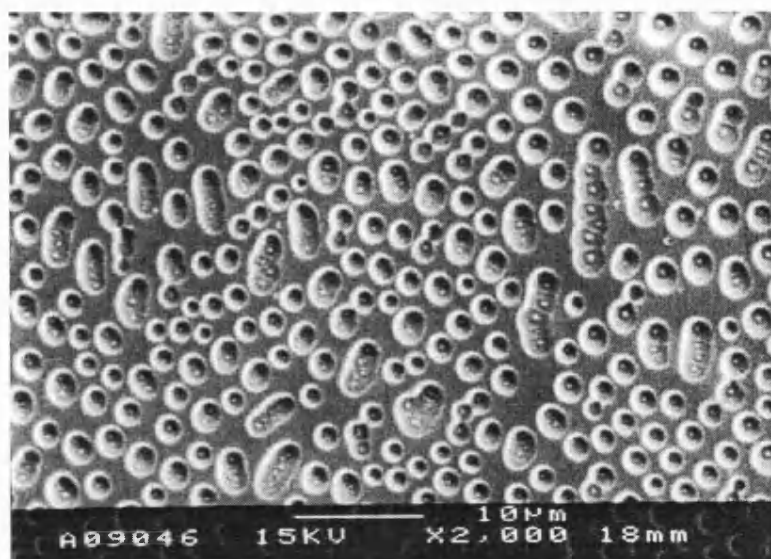


Figure 55: PMMA/PS 1:1 sonicated for 6hrs in THF, mag x2,000

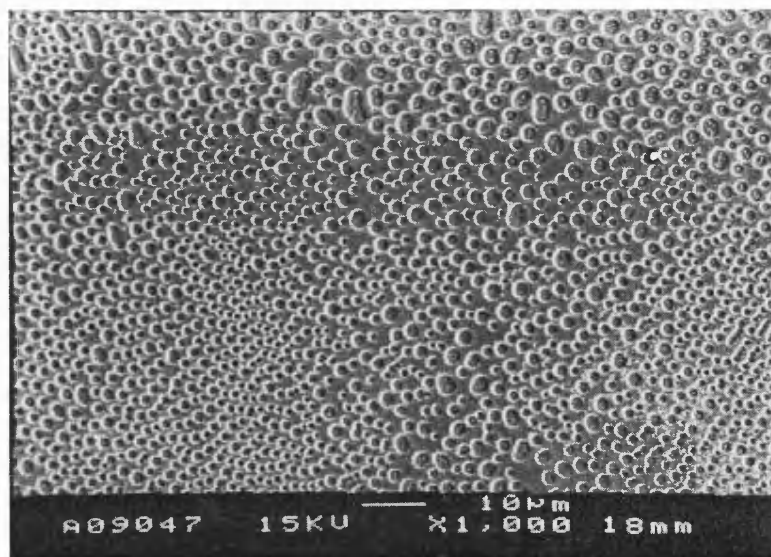


Figure 56: PMMA/PS 1:1 sonicated for 6hrs in THF, mag x1,000

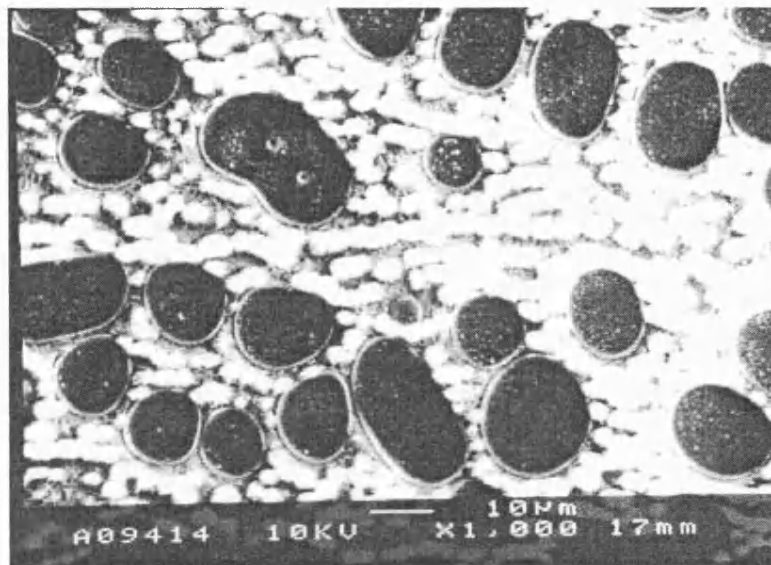


Figure 57: PMMA/PS 1:1, sonicated separately for 6hrs before mixing, mag x1,000

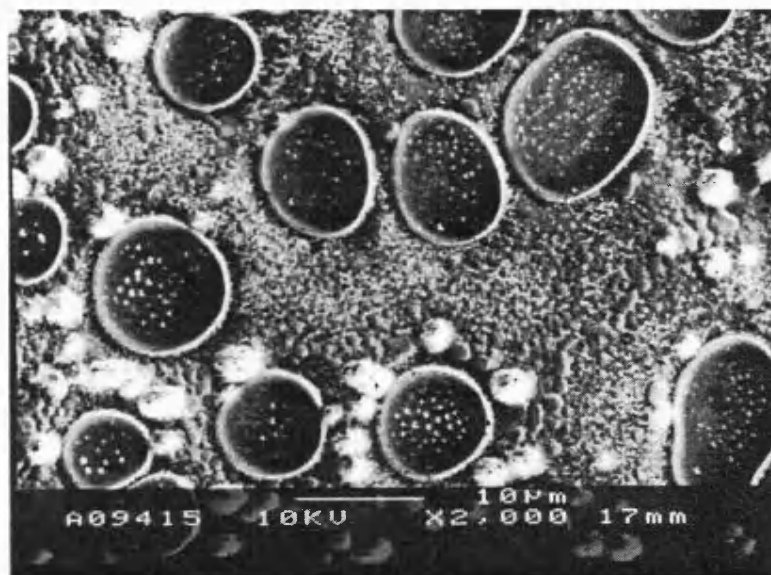


Figure 58: PMMA/PS, 1:1, sonicated separately for 6hrs before mixing, mag x2,000

From the SEM results it can be safely concluded that sonication of this polymer pair does not lead to compatibilisation. In each case the polymers appear distinctly separate.

This result was surprising, but subsequent repeats of this experiment yielded the same images. It is also noted that time zero and sonicated samples appear the same under SEM (small, spherical second phase) whereas sonicated separately and mixed gave larger, irregular phase domains. This difference is due to mixing techniques and will be discussed further, along with possible explanations for the lack of compatibilisation, in the section discussion at the end of this chapter.

7.0.3 Polystyrene/Poly(methylmethacrylate) in Toluene

Further to the problem of polystyrene (PS) and poly(methylmethacrylate) (PMMA) compatibilisation (section 7.0.2), the experiment was repeated using a different solvent (toluene) in order to discount any effects due to tetrahydrofuran causing phase separation. SEM (scanning electron microscopy) showed that the mixture still does not compatibilise as can be seen from the photographs displayed below (0 and 6hrs both polymers sonicated together). In each case one of the polymers has clustered together in many globular formations. A possible explanation is outlined at the end of this chapter. Figure 60, illustrates the experimental problem of the polymer film burning under the electron beam.

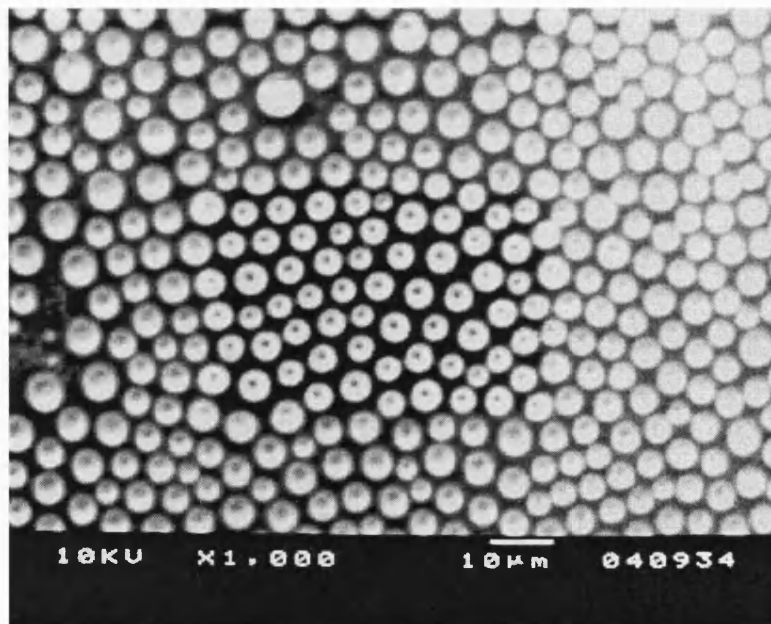


Figure 59: PMMA/PS 1:1 before sonication, in THF, mag x1,000

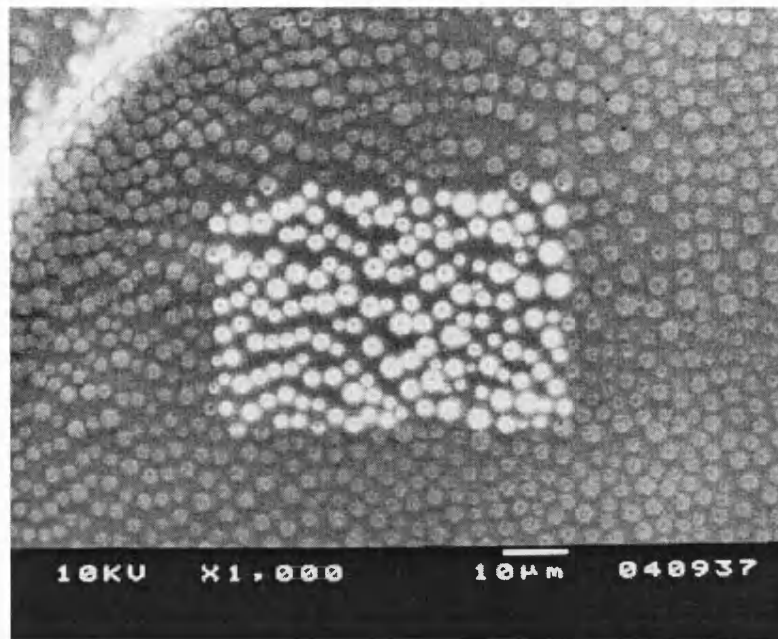


Figure 60: PMMA/PS 1:1 sonicated for 6hrs in THF, mag x1,000
note: bright patch due to 'burning' by the electron beam.

7.0.4 Polyisoprene/Poly(methylmethacrylate)

Solutions of Polyisoprene and Polymethylmethacrylate were prepared in toluene (1% by weight). These were then sonicated separately and mixed as before. The SEM results are displayed below. Figure 61 (mixed polymer, no sonication) shows a good example of a phase separated polymer mix, with the light and dark areas representing each polymer. As the sonication experiment progresses, this can be seen to become less pronounced, indicating that compatibilisation has possibly taken place. Evidence that the process is an *in situ* reaction and not merely due to polymer chain degradation can be seen in Figure 65 where the polymers had been sonicated separately before mixing. In this case phase separation is still very much in evidence.

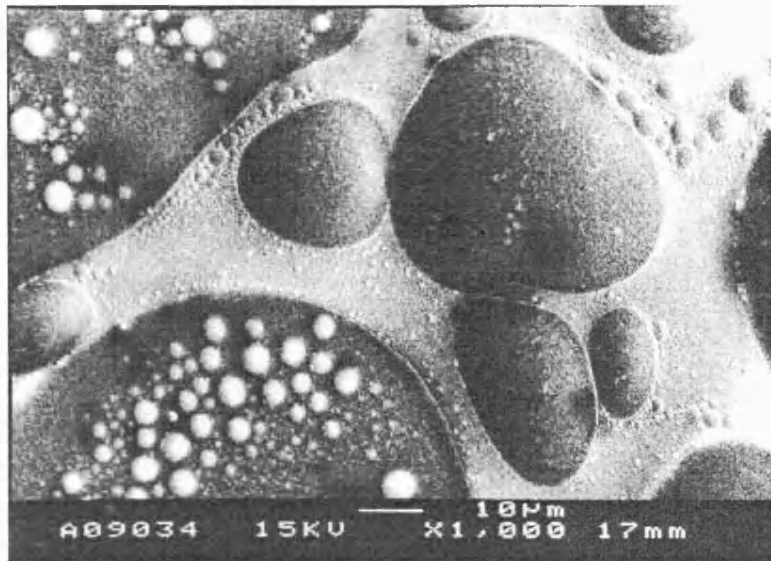


Figure 61: PMMA/polyisoprene (PIP) 1:1 before sonication, in toluene, mag x1,000

It can be seen, quite clearly, that prior to sonication the polymers were very much 'phase separated'.

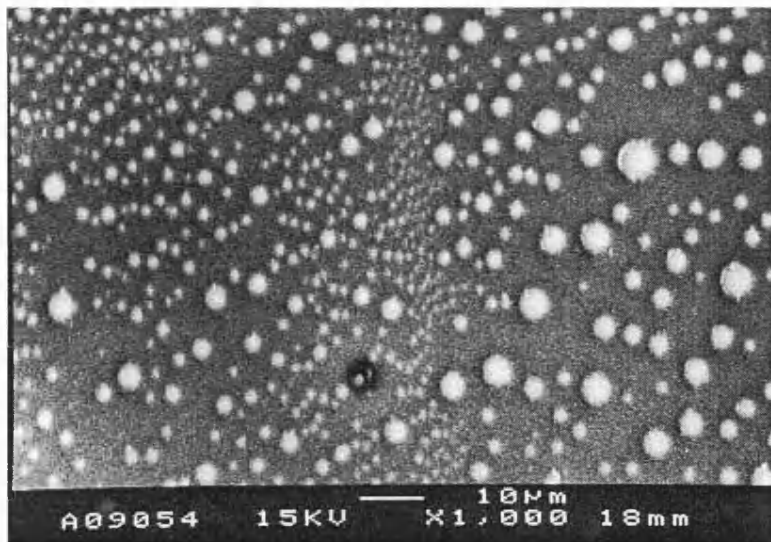


Figure 62: PMMA/PIP 1:1, sonicated for 1hr in toluene, mag x1,000

After 1 hour of sonication, the phase separation has broken down into a more dispersed structure, further sonication reduced the phase separation further still.

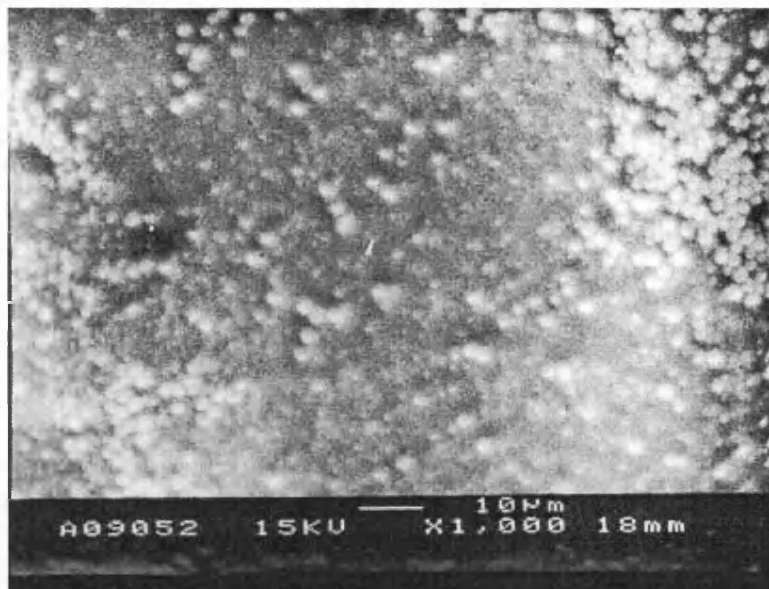


Figure 63: PMMA/PIP 1:1, sonicated 3hrs in toluene, mag x1,000

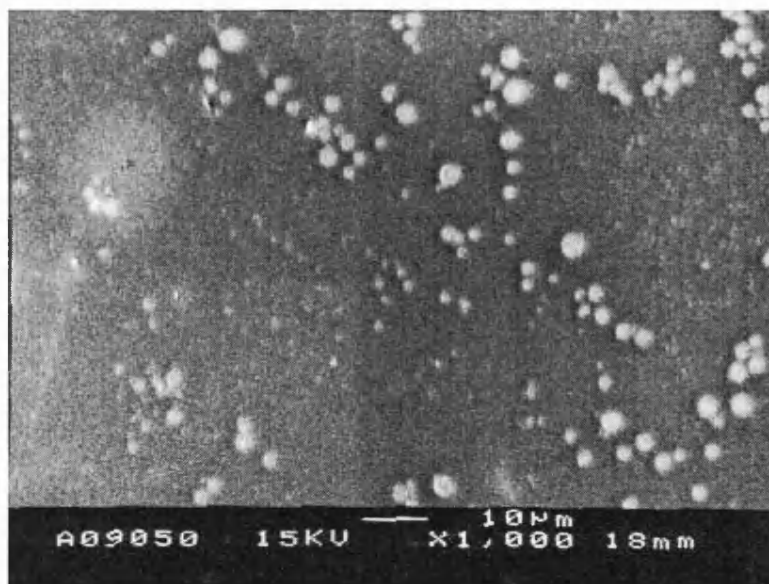


Figure 64: PMMA/PIP 1:1, sonicated for 6hrs in toluene, mag x1,000

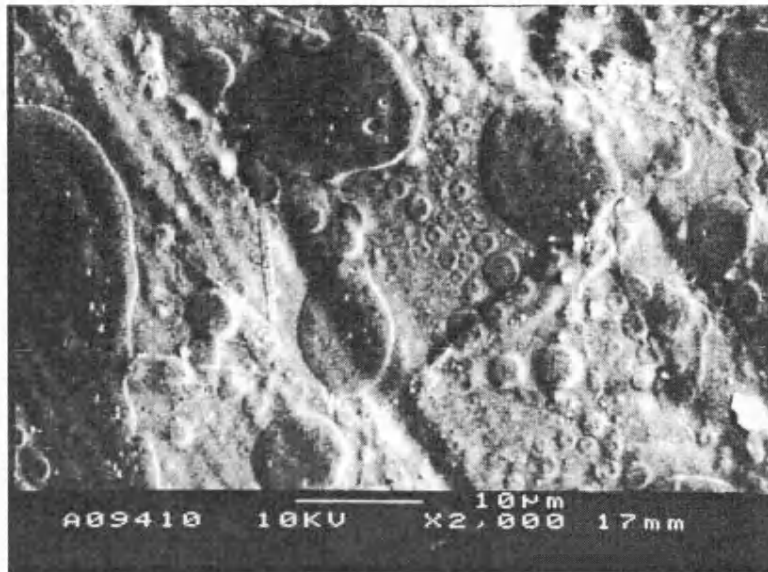


Figure 65: PMMA/PIP 1:1, sonicated separately for 6hrs before mixing, mag x2,000

The SEM results for PMMA/PIP show increasing homogenisation of the polymer mix at a microscopic scale with increasing duration of sonication. Evidence that this is not merely related to chain degradation i.e. shorter polymer chains could give rise to better mixing, is shown by figure 65 in which the polymers were mixed after sonicating separately. In this case the image shows the polymers still very much phase separated.

It could be argued that the polymers in the sonicated together images are merely very finely dispersed due to ultrasonic mixing, but I believe that although this is a major factor in the process, the stability of the resulting mix can only be explained by the presence of copolymers. As the polymers were sonicated in solution and solvent cast to create SEM samples, phase separation due to solvent should have separated the sonicated together polymers, unless some copolymer had been formed which would interfere in this process by stabilising the polymer in the finely dispersed form

7.0.5. Polyethylene / Polypropylene in Decalin

Solutions of polyethylene (PE) and polypropylene (PP), both separately and mixed, were prepared in decalin at 140°C (1% concentration of each polymer). All the solutions were then sonicated (19.92 kHz, 10 W) for 6 hours in a water-jacketed reaction vessel at 95°C. Samples were taken periodically at 0, 3 and 6 hours. The samples from the single polymer solutions were then mixed with each other. Each sample was then solvent cast and sputter coated with gold for observation by SEM.

The results obtained are not as clear cut as for those with polyisoprene/poly(methylmethacrylate) or polystyrene/polyisoprene.

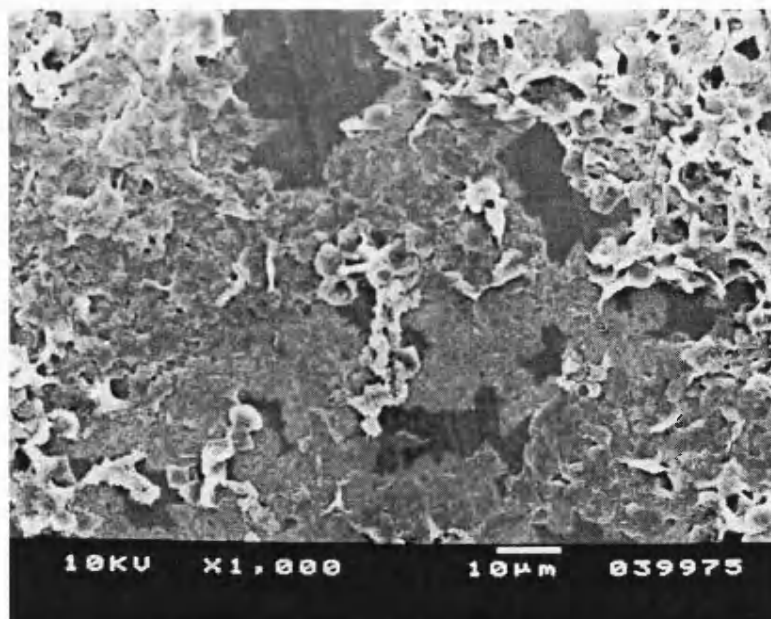


Figure 66: PE/PP 1:1, before sonication, in decalin, mag x1,000

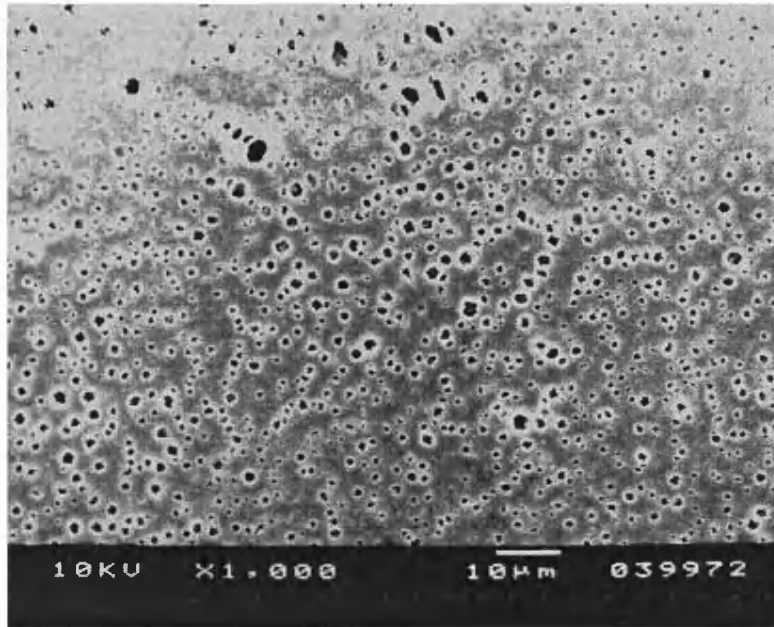


Figure 67: PE/PP 1:1, sonicated for 3hrs in decalin, mag x1,000

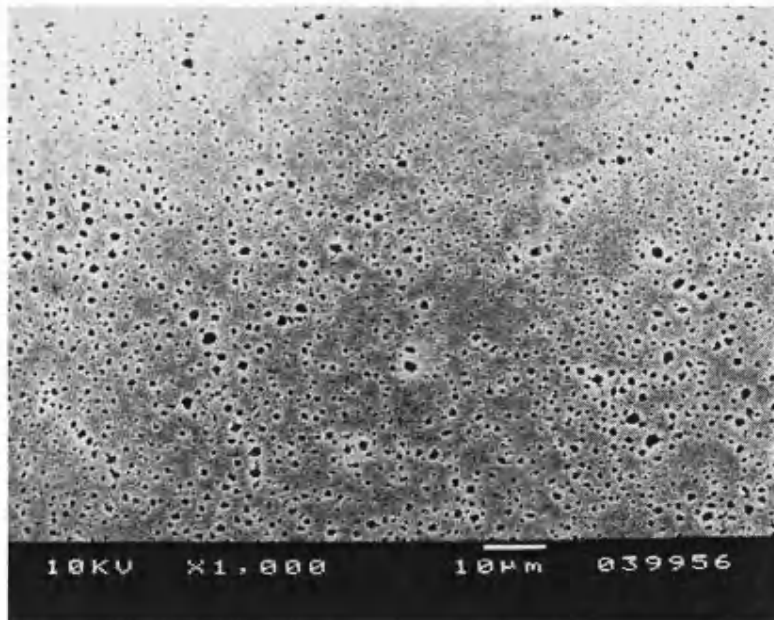


Figure 68: PE/PP 1:1, sonicated for 6hrs in decalin, mag x1,000

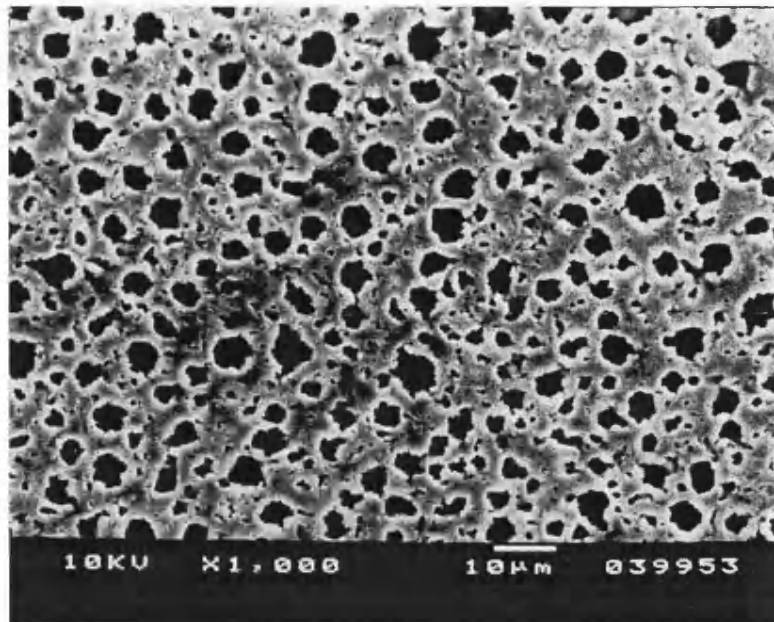


Figure 69: PE/PP 1:1, sonicated separately for 3hrs in decalin before mixing, mag x1,000

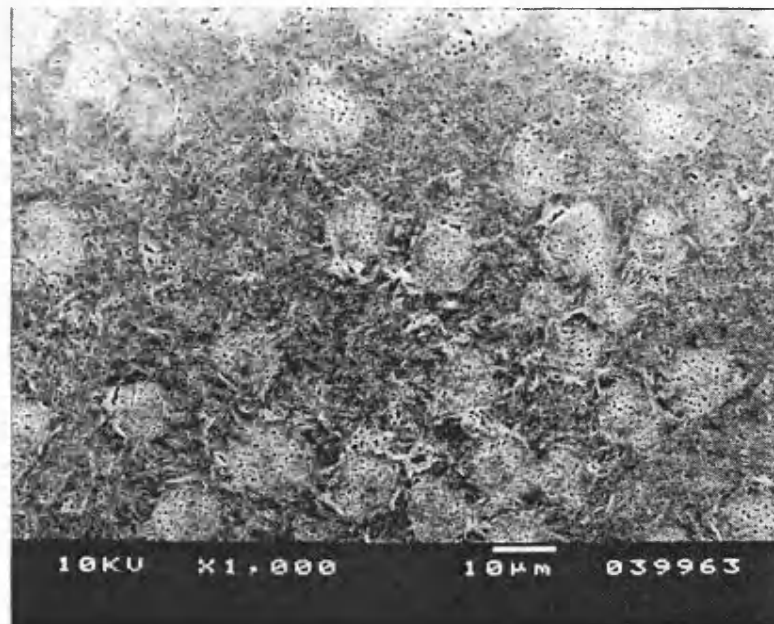


Figure 70: PE/PP 1:1, sonicated separately for 6hrs in decalin before mixing, mag x1,000

7.1 Section Discussion

Practical problems included rapid burn up of some of the polymer samples under the electron beam. This was overcome using a thicker gold coating when preparing the SEM samples. The use of ultrasound to compatibilise immiscible mixtures has noticeable effects on PMMA / PIP, PS / PIP and PE / PP mixtures. However the PS / PMMA mix does not seem to be affected to any significant extent.

The electron micrograph studies of polystyrene/polyisoprene mixtures show the effects of ultrasound. The unsonicated mixture showed many regions of phase separation. These are areas where the polymers form separately from each other due to poor mixing or non-compatibility. The sonicated mixture shows virtually no phase separated regions. The mixture which was sonicated separately and then mixed also showed large areas of phase separation, which discounts the possibility that a simple reduction in molecular weight is the main cause of this effect as polymer degradation will have occurred in both of the sonicated systems. The sonicated together mixture has no phase separations due to the enhanced mixing effect of ultrasound. This is then stabilised by the presence of copolymers, causing the polymers to become more miscible and so preventing the polymers from separating in the highly dispersed mixture. As the polymers were sonicated in dilute solution (1% by weight of each polymer) and cast in solution to make SEM samples, if no copolymer stabilising the dispersed mixture had been present it is very unlikely that anything but a phase separated image would have been seen.

From SEM results it can be concluded that sonication of the PMMA/PS pair does not lead to compatibilisation. In each case the polymers appeared distinctly separate. Interestingly for the sonicated separately polymer results, although the polymers still appear phase separated, the photograph differs from the sonicated results in that the separate phases are much larger and more irregular. This is due to the enhanced mixing effect caused by ultrasonic cavitation, resulting in a more finely dispersed polymer mixture in the case of the sonicated together mixture. As the separately sonicated solutions were simply mixed by pouring together and shaking, a less well mixed image is seen.

The reason for the lack of compatibilisation in this case is unknown. Solvent effects are unlikely as similar results were obtained in both THF and toluene. It is also noted that time zero and sonicated samples appear the same under SEM (small, spherical second phase) whereas sonicated separately and mixed gave larger, irregular phase domains. This difference is due to mixing techniques, the sonicated separately samples were simply poured together and shaken, whilst the time zero samples had been mixed together over a long time period (>1 day) and the sonicated together samples had also been subject to ultrasonic mixing. This indicates that if copolymer was formed, its presence is not sufficient to overcome the repulsive effect between the two polymers. Other explanations could be steric hindrance between the two polymers preventing copolymer formation or it could be that the relative rates of macroradical formation for each polymer differ greatly. If one is much faster than the other, then the possibility of copolymer formation would be reduced as the chances of two different macroradicals meeting would be reduced. However, in the last case it is still possible that some copolymer would form over six hours of sonication.

An interesting observation was that the many globular clusters of one of the polymer phases in the PS/PMMA electron micrographs were indicative of phase separation via nucleation. This phenomena is associated with metastable polymer mixtures, which leads to a possible explanation for the rapid burn up of the polymer film under the electron beam of the SEM. Unlike spinodal decomposition, where the polymer mix phase separates spontaneously, metastable mixtures require a small amount of energy to separate. The difference can be envisaged as such; a spinodally separating polymer mix starts at the top of a free energy curve, so it is unstable and will decompose immediately (see figure 71, below).

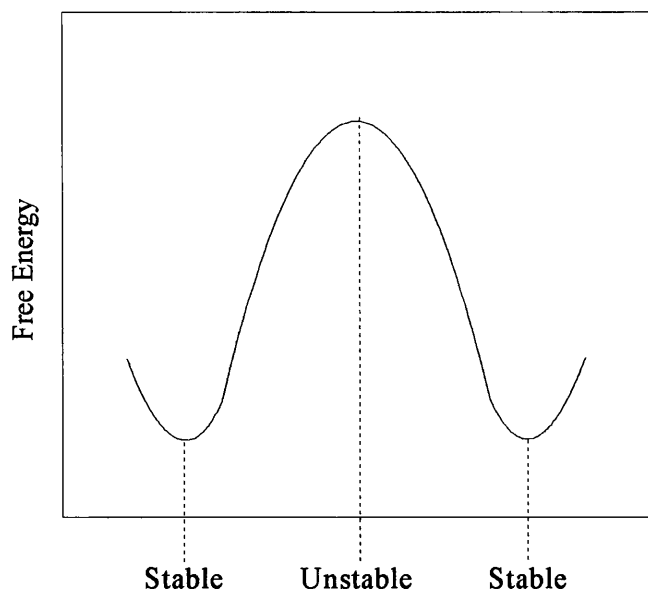


Figure 71. Free Energy curve for a spinodally separating polymer mixture. The polymers are mixed at the top of the curve and separated at the stable regions at the bottom of the curve.

A metastable mix, although not at the point of lowest free energy, is in a small 'potential well', in order to phase separate a small amount of energy is required to push it out of the 'well' (see figure 72. below).

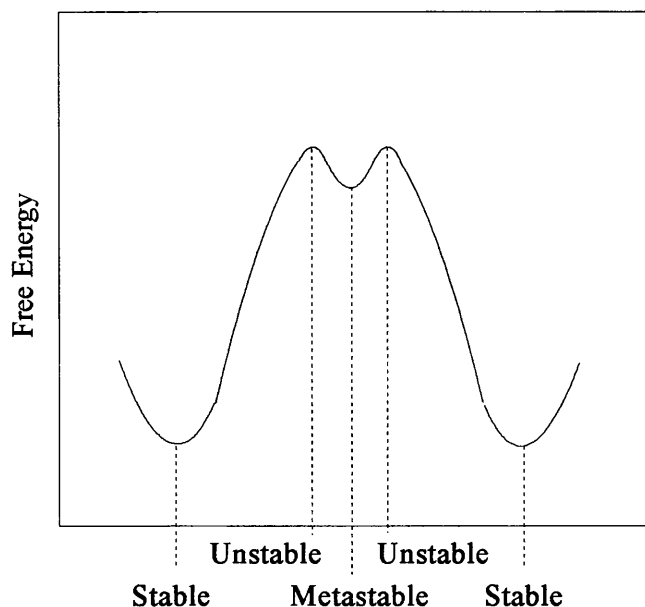


Figure 72. Free Energy diagram for a metastable polymer mix. The polymer mix at the metastable area requires a small amount of energy before it can phase separate to reach the stable areas at the bottom of the curve.

It is possible that the energy from the SEM electron beam is speeding this process, hence the observed burn up of the polymer film as the polymer uses this energy to separate further. This enhancement of nucleation under an electron beam has been shown by SEM studies of 25%PMMA / 75% styrene/acrylonitrile polymer by McMaster¹⁴⁷.

8.0. Polymer Degradation In The Melt

As the final aim of the project was to investigate polymer compatibilisation in the melt, then a logical step was to first carry out sonications of single polymer melts. If polymer degradation increased due to the presence of ultrasound (some thermal degradation may also occur), then radical formation is taking place and so compatibilisation may be possible.

8.1. Observation of Melt Flow due to Ultrasonic Mixing

Before attempting polymer melt degradation, it was thought useful to ascertain whether any effect due to ultrasound was possible in a very viscous medium. The most obvious and easiest effect to detect is that of ultrasonic mixing. Two experiments were devised, which are shown below.

8.1.1 PDMS Melt Flow Simulation

A simple observational experiment was used in order to ascertain the presence of mixing via ultrasound in a viscous solution, such as you would find in a polymer melt. For this a naturally viscous polymer was used, poly(dimethylsiloxane) (PDMS), which also has the advantage of being transparent and colourless. PDMS with a viscosity of 30,000 centistokes was poured into a beaker shaped glass vessel, of similar dimensions found in the furnace. This was then sonicated with the horn at the top of the liquid, and the resulting flow of polymer observed and drawn. This was then repeated with the sonic horn dipped further into the liquid.

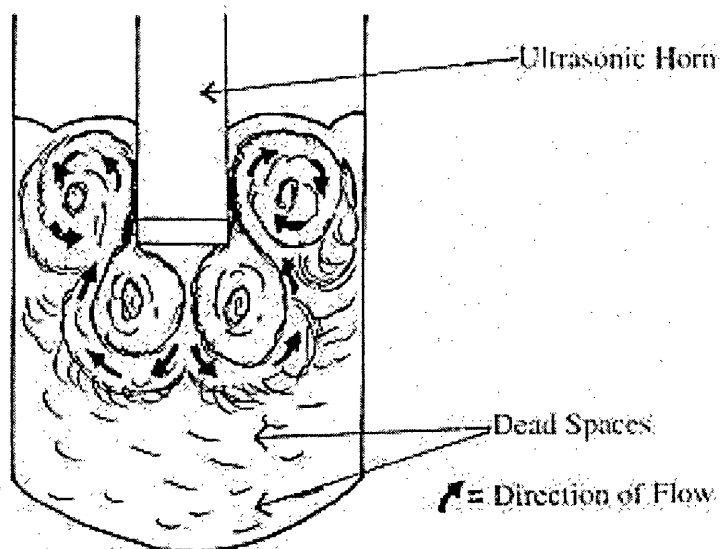


Figure 73: Flow lines of PDMS subjected to ultrasound

The sketches above made from observation of this experiment, show clear regions of intense flow, due to the action of ultrasound. At the bottom of the reaction vessel, there can be observed 'dead spaces', areas with little to no mixing occurring. These observations were useful in the planning of further experiments, especially, when taking samples for further study.

8.1.2 Sonication of PMMA / Silica layers

Layers of Poly(methylmethacrylate) (PMMA) and silica were arranged in a furnace. This was then heated to 240⁰C under vacuum and then sonicated for one hour. The contents were then allowed to solidify before removing the horn and temperature probes. The resulting solid cylinder was then cut in half vertically to show the mixing effects of ultrasound on a polymer melt. If ultrasonic mixing had occurred in the molten system, then the horizontal bands of silica and PMMA would be broken up and disordered, if mixing had not occurred the lines would have been largely intact.

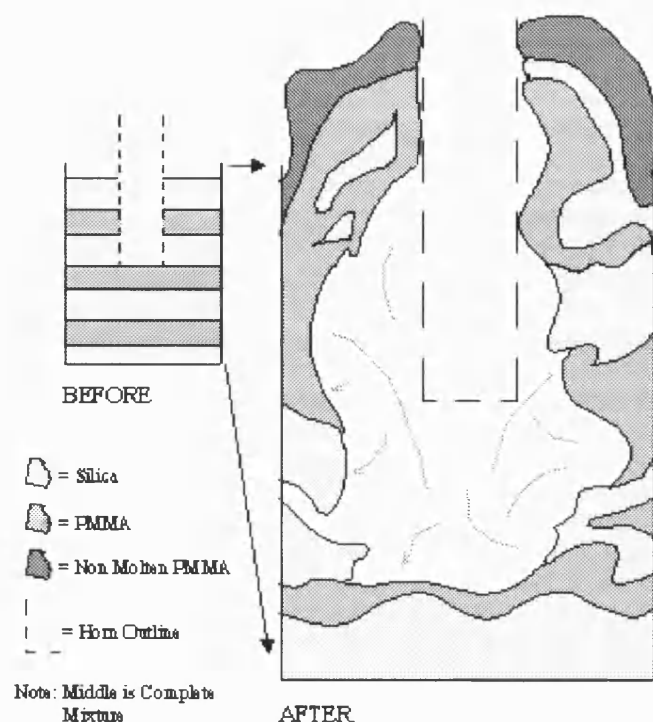


Figure 74: Diagram showing disruption of silica/PMMA layers upon sonication

The patterns displayed show a good correlation with that of the PDMS flow experiment, with the areas of good mixing being directly underneath the horn and along the sides of the horn towards the surface of the reaction vessel. Again the "dead spaces" where at the bottom of the reaction vessel, which indicate the areas least likely to be affected by ultrasound. These two experiments showed where the most likely site of any ultrasonic cavitation will be, and so for all the following experiments, samples were taken from the middle of the polymer melt, slightly underneath the horn.

8.2. Ultrasonic Degradation of Molten Polymers

A major aim of this project was to investigate the behaviour of molten polymers when subjected to ultrasonic irradiation. To do this, a furnace and controller were designed and constructed (page 78) which enabled the experiments to be carried out under controlled conditions. Samples of the sonicated molten polymers were sent to RAPRA for analysis by GPC (page 67) and compared with

blanks which had been subjected to the same temperature without ultrasound for the same length of time.

8.2.1 Polystyrene

Results are shown below for 35g of polystyrene sonicated (19.52 kHz, 10 W) at 240⁰C under vacuum and also for samples subjected to heat only. Each timed run was for a separate 35g sample. The results are presented in a table below, with the Mn values also plotted against time on a graph.

Sonicated Runs

<u>Time</u>	<u>Mn</u>	<u>Polydispersity</u>
0 hr	120000	2.6
3 hr	106000	2.9
7 hr	75000	3.0
9 hr	76000	2.7

Heat Only

<u>Time</u>	<u>Mn</u>	<u>Polydispersity</u>
3 hr	126000	2.6
7 hr	108000	2.7
9 hr	125000	2.8

It was also observed that the temperature in the middle of the melt (i.e. nearest the ultrasonic horn) initially increased by approximately 10⁰C when the ultrasound was applied. This returned to the set temperature as the electronic temperature controller automatically made adjustments. This observation suggests that ultrasonic mixing is occurring as, due to the furnace design, the polymer will be hottest at the edge of the furnace whilst the polymer is being brought up to the required temperature and will slowly even out once it reaches this. Upon sonication, however, the hotter polymer at the edges is mixed with the colder polymer at the core of the furnace, causing this ‘evening-out’ process to speed up.

This is observed by the reading from the temperature probe closest to the core rising sharply as the hotter polymer is mixed in.

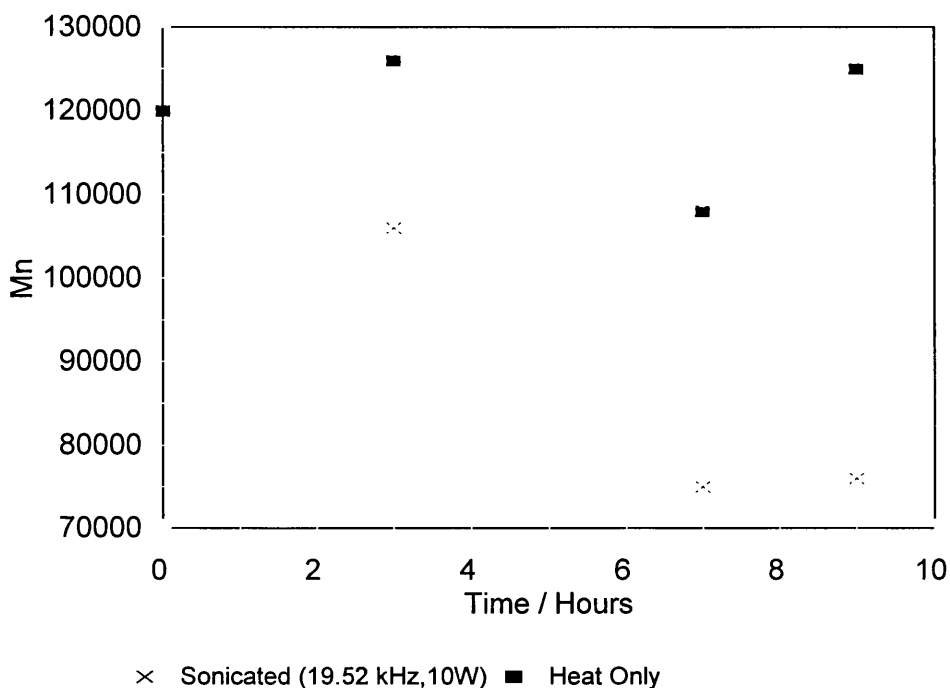


Figure 75: Degradation Plot for Molten Polystyrene

Evidently from the observation of the initial temperature rise upon sonication, mixing is occurring, from the graph it can also be seen that degradation also occurs upon sonication, with the heat only samples showing little variation and no downward trend in comparison to that of the sonicated samples. As each separate time on the graph represents a different sample (it was not possible to take small hourly samples due to the equipment design) some variation in Mn is expected and this is reflected in the heat only samples. However the definite downward trend seen in the sonicated case must be due to increased chain degradation.

8.2.2 Polystyrene (under N_2)

In order to minimise any effects of oxidative degradation, 35g of polystyrene was sonicated in the melt, under a nitrogen atmosphere. The results are presented below. It can be seen that, in comparison to the samples tested under vacuum conditions, the extent of degradation for the sonicated sample is

considerably. Under nitrogen some ultrasonic degradation is still seen to occur in comparison to the heat only samples. It may also be noted that the polystyrene used in this experiment has a higher M_n than the sample used in the vacuum experiment, from this it would be expected that the polymer would degrade faster and show a very large drop in M_n when subjected to ultrasound.

<u>Time</u>	<u>Mn</u>	<u>Polydispersity</u>
0 hr	243,000	4.5
2 hr	225,000	3.8
3 hr	195,000	3.4
4 hr	210,000	3.0
5 hr	228,000	4.0
7 hr	208,000	3.8

Heat Only

<u>Time</u>	<u>Mn</u>	<u>Polydispersity</u>
1 hr	225,000	4.3
2 hr	231,000	5.2
3 hr	223,000	4.1
4 hr	237,000	4.0
5 hr	236,000	3.5

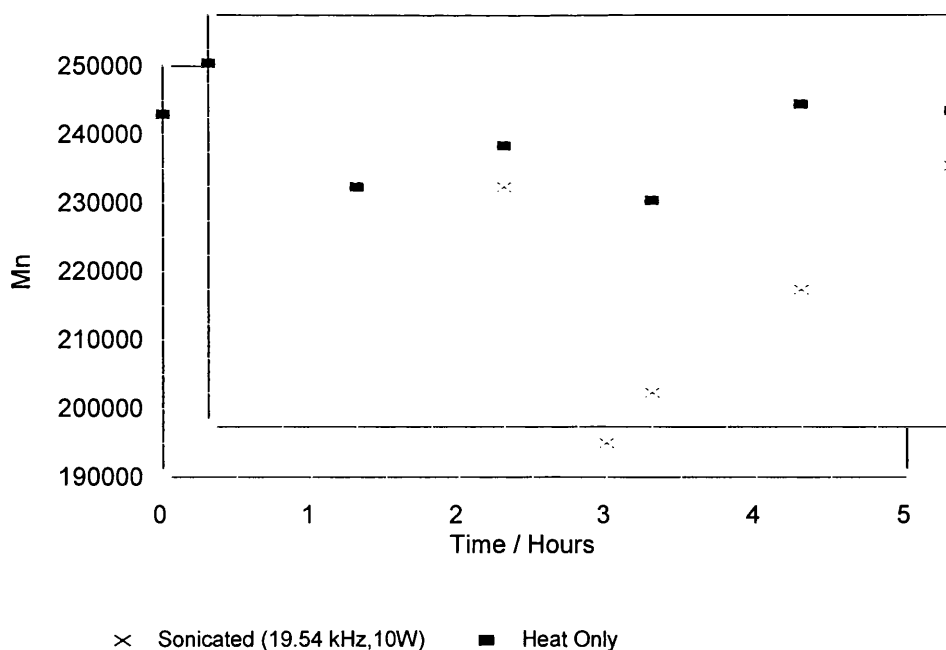


Figure 76: Degradation Plot for Molten Polystyrene Under Nitrogen

The above graph is very different from the graph of sonication of polystyrene under vacuum conditions. Very little, if any, extra chain degradation has occurred in the sonicated under nitrogen samples compared to the heat only samples. After the uncertainties of the GPC measurements and of where the samples were extracted from the samples are taken into consideration it could be safely concluded that no degradation took place.

From the results it seems that degradation occurs more readily under vacuum conditions than under a nitrogen atmosphere. What could be happening is that the 'vacuum' conditions are not perfect, and the ultrasonic mixing effect is efficiently mixing any oxygen present from the partial atmosphere surrounding the furnace causing increased thermal degradation. The use of a nitrogen atmosphere, effectively eradicates this problem, giving similar results for heat only and sonicated samples. A mixing effect could also explain the apparent lowering of polydispersity in the sonicated samples, as smaller polymer chains may move more freely causing a separation of large and small chains, thus creating areas of similar polymer chain length in the melt. It may be possible to prove this by taking many samples from a single sonicated and a single non-sonicated polymer pellet and analysing them by GPC. The non-sonicated polymer should show similar

polydispersities, whereas, if the assumption is correct, many differing polydispersities would be shown for the sonicated samples.

8.2.3 Polymethylmethacrylate

Poly(methylmethacrylate) (PMMA) was studied in the melt. Samples of PMMA (30g) were melted in the furnace at 210⁰C and sonicated (19.57 kHz, 10 Watts, under nitrogen) for up to seven hours. Blanks, where the PMMA was just heated were also carried out. The resulting pellets of polymer were then broken up and samples dissolved in tetrahydrofuran (THF) for analysis by GPC. The GPC results shown below give very similar results for each sample, indicating that little degradation was seen due to ultrasound.

Sonicated Runs

<u>Time</u>	<u>Mn</u>	<u>Polydispersity</u>
0 hr	70400	2.0
4 hr	67500	2.0
5 hr	69300	1.8
7 hr	44900	2.0

Heat Only

<u>Time</u>	<u>Mn</u>	<u>Polydispersity</u>
4 hr	80200	1.9
5 hr	83600	2.0

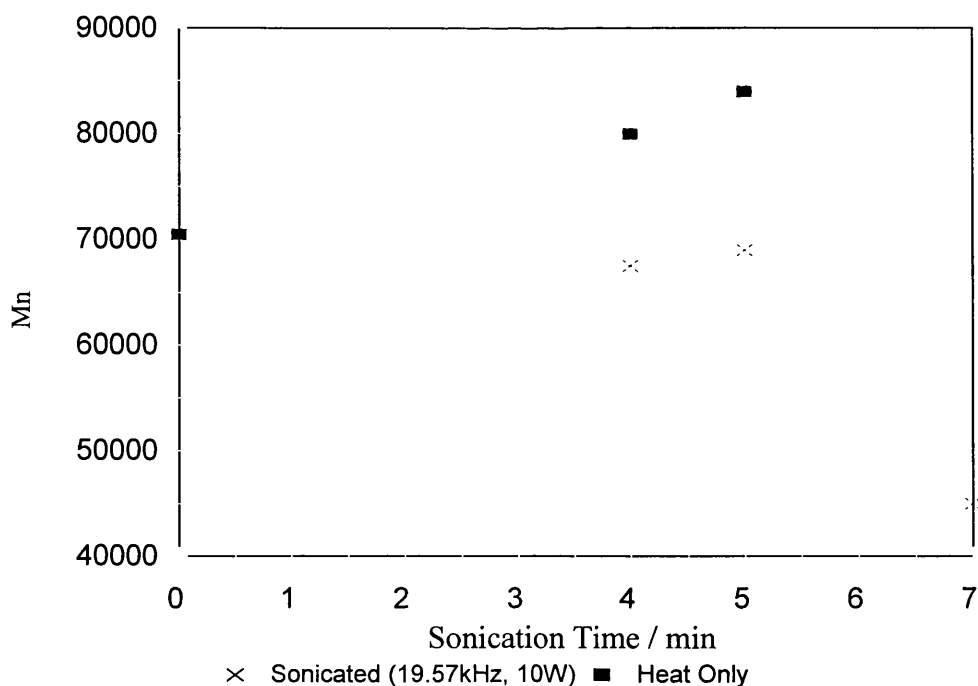


Figure 77: Degradation Plots for Poly(methylmethacrylate) under Nitrogen.

Again, apart from what seems to be an anomalous reading at 7 hrs, extra degradation of the polymer in the sonicated sample is slight. The conclusions drawn from this are similar to that for melt sonication of polystyrene under nitrogen, in that degradation is not occurring. Sufficient difference in polydispersities is not present to lead to any definite conclusions.

8.2.4 Polyethylene

PE was studied in the melt. Samples of PE (35g) were melted in the furnace at 210⁰C and sonicated (19.57 kHz, 10 W, under nitrogen) for up to five hours. Blanks, where the PE was just heated were also made. The results shown below, again show little signs of reduction in Mn, however the polydispersity lowers with increasing sonication time, in comparison to the heat only ‘blanks’, probably due to the mixing effect discussed earlier (page 129).

Sonicated Runs

<u>Time</u>	<u>Mn</u>	<u>Polydispersity</u>
0 hr	76500	5.1
1 hr	76000	5.3
2 hr	77300	5.1
3 hr	75800	5.0
4 hr	77200	4.7
5 hr	63900	4.4

Heat Only

<u>Time</u>	<u>Mn</u>	<u>Polydispersity</u>
1 hr	68500	5.3
2 hr	78000	5.0
3 hr	79800	5.1
4 hr	79100	5.3
5 hr	74300	5.3

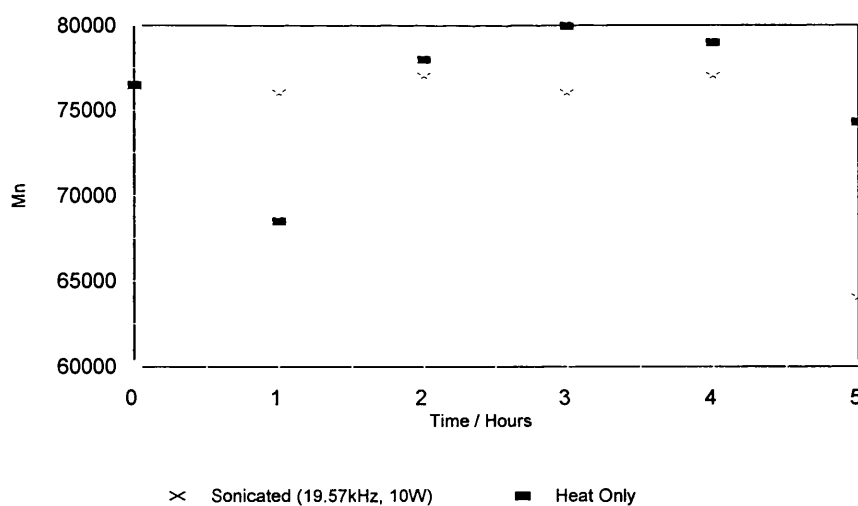


Figure 78: Degradation Plot for Polyethylene under Nitrogen

Again the sonicated samples have a slightly lower M_n , although this is not enough to be significant (especially after considering the effect of sampling position) and represent conclusive evidence of ultrasonic degradation. It is more likely that a small amount of thermal degradation is occurring, aided by ultrasonic mixing.

8.3 Section Discussion

From the PDMS experiment it can be seen that ultrasound is capable of causing a mixing effect in very viscous media such as found in a polymer melt. The silica / PMMA experiment shows that ultrasound does induce mixing in a polymer melt, as the silica / PMMA layers have obviously been broken up due to a mixing effect. These two experiments ease some of the worries of using ultrasound in a viscous fluid. However, the results so far do not indicate that ultrasonic degradation is occurring. Initial results using polystyrene under vacuum were promising giving a degradation curve for the sonicated samples, but not for the non-sonicated. Confusingly, use of a nitrogen atmosphere instead of vacuum showed no degradation. It is possible that the vacuum conditions were allowing a sufficient amount of atmospheric oxygen into the reaction chamber to allow oxidative degradation of the polymer. An ultrasonic mixing effect, then enabled more efficient reaction with the oxygen than in the heat only sample where only the surface would be in contact.

PMMA and PE under nitrogen also showed no degradation which could be accredited to ultrasound. An interesting observation was that in the case of PE and PS, even though no degradation had taken place, a general lowering of the polydispersity was seen in the sonicated samples compared to the non-sonicated samples. Again the suspected mixing effect could also explain the apparent lowering of polydispersity in the sonicated samples, as smaller polymer chains may move more freely, causing a separation of large and small chains, thus lowering the weight distribution at any one point in the melt. It may be possible to prove this by taking many samples from a single sonicated and a single non-sonicated polymer pellet and analysing them by GPC. The non-sonicated polymer

should show similar polydispersities, whereas, if the assumption is correct, many differing polydispersities would be shown for the sonicated samples.

9.0. Melt Compatibilisation

The overall aim of the project was to investigate the possible compatibilising effect of ultrasound on mixtures of two normally incompatible polymers in the molten state. The same apparatus was used as for the single polymer melt studies. The determination of the compatibilising effect was carried out by SEM initially allowing a visual determination of the extent, if any, of phase separation, and later, in some cases, by DSC and DMTA which gave information on the glass transitions of the polymers indicating the extent of the polymer compatibility. The results of these experiments all suggest that a further refinement of the conditions is required to enable ultrasonic cavitation to occur in polymer melts. Improving the coupling between horn and melt by carrying out the sonication under pressure is a possibility explored in the next chapter.

9.0.1. Polyethylene/ Polystyrene electron micrograph studies

A mixture of polystyrene and polyethylene (50/50 by weight) was dissolved in decahydronaphthalene (decalin) at 140⁰C. The decalin was then removed by evaporation in the fume cupboard and via a vacuum chamber. This left a white powder. The sonication and heating was then carried out as described earlier (page 125). The SEM results are shown below (unfortunately some problems were experienced with the SEM camera and as a result black lines can be seen across these images. However, the results are still clear). For all these results the samples were solvent cast onto aluminium planchettes for observation via SEM. Phase separation is seen in both sonicated and non-sonicated samples.

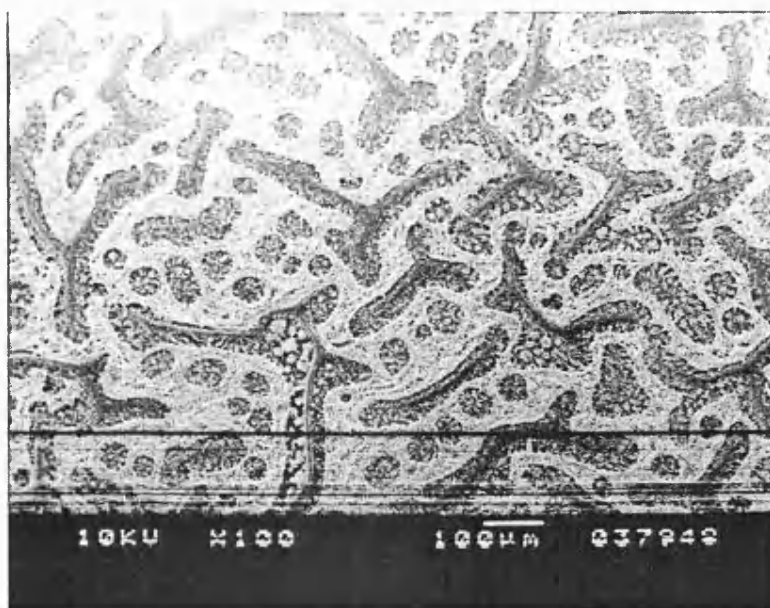


Figure 79: PE/PS 1:1, 5hrs in melt (240⁰C), no ultrasound mag x100

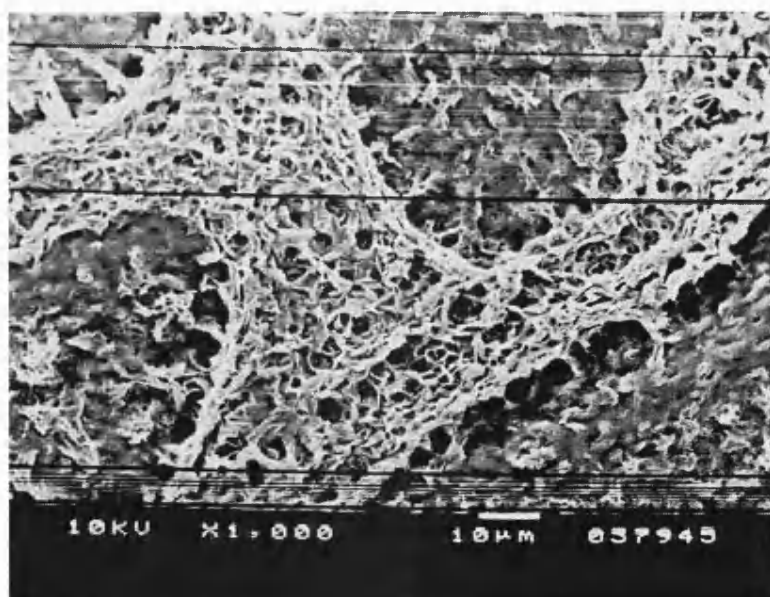


Figure 80: PE/PS 1:1, 5hrs in melt (240⁰C), no ultrasound mag x1,000

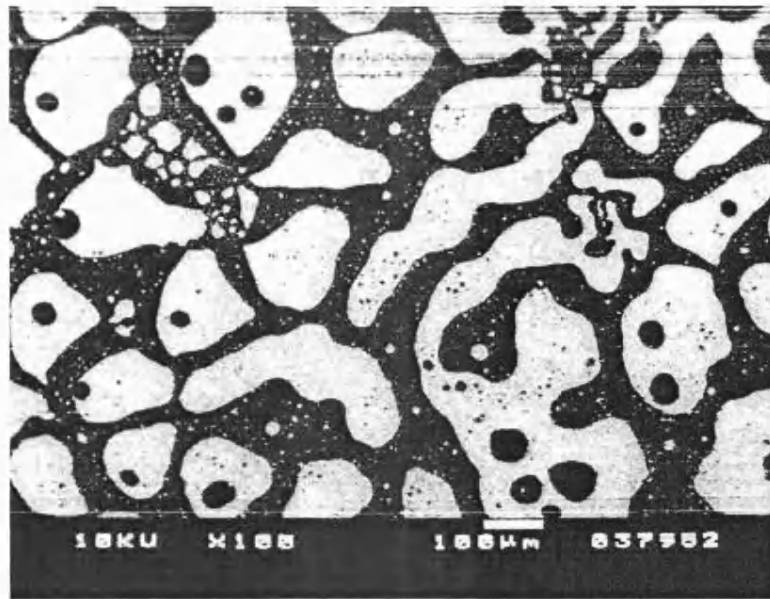


Figure 81: PE/PS 1:1, 5hrs sonicated in melt (240⁰C), mag x100

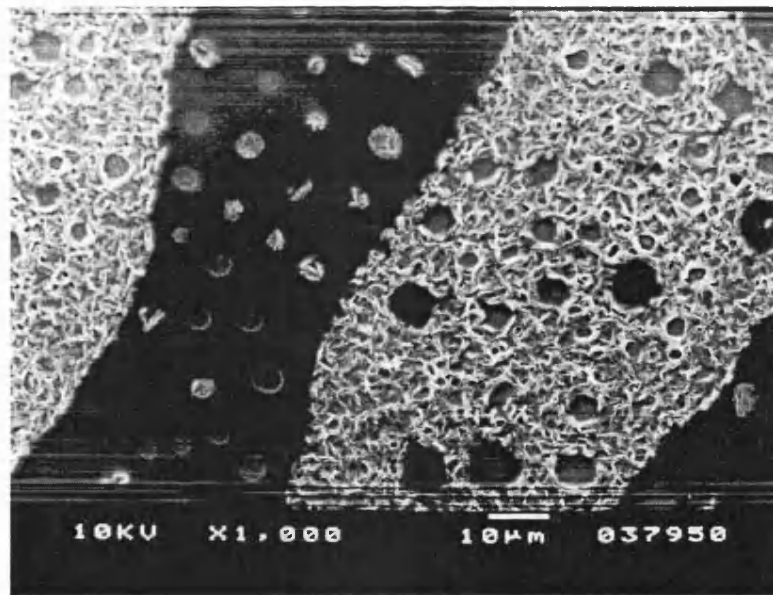


Figure 82: PE/PS 1:1, 5hrs sonicated in melt (240⁰C), mag x1,000

The electron micrographs shown here, especially those at magnification x100, clearly show a phase-separated polymer. The patterns seen are indicative of spinodal decomposition, which is characterised by high levels of phase

interconnectivity in both phases. Obviously the use of ultrasound has not produced compatibilisation.

9.0.2. Polyethylene/Polypropylene electron micrograph studies

A mixture of polypropylene and polyethylene (50/50 by weight) was dissolved in decahydronaphthalene (decalin) at 140⁰C. The decalin was then removed by leaving a white powder, which was much easier to use than the starting granulated polymers and packed into the furnace better.

After sonication, samples were taken from the centre of the pellet obtained from the furnace after cooling. The choice of where to take samples from had been decided from earlier experiments (page 124). For the first observations by SEM the samples were dissolved in decalin and cast onto an aluminium planchette. Subsequent samples were not dissolved, and were simply broken from the polymer pellet and physically fixed to the aluminium disc with Araldite. SEM results from both methods of sample preparation are shown as a conclusion as to what was happening during sonication can eventually be drawn from this. The SEM micrographs are thus labelled as such: samples cast from solvent, and, solid sample (i.e. fixed in place with Araldite).

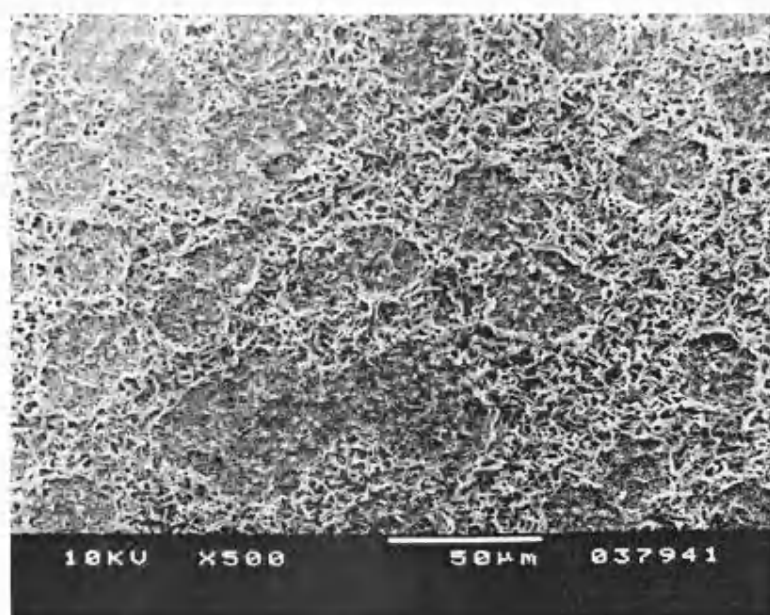


Figure 83: PE/PP 1:1, 5hrs in melt (240⁰C), no ultrasound, mag x500

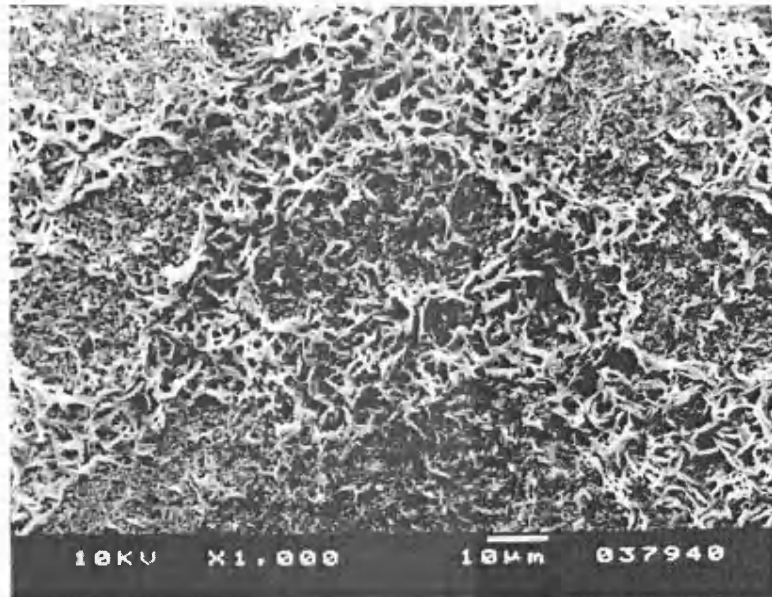


Figure 84: PE/PP 1:1, 5hrs in melt (240°C), no ultrasound, mag x1,000

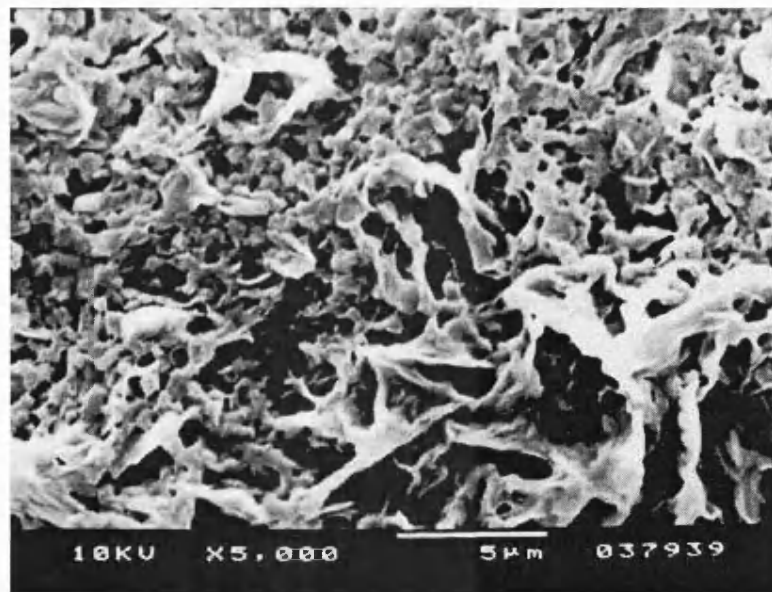


Figure 85: PE/PP 1:1, 5hrs in melt (240°C), no ultrasound, mag x5000

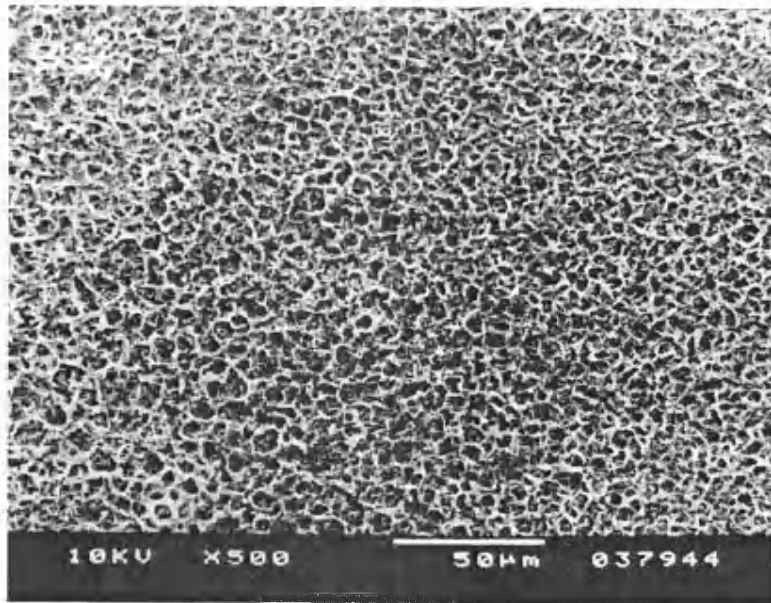


Figure 86: PE/PP 1:1, 5hrs sonicated in melt (240°C), mag x500

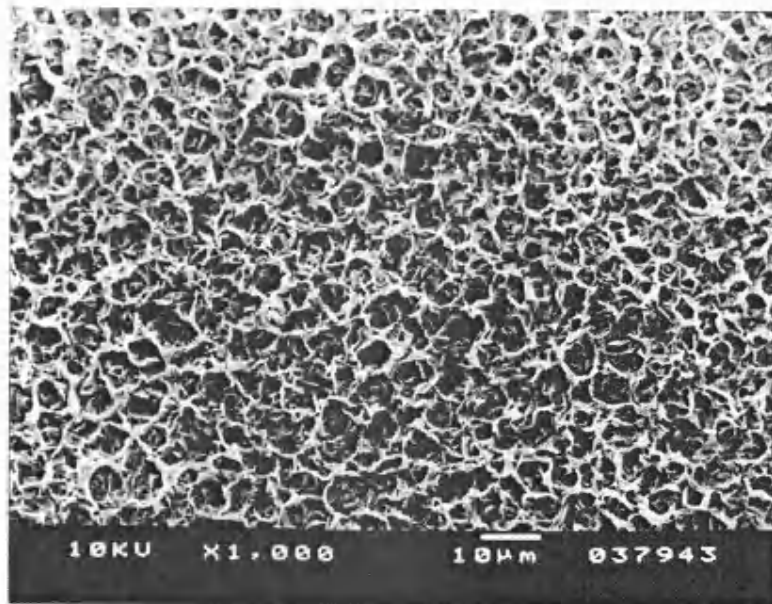


Figure 87: PE/PP 1:1, 5hrs sonicated in melt (240°C), mag x1,000

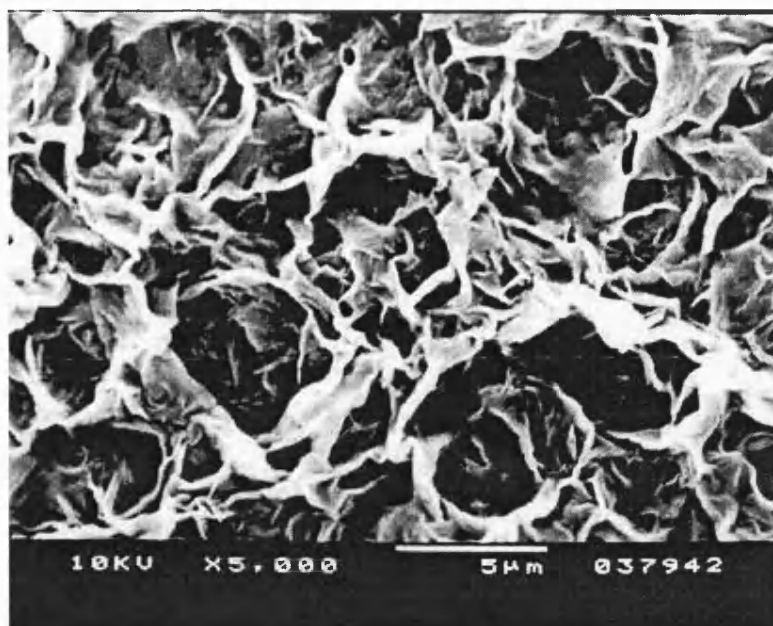


Figure 88: PE/PP 1:1, 5hrs sonicated in melt (240⁰C), mag x5,000

The above SEMs are difficult to interpret, for the heat only samples, especially the x500 and 1,000 examples, circular regions can be seen which show phase separation. From the images of the sonicated samples it cannot be decided whether the samples are phase separated or not. Study of the DSC and DMTA data gathered for these polymers is of help determining this.

9.0.2. Polyethylene/Polypropylene electron micrograph studies

Below are presented SEM results for PE/PP sonicated in the melt (including the heat only blanks), where the samples were fixed directly to the aluminium observation plate. Immediate differences from that of the solvent cast results (above) are evident.

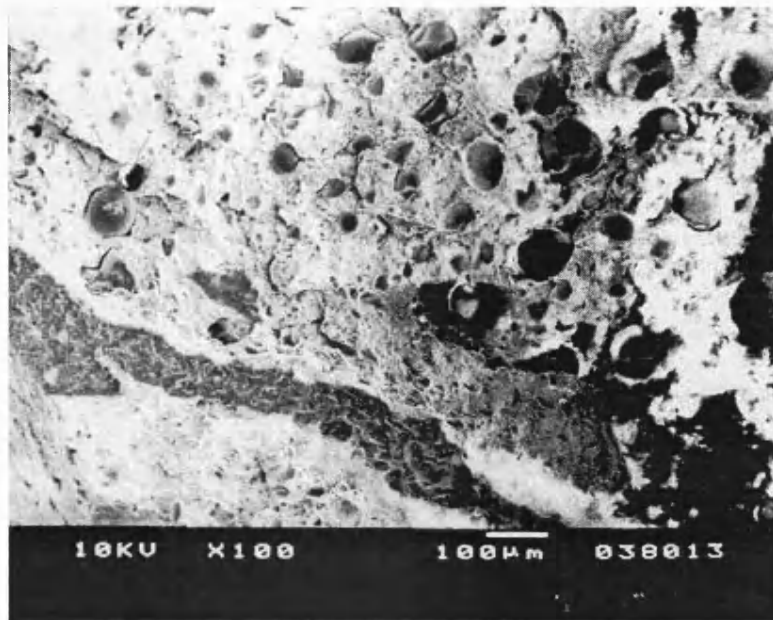


Figure 89: PE/PP 1:1, 5hrs in melt (240°C), no ultrasound mag x100

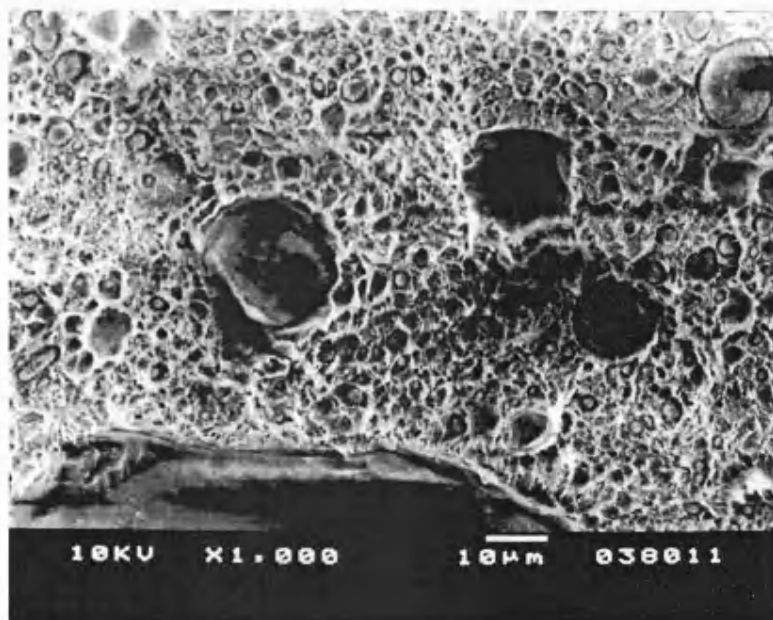


Figure 90: PE/PP 1:1, 5hrs in melt (240°C), no ultrasound mag x1,000

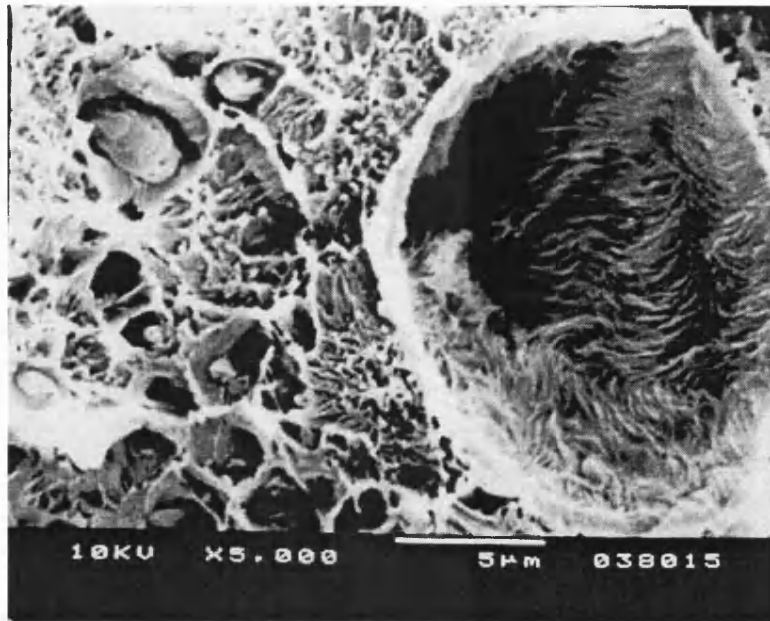


Figure 91: PE/PP 1:1, 5hrs in melt (240°C), no ultrasound mag x5,000

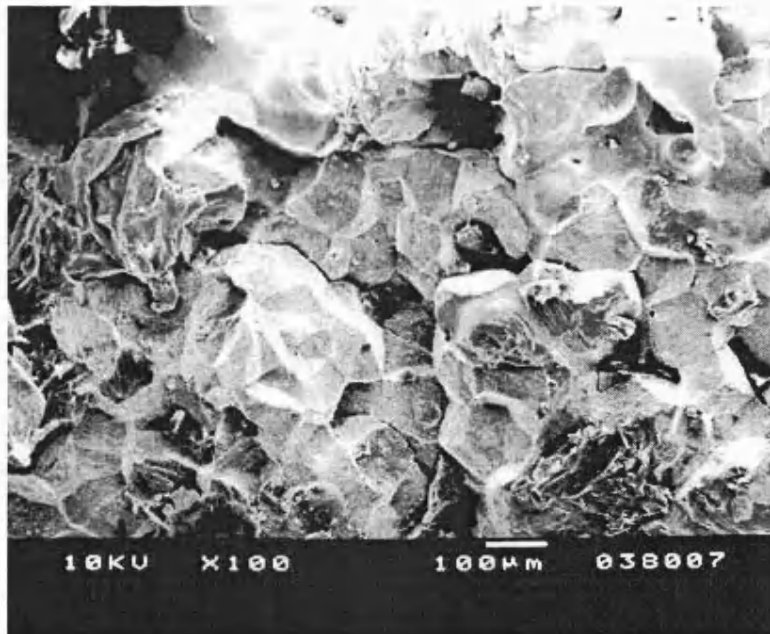


Figure 92: PE/PP 1:1, 5hrs sonicated in melt (240°C), mag x100

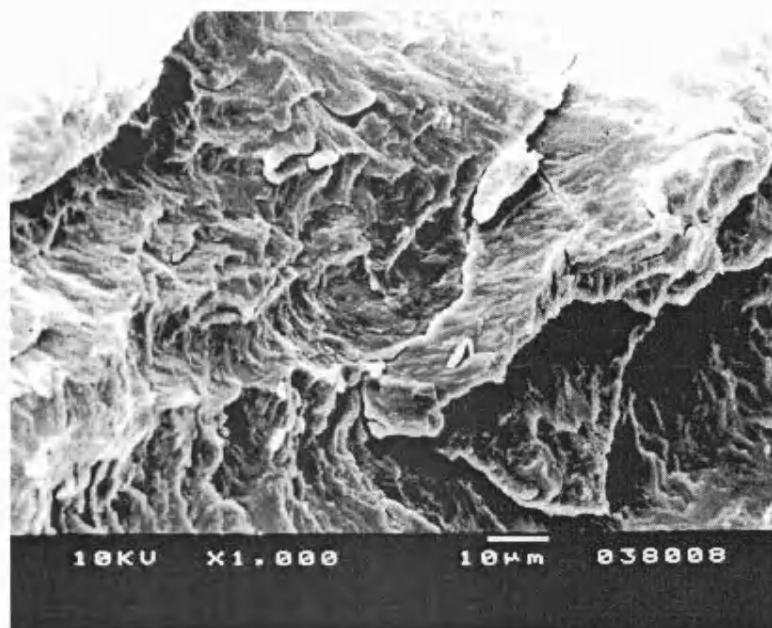


Figure 93: PE/PP 1:1, 5hrs sonicated in melt (240⁰C), mag x1,000

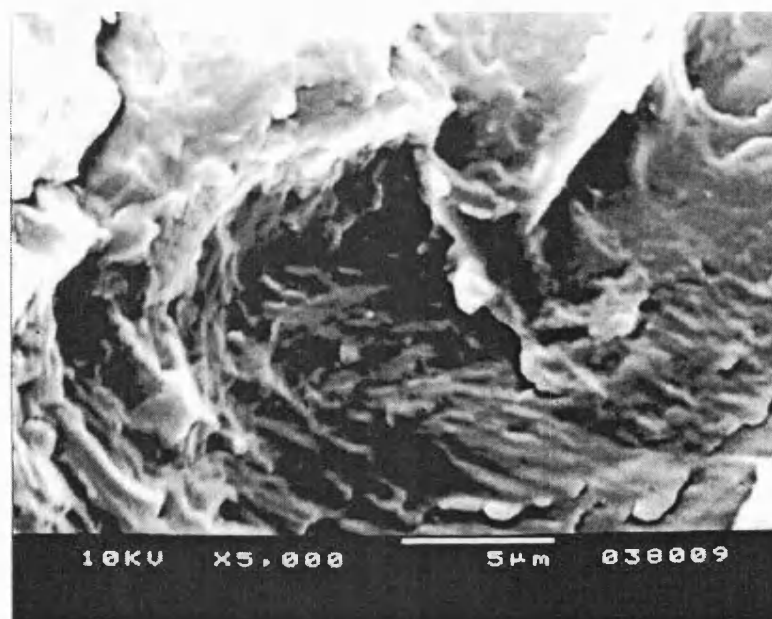


Figure 94: PE/PP 1:1, 5hrs sonicated in melt (240⁰C), mag x5,000

The SEM micrographs above show the characteristic phase separation for the heat only samples, whereas the sonicated samples appear totally homogenous. This suggests one of two conclusions. Either that the use of ultrasound has created an extremely well dispersed mix where phase separation cannot be seen even at

magnifications upto x5,000 or that some copolymer has been formed and the two polymers are now more miscible. Analysis by DSC was used to discern which was the case.

9.0.3 DSC Results for Melt Sonicated PE/PP

Small samples (micrograms) of the polymer pellets were analysed by DSC. If compatibilisation had taken place a shift in the glass transition (T_g) of either or both polymers should be seen to occur. DSC thermographs of the original homopolymers and of the heat only mixes were also produced for comparison.

From the results it is very difficult to actually determine the glass transitions, but from careful analysis they can be seen. For ease of interpretation the T_g 's have been indicated on the graphs, and also listed in a table at the end of this section. The graphs are shown below.

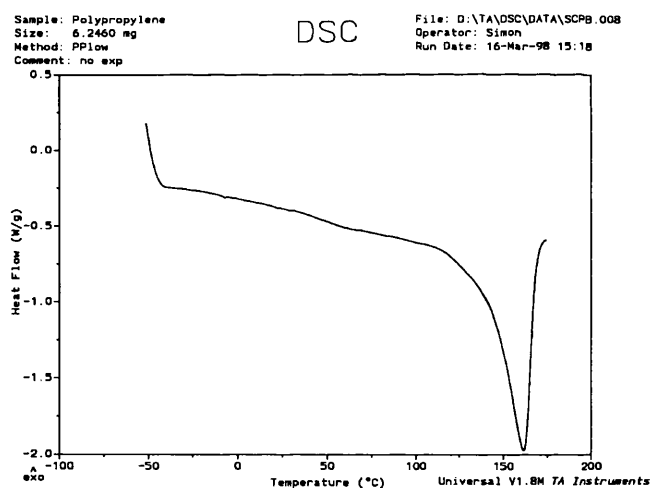


Figure 95: DSC thermogram for Polypropylene

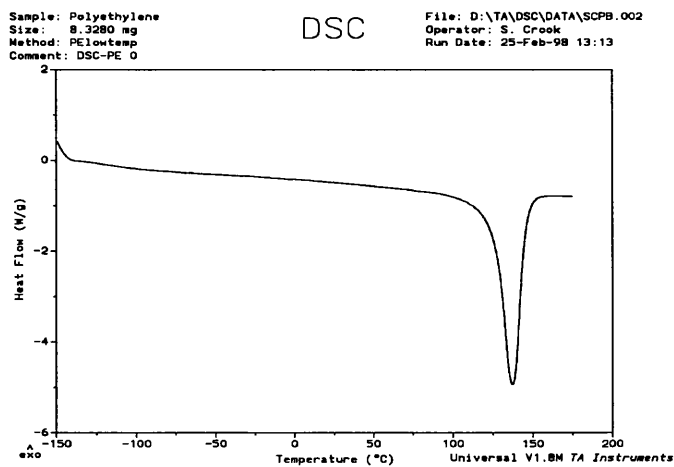


Figure 96: DSC Thermogram for Polyethylene

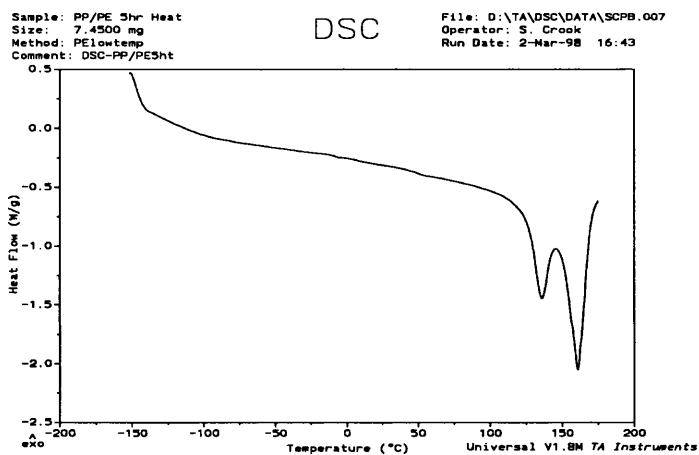


Figure 97: DSC thermogram for PE/PP, 5hr Heat (240°C)

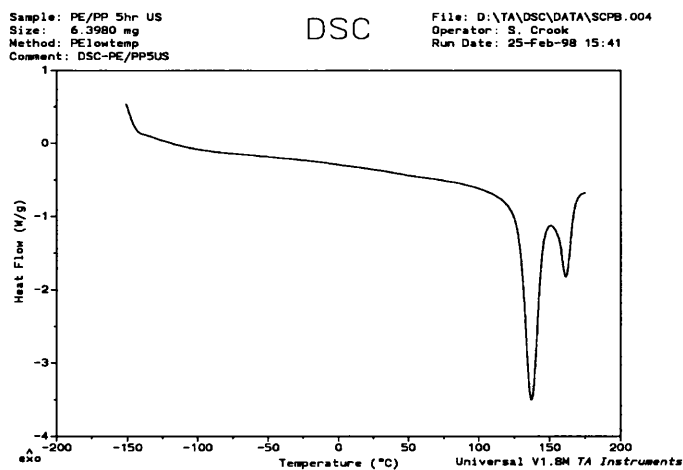


Figure 98: DSC Thermogram for PE/PP, 5hr ultrasound (240°C)

Summary of DSC peaks

<u>DSC</u>	<u>T_g (°C)</u>	<u>T_{c1} (°C)</u>	<u>T_{c2} (°C)</u>
Figure 95: Polypropylene	-10	161	NA
Figure 96: Polyethylene	-100 to -130	137	NA
Figure 97: PE/PP Ht only*	-98 to -130	132	160
Figure 98: PE/PP US*	-98 to -130	137	160

*pp T_g too small to see for figs.97 & 98

From the DSC thermographs the PE glass transition at -100 to -130 can be seen as a broad shoulder on all the graphs. A completely compatible polymer pair would show a single glass transition somewhere between those of the homopolymers. Partial compatibilisation, which is what we expect to find if some copolymer has been made, would still show two T_g's, but one or both of these would have shifted towards the other. As this is not the case and no difference in T_g's are seen between sonicated and non-sonicated samples, it can be concluded that although a superior mix has been formed by use of ultrasound (as seen by the SEM evidence), no copolymer has been produced. This implies that only a small amount or no cavitation and chain degradation effects are taking place in the polymer.

9.0.4 DMTA of PE/PP

DMTA sample bars (20mm x 10mm x 2mm) were made using an aluminium mould. These bars were then tested by the single cantilever bending mode of the DMTA. Graphs were obtained showing both log e' (modulus) and the loss tangent, tan delta, vs temperature. The glass transitions are much easier to see than on the DSC results as the DMTA is a much more sensitive technique. It was found that the DMTA data and DSC results agreed with other and showed that no displacement of T_g was seen in this sonicated samples, indicating that compatibilisation did not take place.

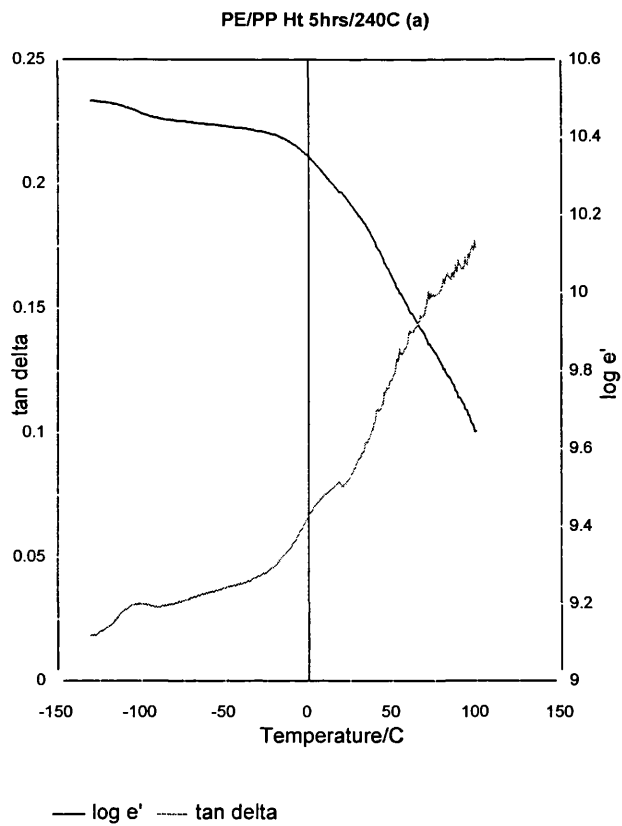


Figure 99: DMTA of PE/PP, heat only (240⁰C)

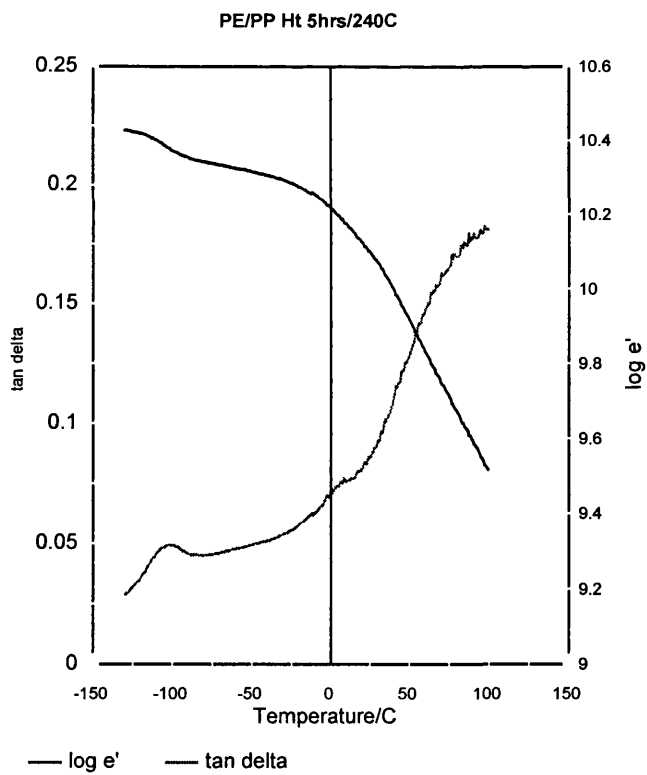


Figure100: DMTA of PE/PP, heat only (240⁰C)

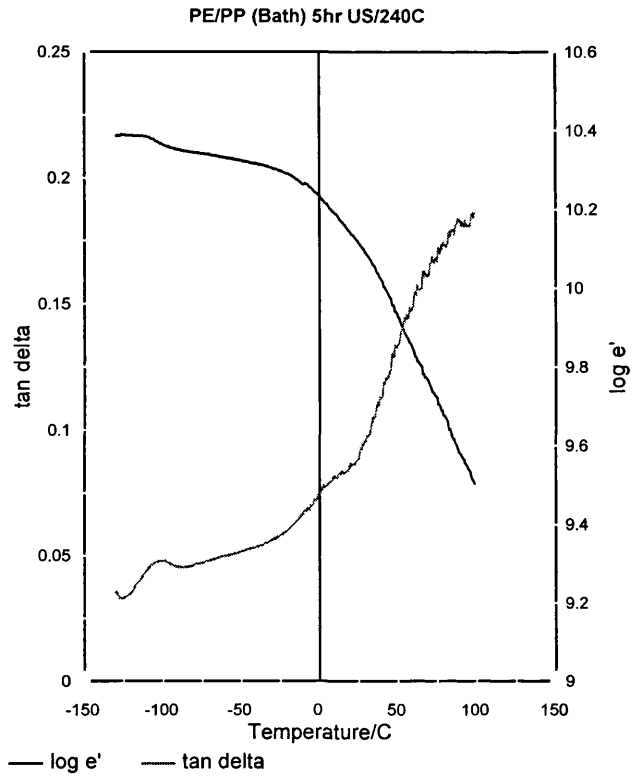


Figure101: DMTA of PE/PP, sonicated 5hrs not pressurised (240⁰C)

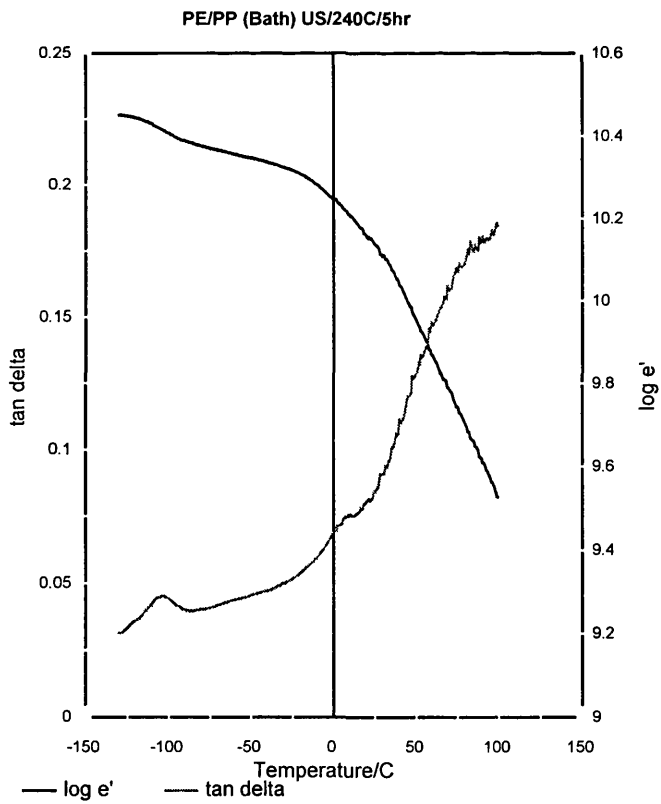


Figure102: DMTA of PE/PP, sonicated 5hrs not pressurised (240⁰C)

9.0.5. Polyvinylidifluoride/Polyethylene electron micrograph studies

Powdered mixtures of PE and PVDF were produced by dissolving the polymers in decahydronaphthalene at 140⁰C, and then removing the solvent by a combination of evaporation on a watch glass and vacuum oven.

The PE/PVDF mixture was then treated as follows; one sample (35g) was heated (240⁰C) and sonicated for six hours (19.41 kHz, 10W), the other sample (35g) was subjected to heat (240⁰C) only. DSC and DMTA analysis was also performed on these samples. The SEM micrographs are displayed below. All the samples shown by the micrographs below were prepared by fixing the solid polymer to the aluminium sample holder (as explained earlier).

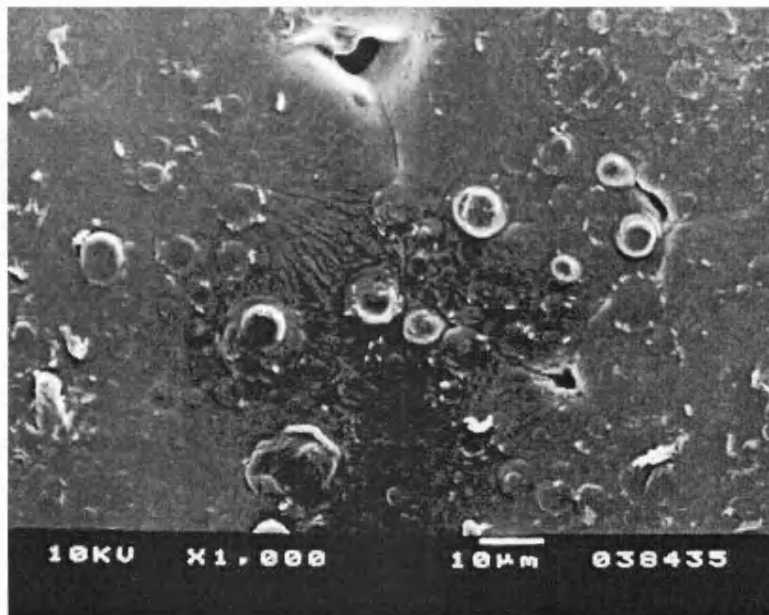


Figure103: PVDF/PE 1:1, 6hrs in melt (240⁰C), no ultrasound mag x1,000

9.0.5. Polyvinylidifluoride/Polyethylene electron micrograph studies

Powdered mixtures of PE and PVDF were produced by dissolving the polymers in decahydronaphthalene at 140⁰C, and then removing the solvent by a combination of evaporation on a watch glass and vacuum oven.

The PE/PVDF mixture was then treated as follows; one sample (35g) was heated (240⁰C) and sonicated for six hours (19.41 kHz, 10W), the other sample (35g) was subjected to heat (240⁰C) only. DSC and DMTA analysis was also performed on these samples. The SEM micrographs are displayed below. All the samples shown by the micrographs below were prepared by fixing the solid polymer to the aluminium sample holder (as explained earlier).

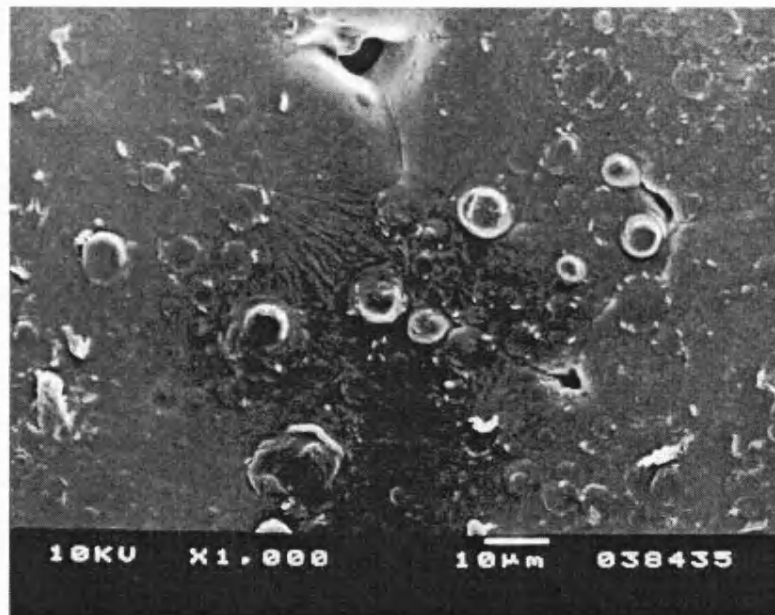


Figure103: PVDF/PE 1:1, 6hrs in melt (240⁰C), no ultrasound mag x1,000

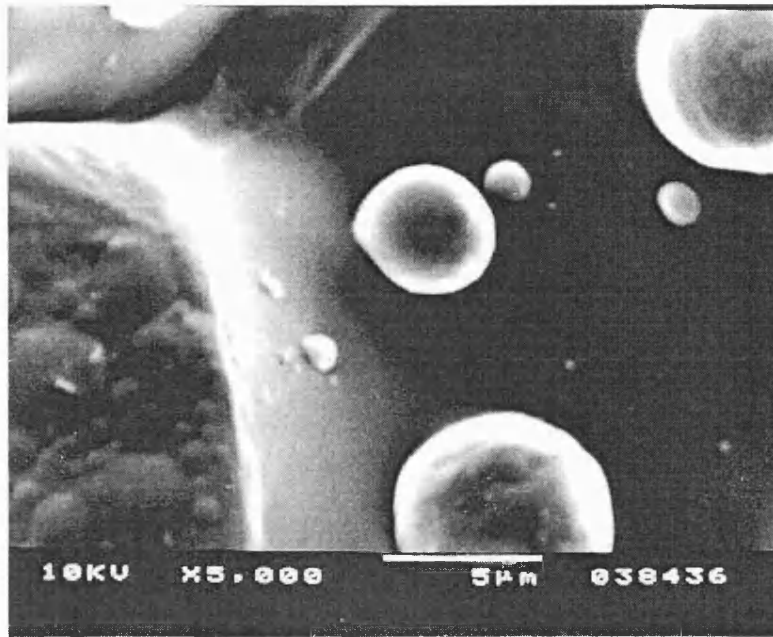


Figure104: PVDF/PE 1:1, 6hrs in melt (240⁰C), no ultrasound mag x5,000

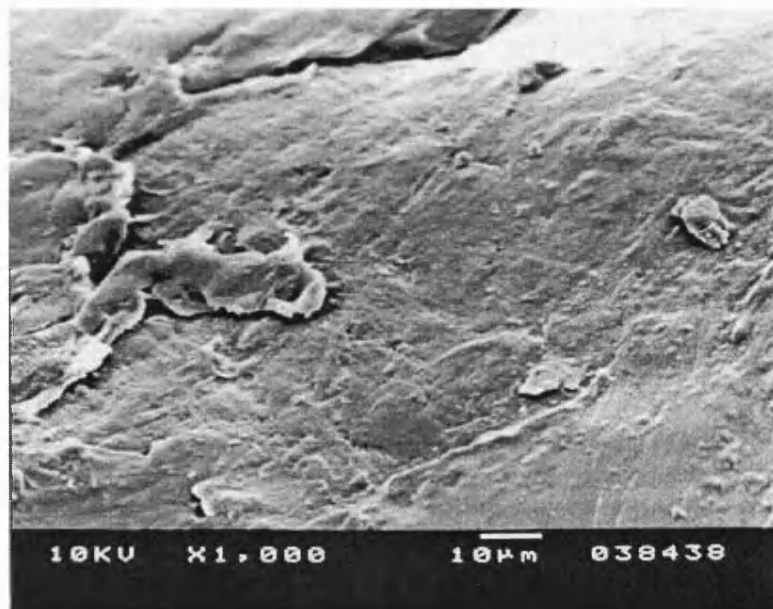


Figure105: PVDF/PE 1:1, 6hrs sonicated in melt (240⁰C), mag x1,000

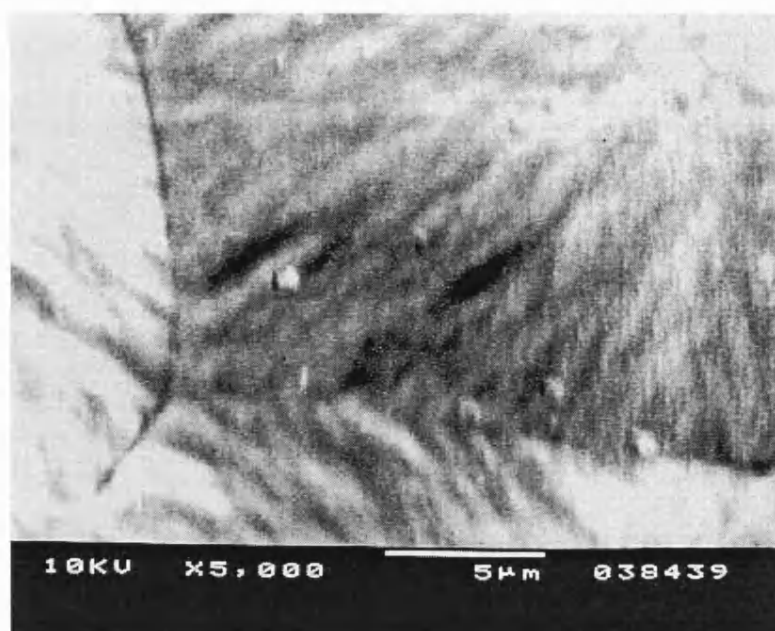


Figure106: PVDF/PE 1:1, 6hrs sonicated in melt (240⁰C), mag x5,000

As with the PE/PP melt sonication, the PVDF/PE SEM results show images associated with phase separation for the non-sonicated samples and a one phase structure for the sonicated sample. Again DSC and DMTA were used to ascertain whether this was merely a very disperse mixture or if the hoped for copolymers had been formed.

9.0.6. DSC results for PE/PVDF Melt Sonication

DSC thermographs were obtained for the sonicated and heat only samples of PE/PVDF. Graphs for PE and PVDF alone are also shown for reference. As with the DSC results for PE/PP the Tg's are difficult to spot. A table of Tg peaks has been included after the DSC graphs. Again the graphs show no displacement of the glass transitions.

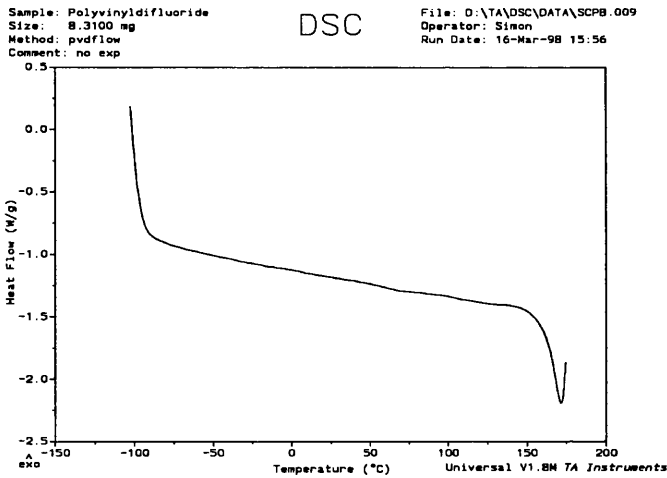


Figure107: DSC Thermogram for Polyvinylidifluoride

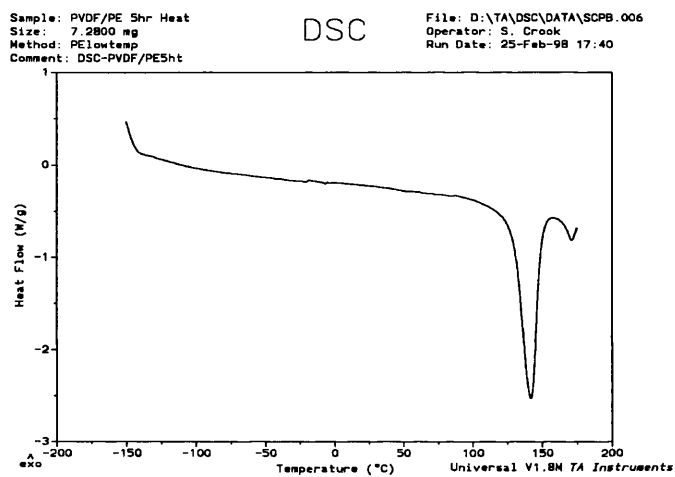


Figure108: DSC Thermogram for PVDF/PE, 5hr Heat (240°C)

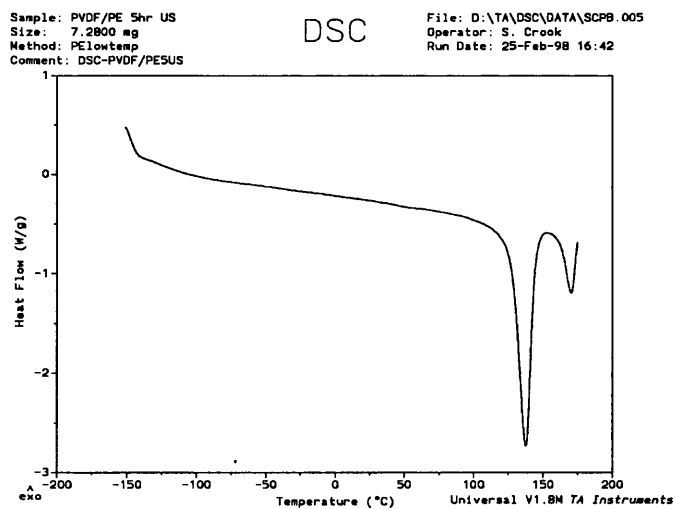


Figure109: DSC thermogram for PVDF/PE, 5hr Ultrasound (240°C)

Summary of DSC peaks

<u>DSC</u>	<u>T_g (°C)</u>	<u>T_{c1} (°C)</u>	<u>T_{c2} (°C)</u>
Figure 96: Polyethylene	-100 to -130	137	NA
Figure 107: Polyvinylidifluoride*	NA	170	NA
Figure 108: PE/PVDF Ht only*	-100 to -130	140	170
Figure 109: PE/PVDF US*	-100 to -130	140	170

*PVDF T_g Too Small to see.

As can be seen from the above, the PE T_g's are in exactly the same space for both sonicated and unsonicated. Unfortunately the PVDF transition was too small to be seen by DSC. Again the conclusion is that no copolymer formation has taken place, as this would result in a shift of the glass transition temperatures, and that the initially promising SEM results are showing the product of the ultrasonic mixing effect.

9.0.7. PVDF/PE DMTA Results

DMTA sample bars (20mm x 10mm x 2mm) were made as before using a specifically designed aluminium mould. These bars were then tested by the single cantilever bending mode of the DMTA. In agreement with the PE/PP results it was found that the DMTA data and DSC results for PE/PVDF agreed with each other, showing no displacement of T_g in the sonicated samples, indicating that compatibilisation did not take place. For the DMTA results the separate unshifted T_g of PVDF can clearly be seen at -40 to -30°C

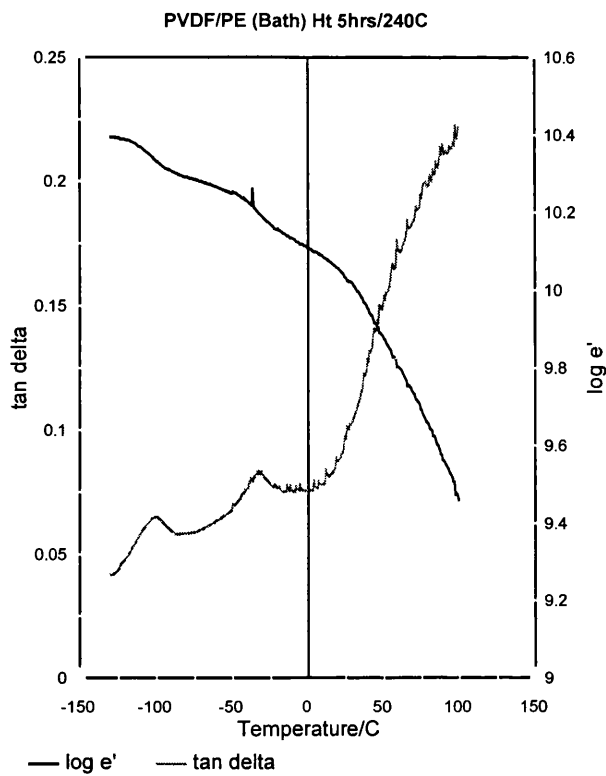


Figure110: DMTA of PE/PVDF, heat only (240⁰C)

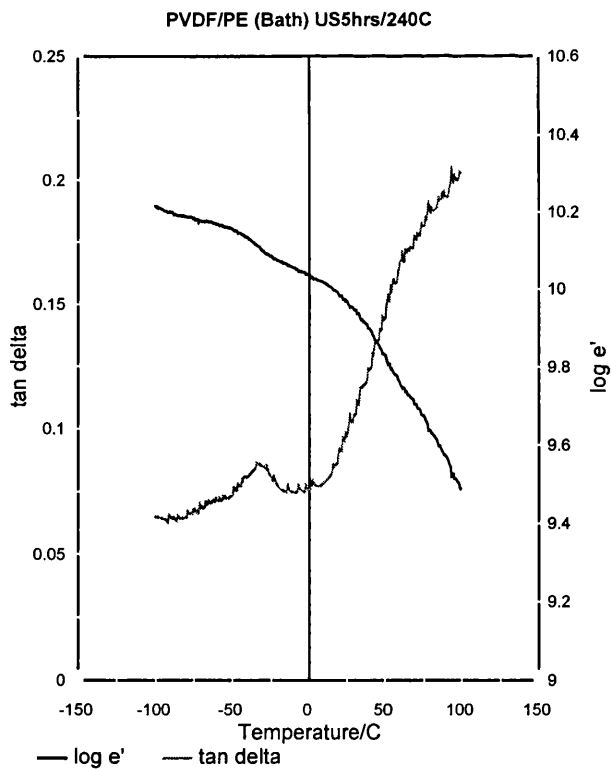


Figure111: DMTA of PE/PVDF, sonicated 5hrs (240⁰C)

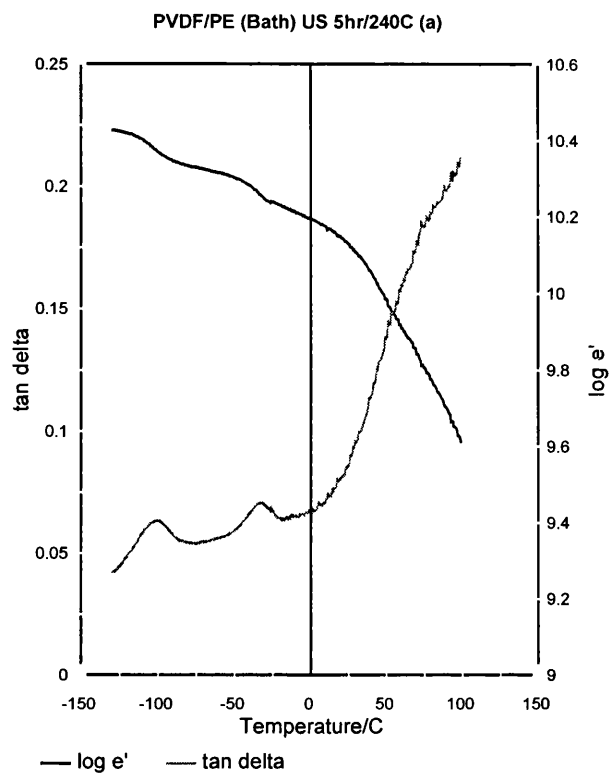


Figure 112: DMTA of PE/PVDF, sonicated 5hrs (240°C)

9.0.8 Polyvinylidifluoride/Polypropylene

Powdered mixtures of polypropylene and PVDF were produced using the methods described in earlier chapters. Sonication of the polymer mix was performed as for the previous polymer pairs (240⁰C,19.41 kHz, 10 W).

SEM samples were only produced using one method, that of fixing a solid piece of the resulting polymer pellet to the aluminium observation disc. These samples showed no difference between that of sonicated or heated, both appearing totally homogenous at magnifications upto x1,000. Further study by DSC was carried out, the results for which also showed no difference between sonicated and non-sonicated samples.

9.1. Section Discussion

From the DMTA and DSC data it can be seen quite conclusively that the attempts made at compatibilisation for PE/PP and PE/PVDF have not worked under the conditions employed. The glass transition temperatures for both sonicated and non-sonicated samples are the same, a clear indicator that no copolymers have been formed and the miscibility not improved.

All the SEM images for the solvent cast samples show phase separated polymers. However in the case of PE/PP and PE/PVDF, the SEM samples prepared without solvent do not show any phase separation. These two observations mean that the polymers are well dispersed after sonication, but in no way compatibilised as they readily separate upon addition of solvent.

Again, as with the single melt sonication experiments in the preceding chapter, effects of ultrasonic mixing have been observed without the accompanying cavitation effects and the predicted polymer degradation. It may be possible that upon sonication the melt is pushed away from the horn and an air pocket is formed which, due to the viscosity of the melt, is not filled by more polymer flowing into it. This would create an effective barrier against cavitation occurring in the melt. Agitation around the air pocket may explain the increased mixing which is seen in all cases.

If this is so, then if the sonication was carried out under pressure sufficient coupling of the horn to the melt may be achieved which would eliminate this problem. This was the next step of the project.

10.0. SONICATION OF PRESSURISED POLYMER MELT SYSTEMS

In order to maximise coupling between the ultrasonic horn and polymer melt, it was decided that using a pressurised system may be of use. Pressure of 20psi was achieved with PE/PP and PE/PVDF studied. A furnace was designed and manufactured at Bath for this work (see page 81). A photograph of the equipment used is shown below (the nitrogen hood is omitted).



Figure 113: Equipment used for pressure sonication of polymer melts

10.1.1. SEM of Polypropylene/Polyethylene

A 1:1 by weight mix of PE/PP precipitated from solution (decalin) was placed in a specially designed aluminium vessel (see page 81). This was then heated to 240°C and sonicated under pressure at 3.5 sec intervals (the maximum obtainable). The resulting polymer was examined under electron microscope and also by DSC and DMTA. The SEMs, for which the samples were produced by fixing a solid piece of the polymer sample to the sample holder, are displayed below:

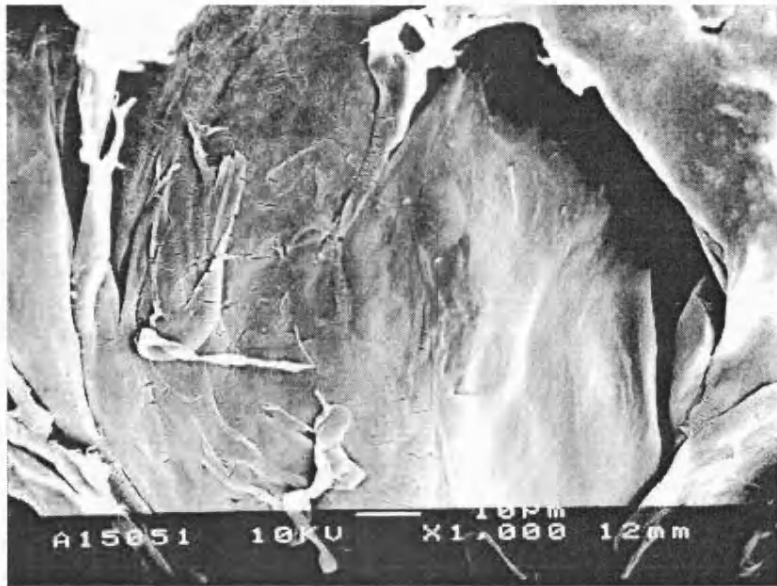


Figure114: PE/PP (8), Sonicated with pressure 20x3.5s, 240⁰C, mag x1,000



Figure 115: PE/PP (8), Sonicated with pressure 20x3.5s, 240⁰C, mag x5,000

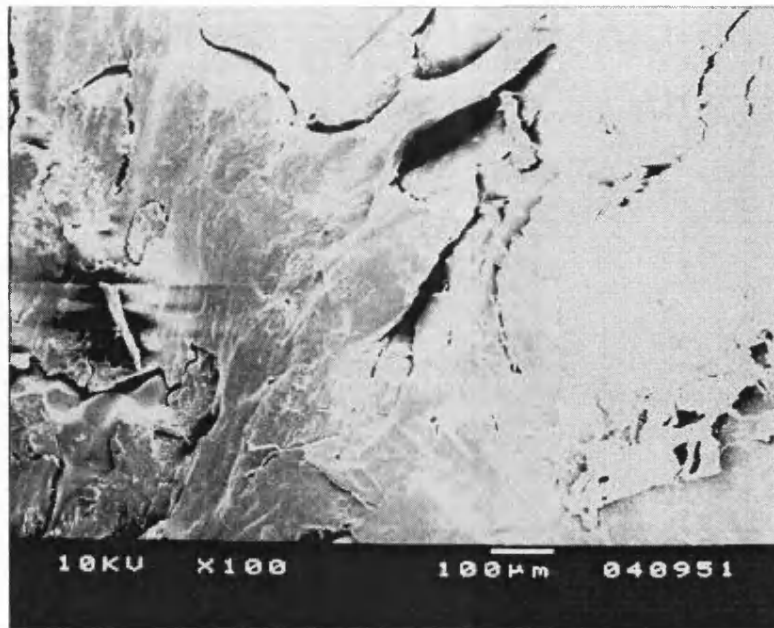


Figure116: PE/PP, Sonicated with pressure 20x3.5s, 240⁰C, mag x1,000

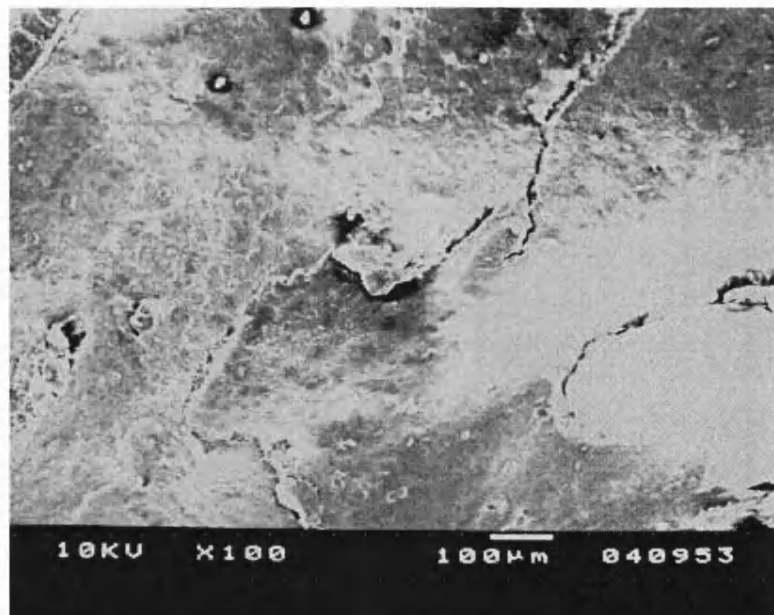


Figure 117: PE/PP, Sonicated with pressure 40x3.5s, 240⁰C, mag x100

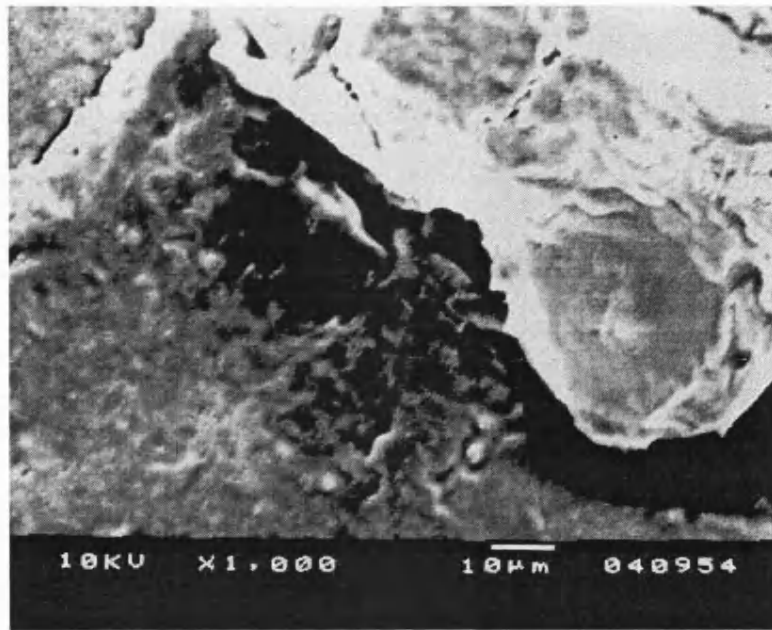


Fig118: PE/PP, Sonicated with pressure 40x3.5s, 240⁰C, mag x1,000

All the above samples appear to show no obvious signs of phase separation, however this alone cannot be taken as evidence of compatibilisation, only as a possible pointer. The next step was to analyse the samples by DSC and DMTA to see if a T_g shift had occurred and/or the polymers properties had changed.

10.1.2. DSC of pressurised melt samples

Samples of PE/PP were produced using the ultrasonic welding apparatus, Both sonicated and heat only samples were analysed via DSC. For each sample, the polymer was cooled to a set temperature (-130⁰C in order to capture the PE T_g) and data recorded as heat was applied. Unlike the DSC results for the non-pressurised systems a T_g shift for polyethylene was observed in the sonicated samples. The results are shown below.

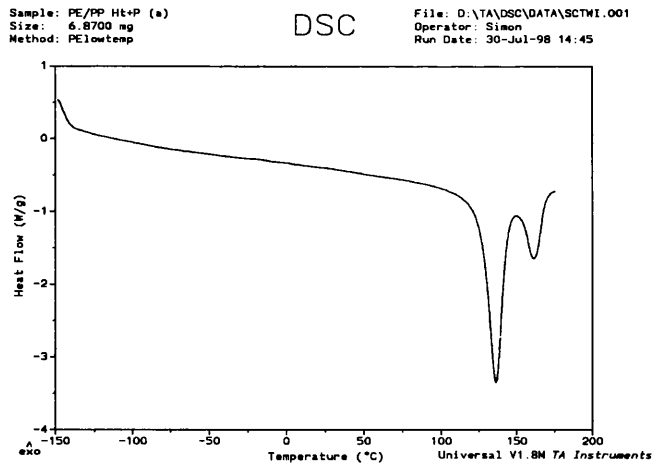


Figure 119: DSC thermogram of PE/PP, heat and pressure only (240⁰C, 20 psi)

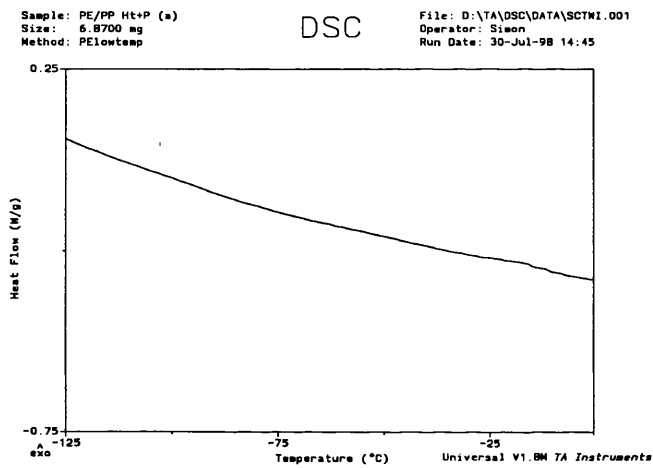


Figure 120: (Zoom of figure 119), DSC thermogram of PE/PP, heat and pressure only (240⁰C, 20 psi)

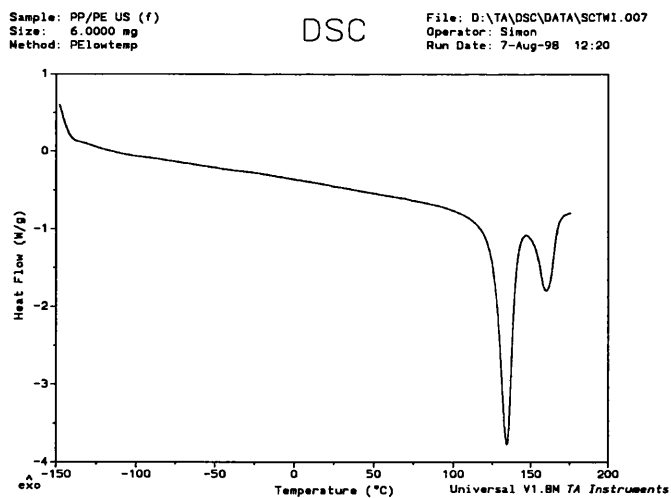


Figure 121: DSC thermogram of PE/PP, sonicated 5x3.5 secs with pressure (240⁰C, 20 psi, 50W)

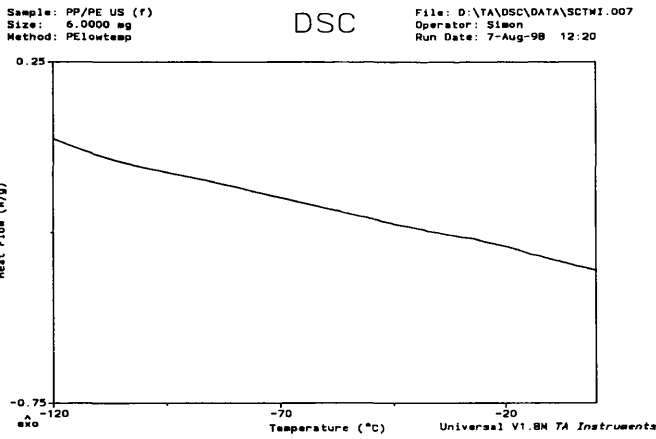


Figure122: (zoom of figure121), DSC thermogram of PE/PP, sonicated 5x3.5 secs with pressure (240°C, 20 psi, 50W)

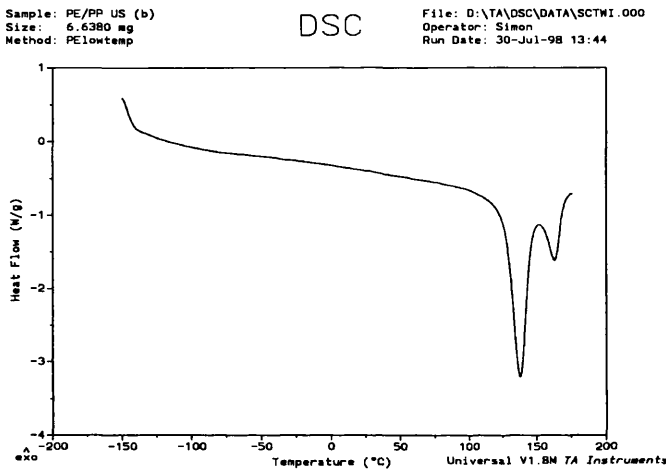


Figure123: DSC thermogram of PE/PP, sonicated 20x3.5 secs with pressure (240°C, 20 psi, 50W)

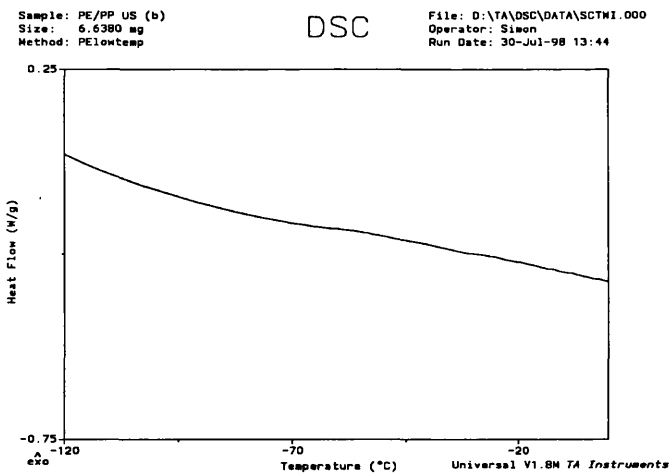


Figure124: (Zoom of figure 123), DSC thermogram of PE/PP, sonicated 20x3.5 Secs with pressure (240°C, 20 psi, 50W)

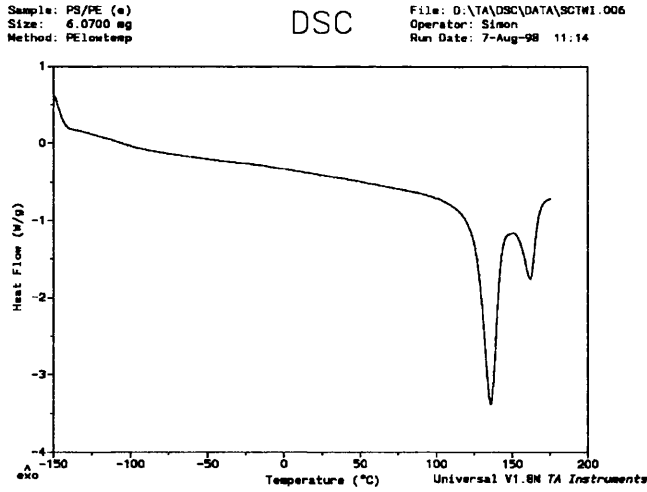


Figure124: DSC thermogram of PE/PP, sonicated 40x3.5 secs with pressure (240°C, 20 psi, 50W)

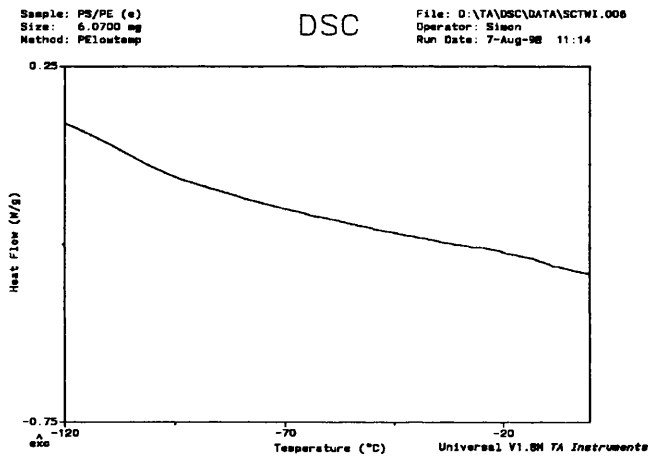


Figure125: (zoom of figure124), DSC thermogram of PE/PP, sonicated 40x3.5secs with pressure (240°C, 20 psi, 50W)

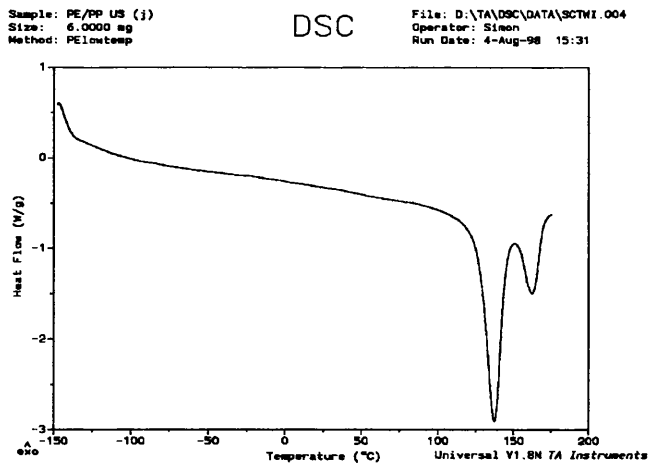


Figure126: DSC thermogram of PE/PP, sonicated 50x3.5secs with pressure (240°C, 20 psi, 50W)

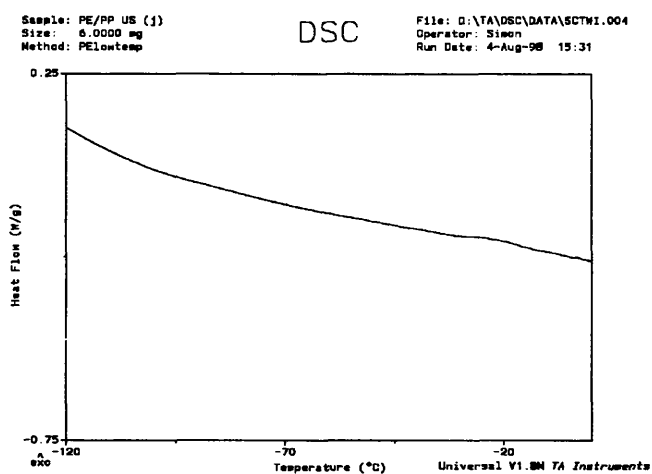


Figure127: (zoom of figure126), DSC thermogram of PE/PP, sonicated 50x3.5secs with pressure (240°C, 20 psi, 50W)

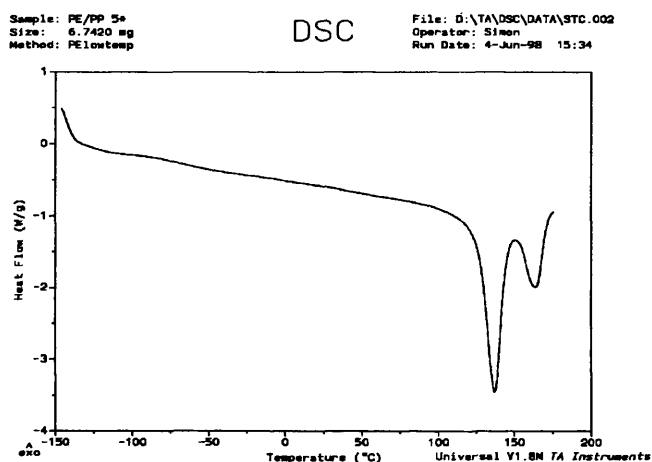


Figure128: DSC thermogram of PE/PP, sonicated 20x3.5secs with pressure (240°C, 20 psi, 50W)

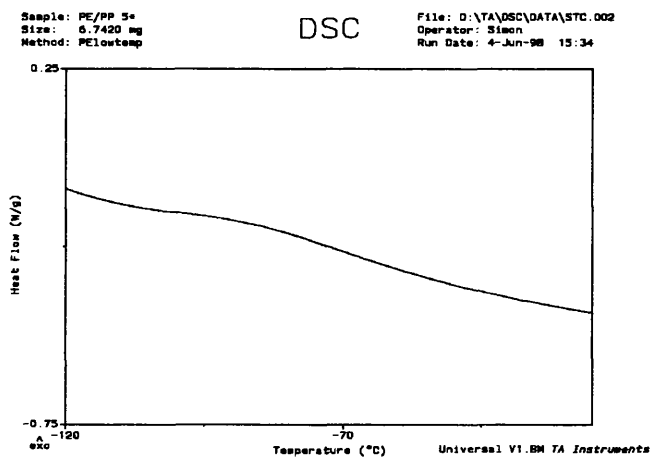


Figure129: (zoom of figure128), DSC thermogram of PE/PP, sonicated 20x3.5secs with pressure (240°C, 20 psi, 50W)

Summary of DSC peaks

<u>DSC</u>	<u>Tg (°C)*</u>	<u>Tc1 (°C)</u>	<u>Tc2(°C)</u>
Figure 119: PE/PP Ht & P only	-98 to -130	137	160
Figure 121: PE/PP US (5x3.5) & P	-75 to -100	137	160
Figure 123: PE/PP US (20x3.5 & P	-35 to -70	137	160
Figure 125: PE/PP US (40x3.5) & P	-10 to -29	137	160
Figure 127: PE/PP US (50x3.5) & P	-10 to -30	137	160
Figure 129: PE/PP US (20x3.5) & P	-72 to -100	137	160

*note: in all DSC containing PE, the original Tg 'shoulder' was still present at around -100 to -130, in some cases broader (sonicated).

All the sonicated samples show a shift in the Tg of Polyethylene (PP was too small to observe). The heat and pressure only sample shows no difference in the Tg compared to the graphs in chapter 9. These two observations suggest that the use of ultrasound with pressure on the molten PE/PP system has caused a degree of compatibilisation to occur. More encouragingly, the longer the sonication time the greater the Tg shift e.g. 25 to 30⁰C shift for 5 secs, 90-100⁰C shift for 50 secs. The cause of this has to be the formation of small amounts of copolymer in the system causing a degree of polymer/polymer miscibility. As there will still be large amounts of unreacted polymer left, the inclusion of the PE Tg at -100 to -130⁰C in all the results is no surprise.

10.1.3. DMTA of pressurised PE/PP Melt

In order to back up the evidence from the DSC and hopefully show the results more clearly, DMTA analysis was performed on the PE/PP samples. The DMTA sample bars were produced as before (page 146). It can be seen that the DMTA results show the same Tg shifts and a change in the properties of the sonicated, pressurised samples, indicated by differences in the log e' plots.

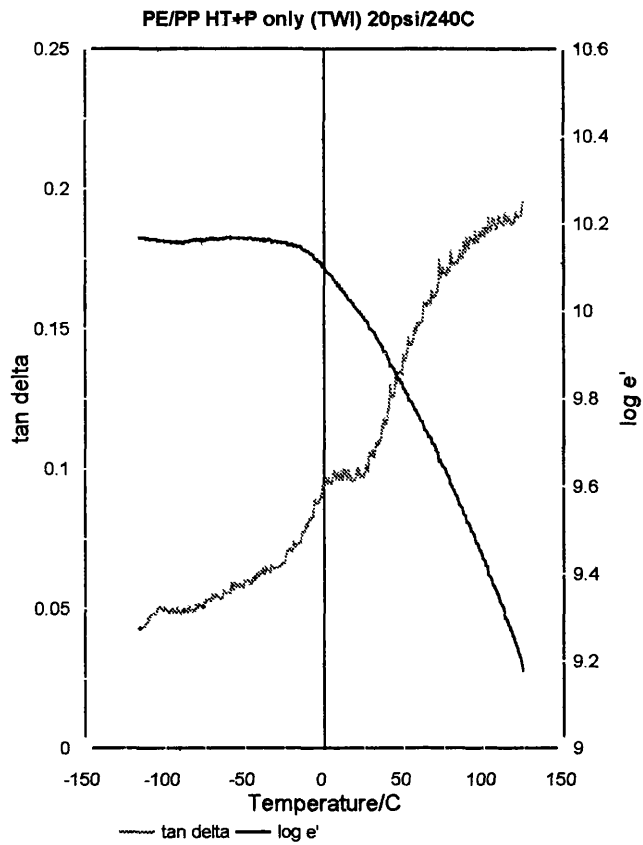


Figure130: DMTA of PE/PP, heat and pressure only (240°C/20psi)

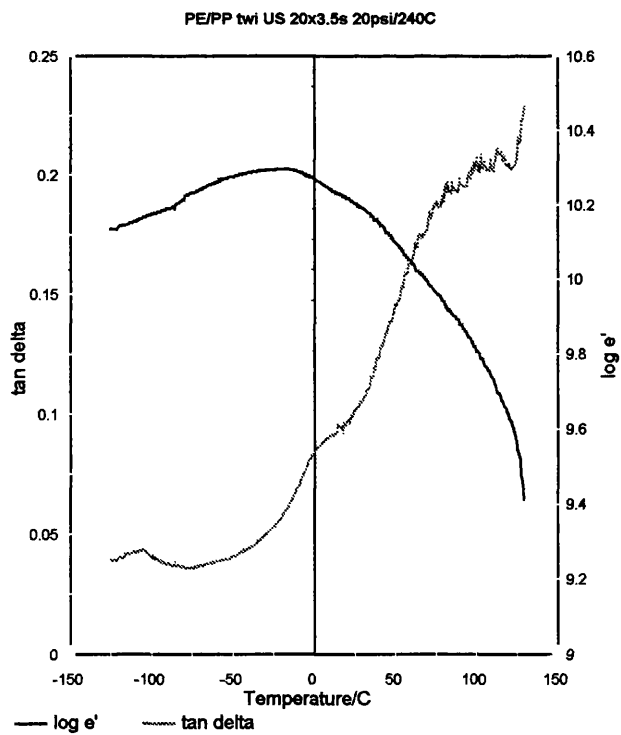


Figure131: DMTA of PE/PP, sonicated for 20x3.5sec under pressure (240°C/20psi)

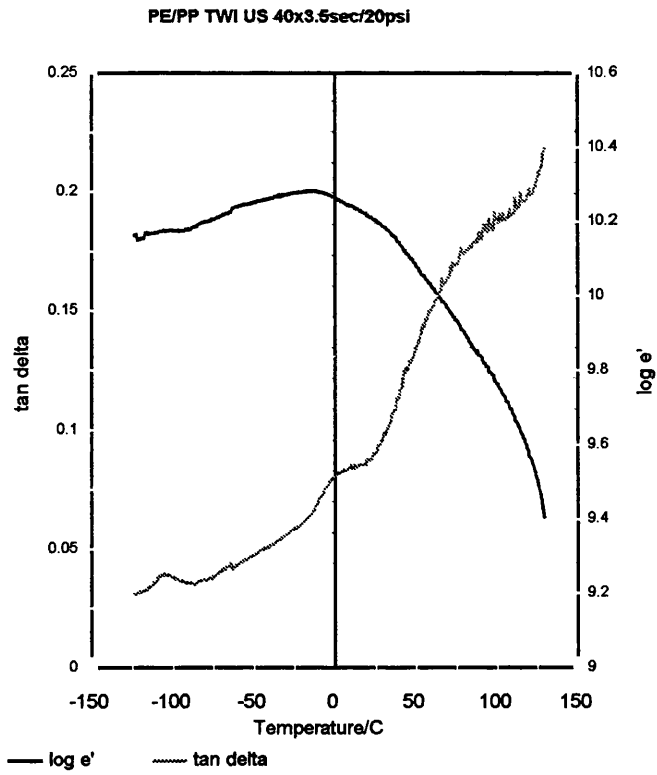


Figure132:DMTA of PE/PP, sonicated for 40x3.5sec under pressure (240°C/20psi)

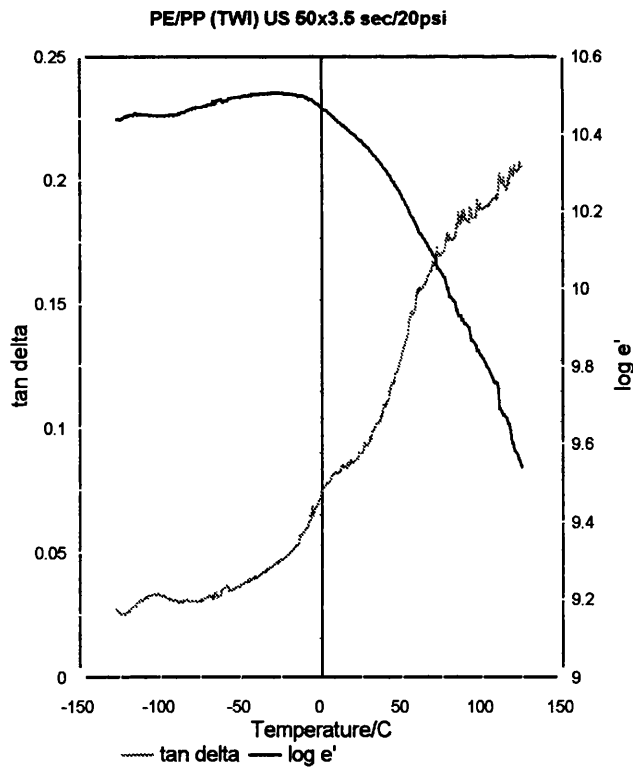


Figure134:DMTA of PE/PP, sonicated for 50x3.5sec under pressure (240°C/20psi)

10.1.4. Sonication of pressurised PE/PVDF in the melt

PE/PVDF was sonicated under pressure using the same method as for PE/PP. DSC and DMTA was used to establish whether compatibilisation of the two polymer had or had not taken place.

10.1.5. DSC of pressurised PE/PVDF

Samples of PE/PVDF which were produced using the ultrasonic welding apparatus (figure 26, page 83), both sonicated and heat only were analysed via DSC. Again, unlike the DSC results for the non-pressurised systems a T_g shift for polyethylene was observed in the sonicated samples. The results are shown below.

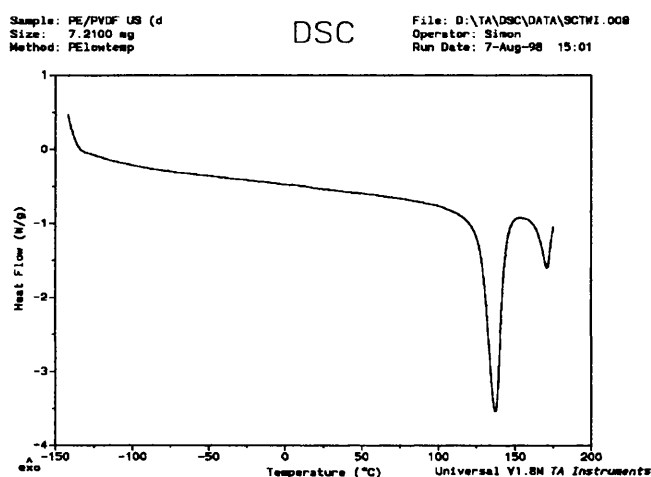


Figure135: DSC thermogram of PVDF/PE, heat and pressure only (240⁰C, 20 psi)

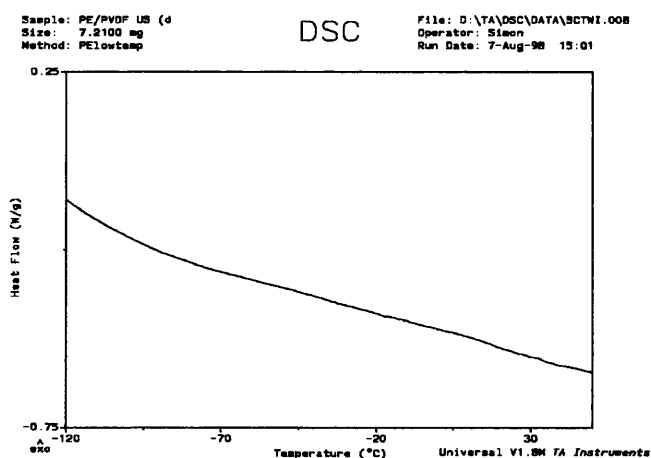


Figure136: (zoom of figure135), DSC thermogram of PVDF/PE, heat and pressure only (240⁰C, 20 psi)

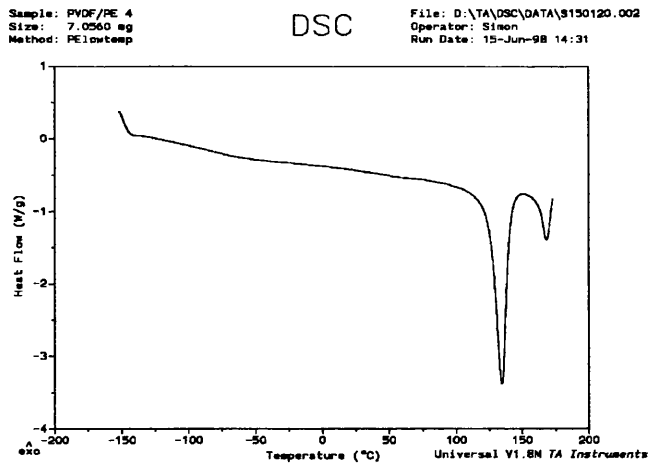


Figure137: DSC thermogram of PVDF/PE, sonicated 20x3.5 secs with pressure (240°C, 20 psi, 50W)

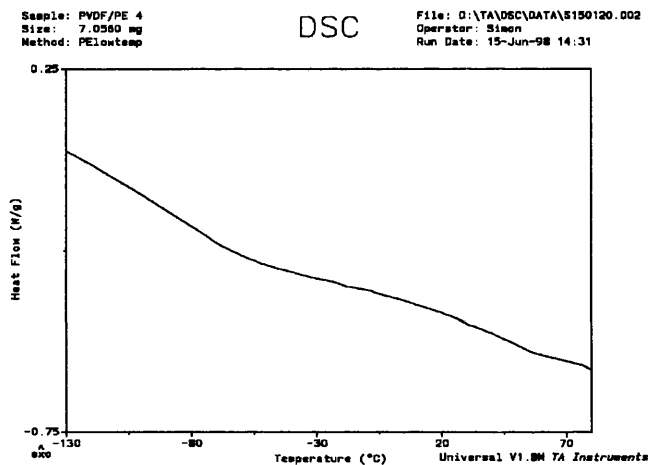


Figure138: (zoom of figure137), DSC thermogram of PVDF/PE, sonicated 40x3.5 secs with pressure (240°C, 20 psi, 50W)

Summary of DSC peaks

<u>DSC</u>	<u>Tg (°C)*</u>	<u>Tc1 (°C)</u>	<u>Tc2(°C)</u>
Figure 135: PE/PVDF Ht & P only	-98 to -100	137	170
Figure 137: PE/PVDF US (20x3.5) & P	-61 to -130	137	170

*note: in all DSC containing PE, the original Tg 'shoulder' was still present at around -100 to -130, in some cases broader (sonicated).

A shift/widening of the PE Tg is shown in the DSC thermographs. As stated earlier this is evidence of partial compatibilisation. These results and all other results in this section will be discussed in more detail at the end of the chapter.

10.1.6 DMTA Results for pressurised sonication of PE/PVDF Melts

DMTA results were obtained for PE/PVDF, the Tg's of both PE and PVDF can be seen easily and are in agreement with the DSC data shown in the previous section.

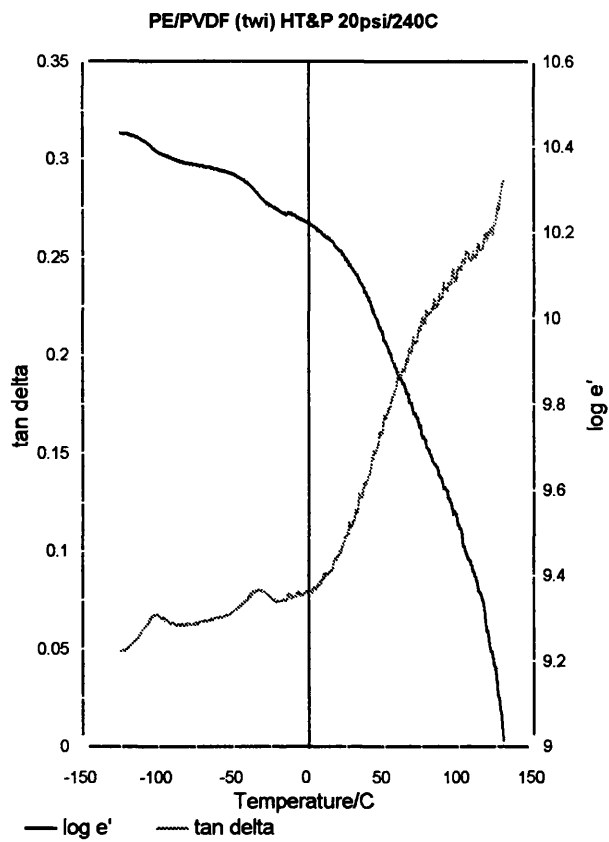


Figure139: DMTA of PE/PVDF, heat and pressure only (240°C/20 psi)

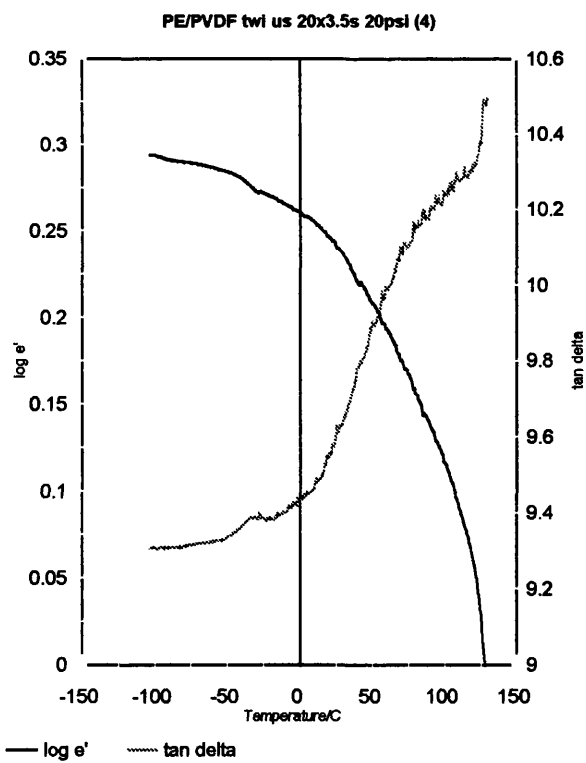


Figure140: DMTA of PE/PVDF, sonicated for 20x3.5 sec under pressure (240°C/20 psi)

10.2 Section Discussion

The DSC plots for PE/PP and PE/PVDF show some differences in the melting peaks volumes indicating a possible change in the crystallinity of the respective components. In the case of the sonicated samples the melting peaks are closer together, although this is not enough to indicate compatibility. More interesting, but much harder to see, are the positions of the polyethylene glass transitions.

From the DSC results for melt mixtures sonicated at atmospheric pressure it was seen that the compatibilisation effect was negligible, with the 'shoulder' of the PE Tg appearing at the same position for heated and sonicated samples (seen at ~ -100 to -130°C). For PP/PVDF and PP/PE DSC results the PP transition was very difficult to spot, but could be seen on a couple of plots at around -5°C . For PVDF/PE and PVDF/PP DSC results the PVDF Tg could be seen at approximately -50°C .

For the pressurised PE/PP and PE/PVDF samples the PE Tg is still at -100 to -130°C for the heat and pressure alone systems. However when ultrasound is used in conjunction with pressure a large shift in Tg is seen in every case. Again for DSC the 'peaks' were hard to see, but a comparison with other graphs showed that, as well as the 'shoulder' seen in all the DSC graphs, a further PE glass transition can now be seen at upto 90°C higher temperatures (see pages 161 & 171). The initial shoulder is also broader. Moreover this shift is more pronounced for longer sonication times (-35 to -60 for the 20x3s sample and -25 to -35 for the longer sonicated samples). Such a shift is seen in many journals as a sign of some degree of compatibilisation taking place^{93,109,149,150,151,152}.

Further evidence of the effect of sonication and pressure is seen in the DMTA results for PE/PP and PE/PVDF. In these it was seen that the heat only and the sonicated without pressure melts gave similar results with no Tg shift. Comparison of the heat and pressure only 'blanks' shown in this chapter again shows a similar plot. However for the sonicated with pressure samples a large difference in the graphs is seen.

On all the PE/PP DMTA plots, distinct broad peaks can be seen on tan delta traces at around -110°C and 0°C . These correspond to the PE and PP Tg's respectively. For the pressure and ultrasound systems a third smaller peak can be seen between the two which corresponds with the shifted Tg peaks seen in the DSC thermographs. Looking at the Log e' trace, for the sonicated with pressure samples the trace immediately raises (in comparison to the drop seen in all other graphs) and stays at a consistently higher value across the temperature range studied, showing evidence of a change in the properties of the polymer pair. This rise in log e' indicates a stiffer material.

Again, for the PVDF/PE plots, the non-sonicated, sonicated without pressure and heat/pressure only samples are all similar. Whereas for the sonicated under pressure graph, the PE Tg at -100 is very small, which is probably because it is spread out over a larger temperature range as seen in the corresponding DSC trace. A third peak is not seen in this DMTA, so it seems that the PE Tg has broadened but not shifted enough to give the separate peak seen for PE/PP. No obvious change in properties are seen.

From the results in this chapter, it is shown that pressure is required to assist the ultrasonic process when sonicating a viscous polymer melt. It would seem that the suspicion outlined in the preceding chapter was correct in that the sonic horn was not coupling with the melt sufficiently to enable cavitation to occur.

Although a truly miscible polymer pair would show one Tg peak, the nature of this method is such that the formation of 100% copolymer is impossible (as some polymer macroradicals will statistically combine with like species). Therefore some areas of each homopolymer will remain in the product displaying their original glass transition temperatures. However, the shifting of the Tg for Polyethylene (seen in both cases) and the change in moduli for PE/PP, indicate that partial miscibility has been achieved from otherwise totally immiscible polymers.

11.0. Discussion & Conclusions

A discussion of all the results in this thesis and also of possible applications and scale up choices is presented in this chapter. This is rounded off with the conclusions, which may be drawn from this work.

11.1 Discussion

This discussion is a summary and bringing together of the main points raised in the end of chapter discussions, which should, hopefully, give an overall picture of the project results. The conclusions to the project are presented immediately after this section.

11.1.1 Sonochemical Polymer Solution Degradation

The typical smooth degradation curves (M_n vs sonication time) which even out at a limiting value were expected^{61,62}, with more concentrated solutions giving more shallow curves. These shallower curves with higher limiting values, imply that the polymers degrade at a slower rate and to a lesser extent at higher concentrations. At low concentrations, the polymer chains are relatively free from contact with other polymer chains, so as cavitation occurs the polymers are readily stretched and broken by the intense shear gradients formed. As the concentration increases, the effect of the shear gradients is diminished as the large volume of polymer chains will hinder the flow of polymers towards the cavitation site so lessening the effect. The net result is that polymers near the bubble site will still be degraded, but the range of the shock wave will be smaller, so reducing the overall reduction in molecular weight, and reducing the rate.

Sonication of polystyrene (PS) which had already been investigated was the starting point and gave the expected results shown in the literature^{58,59,61,62}, with smooth degradation curves and the previously mentioned effect of less degradation at increasing concentrations (shallower curves and higher limiting values of M_n). However, sonication of previously uninvestigated polybutadiene gave a more interesting, unexpected result. Erratic degradation plots were produced, with actual increases in M_n seen at some points, although the overall effect was the

expected decrease in M_n . It was thought that the double bond present in the backbone of the polymers was responsible for this, as this made the occurrence of chain branching reactions possible. Evidence for this reaction was shown by ^{13}C spectroscopy showing the presence of an unprotonated sp^2 carbon in the sonicated polybutadiene samples.

The Schmid plots for polystyrene show a good fit (straight line) for about the first 200mins, after which the plots break down. Overall plots give much better results, with straight-line fits given over greater time periods (upto 300mins). The plots of k against concentration for both methods, show a declining rate with increasing concentration. This would agree with the comments earlier in the discussion, in that the increasing viscosity lowers the rate. Due to the branching reactions of polybutadiene, the Schmid plots presented below these degradation plots in Chapter 6 did not give a reliable k value from which corresponding k vs concentration graphs could be plotted.

11.1.2. Compatibilisation

Limited investigation of solution compatibilisation of polymers has been published prior to this project⁹⁸. As melt compatibilisation was the ultimate aim, some research into solution chemistry using previously unstudied polymer pairs was deemed appropriate. From the theory outlined in chapter 3 it was expected to that the sonicated polymer pairs would form copolymers which would improve the miscibility of the two. Evidence of this was to be seen via SEM from which the degree of phase separation was expected to decrease with sonocation time.

This theory seemed to work well with polymer pairs of PS/polyisoprene (PIP), poly(methylmethacrylate) (PMMA)/PIP and to a lesser extent for polyethylene (PE)/polypropylene (PP). However, for PS/ PMMA no evidence at all was seen of diminishing phase separation. In every case the PMMA/PS SEM images show a distinctly phase separated polymer pair. The lack of compatibilisation effects for PS/PMMA was surprising, but subsequent repeats of this experiment yielded the same images. Solvent effects are unlikely as similar results were obtained in both tetrahydrofuran (THF) and toluene. It was observed that time zero and sonicated samples appeared the same under SEM (small

spherical second phase) whereas sonicated separately then mixed samples gave larger, irregular phase domains. This difference is probably to the mixing techniques used, the sonicated separately samples were simply poured together and shaken, whilst the time zero samples had been mixed together over at least 24 hours and the sonicated together samples had also been subject to ultrasonic mixing on top of this.

It may be possible that if copolymer was formed, its presence is not sufficient to overcome the repulsive forces between the two polymers, so phase separation persists. Other explanations could be steric hindrance between the two polymers preventing copolymer formation or it could be that the relative rates of macroradical formation for each polymer differ greatly. If one were much faster than the other, then the possibility of copolymer formation would be slight as the chances of two different macroradicals meeting would be reduced.

The observation of this phase separation, possibly via nucleation, for PMMA/PS mixtures can be used to give weight to the compatibilisation claims for the other polymer pairs. As these pairs are immiscible (as seen by the time zero images), phase separated results would be seen if no effect had taken place. It may be argued that the diminished evidence of phase separation is merely the result of an ultra fine dispersion of the two polymers caused by ultrasonic mixing. However if this was the case the polymers should readily separate out in the solvent upon ceasing the sonication. The fact that this doesn't happen suggests that copolymers have been formed, by the suggested chain degradation/macroradical formation mechanism, and are stabilising the dispersion. This is highly likely as the solution degradation of single polymers in similar dilute solutions was seen to occur, with free radical formation being the best explanation (especially in the case of polybutadiene chain branching).

11.1.3. Melt Sonochemistry-Atmospheric Pressure

Apart from a misleading polystyrene result where the possible presence of oxygen gave increased degradation, no evidence of ultrasonic degradation could be found in any of the polymers tested. However, there was circumstantial evidence which suggested that ultrasound had a mixing effect on the polymer melt, in

agreement with the poly(dimethylsiloxane) (PDMS) and silica/PMMA sonication which gave direct evidence for ultrasonic mixing. This consisted of a general lowering of the polydispersity of the sonicated samples. It is possible that lower mass polymer chains are moved more easily by the mixing effect, which would have the result of a smaller range of molecular weights wherever this occurred i.e. the polydispersity would be lowered. It may be possible to test for this, by taking many samples from a sonicated melt polymer and analysing them by GPC. If the above phenomena had occurred then many different molecular weight averages would result, which in comparison to a heat only blank which would show roughly similar results for all samples.

The melt compatibilisation experiments carried out at atmospheric pressure also agreed with these observations. DSC and DMTA results collected for some of the polymer pairs investigated (PE/PP, PE/PVDF & PP/poly(vinylidene fluoride) (PVDF) showed no difference between sonicated and non-sonicated samples. The hoped for T_g shift, which is a good indicator of increased miscibility/compatibilisation, was not observed at all. However, SEM results gave more evidence of ultrasonic mixing. Due to the fact that the initial SEM samples of sonicated polymer pairs were made by dissolving the sample in solvent and then casting it onto the observation disk and that later samples were fixed to the sample holder without solvent, an interesting observation was made.

For the solvent cast samples, the polymers appeared phase separated, whether sonicated or non sonicated. Yet, when the SEM sample was prepared without solvent no phase separation was seen in the sonicated PE/PP, PE/PVDF and PP/PVDF pairs, but was present in the non-sonicated samples. This suggests that the polymers were being well dispersed amongst each other via sonication. Upon addition of solvent the polymers separate out again as no copolymer is present to stabilise the dispersed polymers (absence of copolymers was shown by DSC and DMTA).

Before melt sonication was abandoned as a means of producing miscible polymer pairs another possibility was left to investigate. This was that due to the high viscosity of the polymer melts, inadequate coupling of the sonic probe to the melt was occurring, preventing cavitation and the associated macroradical

formation. It was possible that upon commencing sonication the polymer melt was forced away from the probe tip, and was too viscous to refill the gap left behind. The air pocket formed by this would then serve as a barrier to the ultrasonic waves between the probe and melt, so cavitation would be impossible. Mixing may still occur, due to agitation of the melt around the edges of the air pocket.

In order to test this, two of the polymer pairs were sonicated in a pressurised environment, which should prevent formation of an air pocket and so improve probe/melt contact.

11.1.4. Pressurised Melt Sonication

Sonication of pressurised (20 psi) melts (PE/PP & PE/PVDF) again gave SEM results (samples cast without solvent) which showed no phase separation. Although, this time the DSC and DMTA data showed a distinct difference between the sonicated and non-sonicated samples. Comparison of the pressure non-sonicated samples with the earlier 'atmospheric pressure' sonication results shows that the DSC and DMTA results are almost identical i.e. no improvement in miscibility. However, for the pressure sonicated samples a shift, and in the very least a broadening, of the polyethylene Tg in all cases was seen. This shift was towards the Tg of the other polymer in the pair.

For the PE/PP samples, in particular, a third Tg peak is seen between the original PE Tg and that of PP (very clear from the DMTA results; peaks in the $\tan \delta$ plot and corresponding small losses in the $\log e'$ plot). The results do not show a complete compatibilisation of the polymer pair, but rather a partial compatibilisation. The original Tg peaks are still present, but the appearance of a third peak in between these two, indicates the presence of small amounts of copolymer. Complete conversion of the polymers into copolymer is statistically impossible by this method. Also, as the sonication times were very short due to the equipment used, it is to be expected that the original Tg peaks will still be present and larger than the copolymer peak, as they represent the unconverted homopolymer in the mix. The effect of this small copolymer addition to the mix can be seen upon inspection of the $\log e'$ (modulus) plot on the DMTA results for PE/PP. A marked change can be seen in the sonicated samples, with the moduli

having a consistently higher value across the temperature range studied. This indicates a stiffer material.

This effect is more difficult to discern from the PE/PVDF results, as the amount of copolymer produced appears to be less for these samples. A broader PE T_g was seen, but not a distinct third peak (the greater the amount of copolymer the greater the T_g shift, the reverse also being true). Longer sonication would most probably produce greater effects. Unfortunately this was not possible with the equipment used for these experiments.

11.1.5. Possible Uses & Industrial Scale Up

This process could have various possible implications and uses in industry and research. As detailed in chapter 4 a major area of possible use would be in the recycling of waste polymers. Large amounts of polymers are buried in landfill sites or simply burned as the current technology to deal with recycling them cannot handle the huge quantities involved or are not cost effective i.e. new polymer is cheaper than the recycled product. One of the main problems is that of separation of different polymers into homopolymer components. The use of the ultrasonic technique could negate this cost by sonication of the non-sorted polymers to form a single useful product. This would probably be low grade, but will still have use, and therefore commercial value, in many low specification, high volume products e.g. children's toys, some forms of packaging, shoe soles etc. Further research could identify easily sorted groups of polymers, which can be used to make higher performance products.

It may also be possible to create new materials from pairs of polymers with properties outstripping those of the starting polymers. Also it could simplify the synthesis of already manufactured copolymer containing polymeric materials, as the copolymer are created *in situ*, with the need for addition of expensive copolymer to the mix avoided. Indeed, in many research papers, polymer pairs are copolymerised by addition of copolymers produced by laborious processes.

Scale up of this technique could be achieved in a variety of ways. Normal industrial sonication can be achieved through batch and flow reactors¹⁴⁸ shown below. Flow reactors are probably unsuitable as pumps are required which would

have difficulty handling a viscous polymer melt. The introduction of pressure may prove difficult also. Batch processing is a possibility, as an effective closed system is used which could easily be pressurised with the bonus of also being able to control the atmosphere i.e. no oxygen to prevent thermal degradation. Problems with this system would include a slow turnover rate as it is not continuous and also the occurrence of 'dead spaces' in the melt where the polymer remains unaffected due to insufficient mixing (this may be overcome by some method of mechanical stirring).

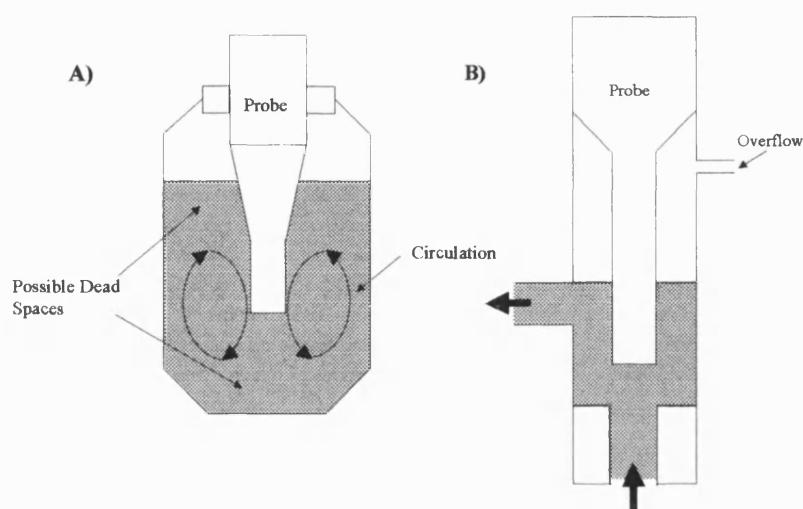


Figure 141: A) Batch Reactor B) Flow Cell

A good industrial technique for this process would be to use an ultrasonic horn attached to the end of a plastic extruder as used by Isayev et al ¹³⁴⁻¹⁴¹. He is using this technique to ultrasonically devulcanize rubber, for which the extruder offers the advantages of efficient melting and flow past the sonic probe. It would also have the bonus of applying pressure to the system, making the sonication of polymer mixtures shown in this project possible. Isayev currently holds patents^{137,138} on this idea (shown schematically below), which would make industrial sonication of polymer mixtures using this technique commercially difficult.

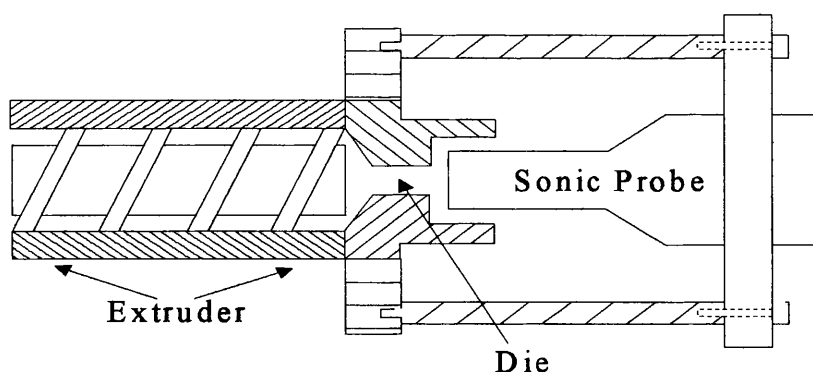


Figure 142: Extruder with sonic horn attached to die outlet.

11.2. Conclusions

The aim of this project was to investigate and achieve the ultrasonic compatibilisation of polymer mixtures in the melt, and gain some further understanding of the process. Also the broadening of understanding of the effect of ultrasound on polymers in solution, both single polymer solutions (degradation) and in pairs (compatibilisation) was envisaged.

These aims have been met in that it was discovered that sonication of polymer melt systems under atmospheric pressure proceeded without the presence of cavitation effects, although some effects attributable to ultrasonic mixing were observed. This lack of cavitation is thought to be due to insufficient coupling of the sonic horn to the polymer melt and can be overcome by carrying out sonication of the melt under pressurised conditions (20 psi in all the examples in this thesis). Sonication under pressure, even for short time periods, has noticeable effects on the two polymer mixtures studied by this method, polyethylene/polypropylene and polyvinylidene fluoride/polyethylene. Shifts in the T_g of polyethylene are seen in each case, and in the case of PE/PP a third T_g is seen showing the presence of copolymer. It may be possible to scale up this process using a batch reactor. The best option of using the extrusion process pioneered by Isayev¹³⁴⁻¹⁴¹ is probably unavailable due to patent issues.

Sonication of solution polymers has shown that high polymer concentrations in solution degrade slowly and somewhat erratically. Previous studies had only used low concentrations. The sonication of polybutadiene solutions has shown the unsuspected occurrence of chain branching reactions via

the double bond of the polymer backbone. NMR studies of sonicated polybutadiene gave weight to the suggested mechanism.

The sonication of polymer/polymer solutions has shown that a degree of compatibilisation is possible for PS/PIP, PIP/PMMA and PE/PP. However, PS/PMMA does not conform to the copolymer formation theory and does not appear to compatibilise at all. A probable mechanism for the phase separation has been suggested from study of the SEM data (metastable polymer mix breaking down via nucleation and growth), but the reason for the lack of copolymerisation is still unknown.

11.3. Further Work Arising From This Research

The first priority would be to develop apparatus that would enable longer and continuous sonication of molten polymers under pressure. The equipment used only allowed sonication at intervals of 3.5 seconds with the reaction vessel barely surviving many repetitions. Overheating of the horn was also a problem after many repetitions.

Experimenting with different ratios of polymers and various polymer pairs, gathering material properties (via DMTA and other testing methods e.g. tensile etc.) could also keep one researching for years. The use of solid state NMR may be a possibility in detecting the presence of copolymer in the sonicated sample by showing the presence of the adjacent atoms of each polymer the polymer/polymer interface of the copolymer.

Investigation into other polymers, which are relevant to the recycling problem, would also be an area for further investigation. Results shown in this thesis for PE and PP (two major commodity polymers) are promising. Other commonly found waste polymers, which could be investigated, include PET (polyethyleneterephalate) and PS.

Scale up of this process, probably using the batch reactor system with mechanical stirring is an area which needs further research before the process presented in this thesis may be augmented on an industrial scale.

REFERENCES

- 1) N.Serpone & P.Colarusso, Res Chem Intermediates, **20 No.6**, 635, 1994
- 2) K.S.Suslick, Science, **247**, 1439, 1990
- 3) T.J.Mason. In: Chemistry With Ultrasound, T.J.Mason (Ed), Elsevier Applied Science; London, 1990
- 4) G.J.Price. In: Current Trends In Sonochemistry, G.J. Price (Ed), RSC; Cambridge, 1992
- 5) P.D.Lickiss & V.E.McGrath, Chem.Br., **47**, March 1996
- 6) T.J.Mason, Education in Chem., **102**, July 1987
- 7) W.L.Whitlow,The Sonar of Dolphins, W.L.Whitlow(ed) ,Springer-Verlag 1993
- 8) T.G.Leighton. In: The Acoustic Bubble, T.G.Leighton (Ed), Academic Press, 1994
- 9) J.P.Lorimer, T.J.Mason, Chem.Soc.Rev., **239**, 1987
- 10) S.D.Lubetkin, Chem.Soc.Rev., **24**, 243, 1995
- 11) Lord Rayleigh, Philos.Mag., **34**, 94, 1917
- 12) K.S.Suslick & E.B. Flint, Science, **253**, 1397, 1991
- 13) K.S.Suslick, M.M.Fang & T.Hyeon, J.Am.Chem.Soc., **118**, 11960, 1996
- 14) K.S.Suslick, Chem.Mater., **9**, 2172, 1996
- 15) K.S.Suslick, M.M.Mdleleni & J.T.Ries, J.Am.Chem.Soc., **119**, 9303, 1997
- 16) K.S.Suslick, Chem.Mater., **8**, 2172, 1996
- 17) J.I.Thornycroft & S.W.Barnaby, Proc. Inst. of Civil Engineers, **122**, 51, 1895
- 18) D.Bremner, Adv.Sonochem., **1**, 1, 1990
- 19) A.L.Loomis & W.T.Richards, J.Am.Chem.Soc., **49**, 3086, 1927
- 20) A.L.Loomis & G.Wood, Philos.Mag., **4**, 414, 1927
- 21) E.W.Flosdorf & L.A.Chambers, J.Am.Chem.Soc., **55**, 3051, 1933
- 22) A.Szent-Gyorgyi, Nature, **131**, 278, 1933
- 23) H.Frentzel & H.Z.Schultz, Naturforsch, **7b**, 484, 1952
- 24) French Pat. No.823321, Chem.Abstr. **32:5490**, Jan 17 1938
- 25) B.E.Noltlingk & E.A.Neppiras, Proc.Phys.Soc., **B36**, 674, 1950
- 26) B.E.Noltlingk & E.A.Neppiras, Proc.Phys.Soc., **63B**, 674,1950
- 27) B.E.Nottlingk & E.A.Neppiras, Proc.Phys.Soc., **B64**, 1032, 1951

- 28) V.Griffing, M.Fitzgerald, J.Sullivan, J.Phys.Chem, **25**, 926, 1956
- 29) V.Griffing, J.Phys.Chem, **20**, 939, 1952
- 30) V.Griffing, J.Phys.Chem, **18**, 997, 1950
- 31) J.P. Perkins, Sonochem.Symp. Annual Chem. Congress, 8-11 April 1986
- 32) L.Crum & K.Hynynen, Phys.World, **28**, August 1996
- 33) T.J.Mason, Ultrasonics Sonochem., **1 No.2**, S131, 1994
- 34) M.A.Margulis, Ultrasonics Sonochem., **1, No.4**, S87, 1994
- 35) M.A.Margulis, Ultrasonics Sonochem., **1 No.2**, S87, 1994
- 36) T.Lepoint, D.De Pauw & F.Lepoint-Mullie, J.Phys.Chem., **100**, 12138, 1996
- 37) S.Putterman, Physics World, May 1998
- 38) T.Lepoint, D.De Pauw & F.Lepoint-Mullie, J.Acoust.Soc.Am., **101(4)**, 2012, 1997
- 39) K.Suslick & E.B.Flint, J.Phys.Chem., **100**, 6612, 1996
- 40) D.F.Gaitan & L.A.Crum, J.Acoust.Soc.Am., **Supp.1, 87**, S141, 1990
- 41) K.S.Suslick & D.J.Casadonte, J.Am.Chem.Soc., **109**, 3459, 1987
- 42) K.S.Suslick, Scientific American, **260**, No.2, 62, 1989
- 43) D.Peters, J.Mater.Chem., **6**, 1605, 1996
- 44) J.L.Luche, Ultrasonics, **25**, 40, 1987
- 45) T.Kitazume, Ultrasonics, **28**, 322, 1990
- 46) M.Koenig, Tetrahedron Lett., **42**, 5965, 1989
- 47) K.S.Suslick, Science, **247**, 1067, 1990
- 48) J.L.Luche, C.Petrier, M.Micolle, G.Melin & G.Reverdy, Environ.Sci. Technol., **26**, 1639, 1992
- 49) G.J.Price, P.Matthias & E.J.Lenz, Trans IChemE, **Vol 72**, Part B, Feb 1994
- 50) H.S.Huang, Environmental Progress, **Vol 11 No.3**, 195, 1992
- 51) A.J.Johnston & P.Hocking, Emerging Technologies in Hazardous Waste Management, 1993
- 52) J.R.Thomas, J.Phys.Chem., **63**, 1725, 1959
- 53) M.Okuyama and T.Hirose, J.Appl.Polymer Sci., **7**, 591, 1963
- 54) G.Gooberman, J.Polym.Sci., **4**, 101, 1960
- 55) J.Reisse & Y.Kegelars, Proc. 6th Meeting of the Eur.Soc.Sonochem., 1998
- 56) R.E.Harrington and B.H. Zimm, J.Phys.Chem., **69**, 161, 1965

- 57) D.E.Hughes and W.L.Nyborg, Science, **138**, 108, 1962
- 58) G.J.Price, Trends in Polym.Sci., **2**, No.5, 174, 1994
- 59) G.J.Price, Chem.Ind., 75, 1993
- 60) Hwan Kyu Kim & K.Matyjaszewski, J. Polym.Sci.:Part A Polym. Chem., **31**, 299, 1993
- 61) G.J.Price, P.J.West & P.F.Smith, Ultrasonics Sonochem., **1**, No.1, S51, 1994
- 62) G.J. Price & P.F.Smith, Polymer, **34**, No.19, 4111, 1993
- 63) S.L.Malhotra, J. Macromol.Sci.Chem., **A18 (7&8)**, 1055, 1982-3
- 64) R.Langer, Macromolecules, **25**, 511, 1992
- 65) M.S. Doulah, J. App.Polym.Sci., **22**, 1735, 1978
- 66) M.A.K.Mostafa, J.Polym.Sci., **28**, 519, 1958
- 67) T.Q.Nguyen, Q.Z.Liang & H.H.Kausch, Polymer, **38 No.15**, 3783, 1997
- 68) G.J.Price, Adv.Sonochem., **1**, 231, 1990
- 69) G.Schmid, Z.Phys.Chem., **A186**, 113, 1940
- 70) D.W.Ovenall, G.W.Hastings & P.E.M.Allen, J.Polym.Sci., **33**, 207, 1958
- 71) D.W.Ovenall, G.W.Hastings, P.E.M.Allen, G.M.Burnett & H.W.Melville
J.Polym.Sci., **33**, 213, 1958
- 72) A.Henglein, Makromol.Chem., **15**, 188, 1955
- 73) H.Fujiwara & K.Goto, Polymer Bulletin, **23**, 865, 1990
- 74) T.Sato & D.E.Nalepa, J.Appl.Polym.Sci., **22**, 865, 1978
- 75) M.Tabata et al, Chem.Phys.Lett., **73**, 178, 1980
- 76) D.L.DeVries and J.R.Thomas, J.Phys.Chem, **63**, 254, 1959
- 77) P.Kruus, Ultrasonics, **21**, 201, 1983
- 78) G.J.price, Ultrasonics, **29**, 166, 1991
- 79) G.J.Price, D.J.Norris & P.J.West, Macromolecules, **25**,(24), 6447, 1992
- 80) R.Langer, Macromolecules, **25**, 123, 1992
- 81) G.J.Price, Ultrasonics Sonochem., **3**, S229, 1996
- 82) T.J. Mason & J.P. Lorimer, Ultrasonics Sonochem., **79**, 1995
- 83) G.Portenlanger & H.Heusinger, Ultrasonics Sonochem., **1 No.2**, S125,
1994
- 84) R.Katoh, E.Yanase, H.Yokoi, S.Usuba, Y.Kakudate & S.Fujiwara,
Ultrasonics Sonochem., **5**, 37, 1998

- 85) C.Booth & C.Price, Comprehensive Polymer Science, 2, chp5, Pergamon Press, Oxford U.K. 1989
- 86) O.Olabisi, Polymer-Polymer Miscibility, Academic Press London, 1979
- 87) R.Jérôme, N.Ropson, P.Dubois & P.Teyssié, J.Polym.Sci., 35, 183, 1997
- 88) D.G.Pfeiffer & M.Rabeony, J.Appl.Polym.Sci., 51, 1283, 1994
- 89) A.H.Gabor & C.K.Ober, Chem.Mater., 8, 2272, 1996
- 90) S.P.Armes, A.B.Lowe & N.C.Billingham, Chem.Commun., 1035, 1997
- 91) R.E.Cohen & J.Gratt, Macromolecules, 30, 3137, 1997
- 92) J.Lub, A.Omenat, R.Hikmet & P.van der Sluis, Macromolecules, 29, 6730, 1996
- 93) F.C.Chang, W.B.Liu, W.F.Kuo & C.J.Chiang, Euro.Polym.J., 32, No.1, 91, 1996
- 94) W.H.Jo, C.D.Park & M.S.Lee, Polymer, 37, No.9, 1709, 1996
- 95) J.K.Kim, S.Kim & C.E.Park, Polymer, 38, No.9, 2155, 1997
- 96) Z.Horák, V.Fort, D.Hlavatá, F.Lednický & F.Vecerka, Polymer, 37, No.1, 65, 1996
- 97) E.Vaccaro, A.T.Dibenedetto & S.J.Huang, J.Appl.Polym.Sci., 63, 275, 1997
- 98) G.J.Price & P.J.West, Polymer, Vol 37, No.17, 3975, 1996
- 99) F.Grieser, G.Cooper & S.Biggs, J.Colloid & Interface Sci., 184, 52, 1996
- 100) J.G.Van de Velde, R.E.Wetton & R.D.L.Marsh, Thermochemica Acta, 175, 1, 1991
- 101) E. Kaisersberger, Thermochemica Acta, 93, 291, 1985
- 102) L.D'Orazio, R.Guarino, C.Mancerella, E.Martuscelli & G.Cecchin, J.Appl. Polym.Sci., 65, 1539, 1997
- 103) D.Graebing., J.Appl.Polym.Sci., 66, 809, 1997
- 104) A.K.Nandi & P.Maiti, Polymer, 38, No.9, 2171, 1997
- 105) C.W.Macosko, P.Guégan, A.K.Khandpur, A.Nakayama, P.Marechal & T.Inoue, Macromolecules, 29, 5590, 1996
- 106) F.C.Chang & C.C.Huang, Polymer, Vol 39, No. 9, 2135
- 107) A.Amash, P.Zugenmaier, J.Appl.Polym.Sci., 63, 1143, 1997
- 108) Y.J.Sun, G.H.Hu, M.Lambla & H.K.Kotlar, Polymer, 37, No.18, 4119, 1996

- 109) T.Vainio, G.H.Hu, M.Lambla & J.Seppälä, J.Appl.Polym.Sci., **63**, 883, 1996
- 110) Y.Jinghua, C.Xue, G.C.Alfonso, A.Turturro & E.Pedemonte, Polymer, **Vol 38, No.9**, 2127, 1997
- 111) P.Magagnini, G.Poli, M.Paci, R.Scaffaro & F.P.La Mantia, Polym.Eng.Sci., **Vol 36, No.9**, 1244, 1996
- 112) C.W.Macosko, P.Guégan, J.J.Cernohous, A.K.Khandpur & T.R.Hoye, Macromolecules, **29**, 605, 1996
- 113) G.Menges, R.Fischer & V.Lackner, Intern.Polym.Process., **VII, 4**, 291, 1992
- 114) G.Tesoro & Y.Wu, Plastics, Rubber & Paper Recycling, 502, 1995
- 115) N.Yoda, Macromol.Symp., **98**, 1293, 1995
- 116) R.W.Cole, ACS 146th Meeting, October 11-14th 1994
- 117) B.Dubrelle D'Orhcel. In: Recycling Of PVC & Mixed Plastic Wastes, ChemTec Publishing, Canada, 1996
- 118) C.J.Kibert, Proc.Instn.Civ.Engnrs.Structs. & Bldgs, **99**,455, 1993
- 119) P.Peuch, Mater.World, 313, 1994
- 120) R.A.Pett et al, Plastics, Rubber & Paper Recycling,p 47, 1995
- 121) G.J.Xu, D.F.Watt & P.P.Hudec, J.Mater.Process.Technol., **48**, 385, 1995
- 122) Article, British Plastics and Rubber, 32, June 1997
- 123) Article, European Chemical News, **47**, 10, November 1997
- 124) M.Buggy, L.Farragher & W.Madden, J.Mater.Process.Technol., **55**, 448, 1995
- 125) T.Endo, T.Suzuki, F.Sanda & T.Takata, Macromolecules, **29**, 3315, 1996
- 126) S.J.Huang, J.M.S. Pure Appl. Chem., **A32(4)**, 593, 1995
- 127) P.Hornsby & S.Pickering, Mater.World, 426, September 1995
- 128) Z. Jedlinski, P.Kurcock, J.M.S. Pure Appl. Chem, **A32(4)**, 797, 1995
- 129) J.D.Hamilton, J.V.Hagan & W.V.Lord, J.Air & Waste Manage.Assoc., **45**, 247, 1995
- 130) A.D.Read, P.S.Phillips & A.Murphy, Resources, Conservation & Recycling, **20**, 153, 1997
- 131) A.D.Read, P.S.Phillips & G.Robinson, Resources, Conservation & Recycling, **20**, 183, 1997
- 132) M.A. Barlaz et al, Waste Management & Research, **11**, 463, 1993

- 133) M.A. Petrich & A.A. Merchant, AIChE Journal, **39**, No.8, 1370, 1993
- 134) A.I.Isayev, S.P.Yushanov & V.Y.Levin, J.Polym.Sci., **B34**, 2409, 1996
- 135) A.I.Isayev, S.P.Yushanov & J.Chen, J.Appl.Polym.Sci., **59**, 803, 1996
- 136) A.I.Isayev, A.Tukachinsky & D.Scworm, Rubber Chem. & Technol., **69**, 92, 1995
- 137) A.I.Isayev, International Patent, No.C08F 2/46, 2/56, B06B 1/00, 1994
- 138) A.I. Isayev et al, U.S. Patent No. 5,284,625, 1994
- 139) A.I.Isayev, A.Tukachinsky & J.Chen, 146th Rubber Division Meeting, Paper 69, Pittsburgh, 11th-14th October 1994
- 140) A.I.Isayev, A.Tukachinsky & J.Chen, Rubber Chem. & Technol., **68**, 267, 1995
- 141) A.I.Isayev, S.P.Yushanov & J.Chen, J.Appl.Polym.Sci., **59**, 815, 1996
- 142) C.M. Langton, J. Alloys & Compounds, **211/212**, 419, 1994
- 143) G.Paula, Mech.Eng., 14, March 1997
- 144) J.R.Ellis, Plastics, Rubber & Paper Recycling, 62, 1995
- 145) C.P.Rader & R.F.Stockel, Plastics, Rubber & Paper Recycling, 2, 1995
- 146) R.S.Stein, Plastics, Rubber & Paper Recycling, 27, 1995
- 147) L.P.McMaster, Adv.Chem.Ser., **142**, 43, 1975
- 148) T.J.Mason, Ultrasonics, **30 No.3**, 192, 1992
- 149) M.Cortazar & M.A.Gomez, Macromolecules, **29**, 7038, 1996
- 150) C.Galan, C.A.Sierra, J.M.Gomez-Fatou & J.A.Delgado, J.Appl.Polym.Sci., **62**, 1263, 1996
- 151) Y.Zhihui, Z.Xiaomin, Z.Yajie & Y.Jinghua, J.Appl.Polym.Sci., **63**, 1857, 1997
- 152) B.Jurkowski & Y.A.Olkhov, J.Appl.Polym.Sci., **65**, 1807, 1997